博士学位論文

Doctoral Dissertation

論文題目

Comprehensive Glycomics for the Discovery of New Biomarkers in Neurodegenerative Diseases

(神経疾患新バイオマーカーの探索のための総合的グライコミクス)

氏名

Solomon Tebeje Gizaw

北海道大学大学院生命科学院

Graduate School of Life Science, Hokkaido University

September 2015

Contents

Abbreviations

AD	Alzheimer's disease
Aß	Amyloid ß
aoWR	Na (aminooxy-acetyl) tryptophanylarginine methyl ester
BCA	Bicinchoninic acid assay
BOA	O-Benzylhydroxylamine hydrochloride
CDG	Congenital disorders of glycosylation
CNS	Central nervous system
CSF	Cerebrospinal fluids
DHB	2, 5-Dihydroxybenzoic acid
DSA	Datura stramonium
DTT	Dithiothreitol
ELISA	Enzyme-Linked immunosorbent assay
Fu	Fucose
Gal	Galactose
GalNAc	*N*-acetylgalactosamine
Glc	Glucose
GSL-omics	Glycosphingolipidomics
HBSFRC	Human Brain and Spinal Fluids Resource Center
Hex	Hexose

HexNAc	*N*-acetylhexosamine
HD	Huntington's disease
HRP	Horseradish peroxidase
IAA	Iodoacetamide
IgG	Immunoglobulin G
LCA	Lens culinaris
KDN	2-keto-3-deoxynonulosonic acid
Man	Mannose
MeOH	Methanol
MS	Mass spectrometry
MTT	3-methyl-1-p-tolytriazene
MALDI-TOF MS	Matrix-assisted laser desorption ionization-time of flight mass spectrometry
NeuAc	*N*-acetylneuraminic acid
NeuGc	*N*-glycolylneuraminic acid
PAS	Periodic Acid-Schiff
PB	Phosphate buffer
PBS	Phosphate buffer saline
PD	Parkinson's disease
PHA-E4	Phaseolus vulgaris
PHM	1-Propanesulfonic acid-2-Hydroxyl-3-Myristamido
PNA	Arachis hypogaea
PNGase F	Peptide *N*-glycosidase F

PTM	Post-translational modification
PolyQ	Polyglutamine
SSA	Sambucus sieboldiana
TBS	Tris-buffer saline
TMB	3, 3’, 5, 5’-Tetramethylbenzidine
TOF	Time of flight
WT	Wild type

Chapter 1

General Introduction

1.1. Neurodegenerative Diseases

Neurodegeneration is the umbrella term that can be applied to several conditions result in progressive loss of neuronal structure, function and death. Neurodegenerative diseases are heterogeneous groups of disorders, chronic and progressive. These central nervous system (CNS) disorders are characterized by selective and symmetric loss of neurons in motor, sensory, or cognitive systems. Pathophysiologically classified by the patterns of cell loss and identifications of disease-specific cellular markers, such as senile plaques, neurofibrillary tangles, neuronal loss, acetylcholine deficiency, Lewy bodies, depletion of dopamine, cellular inclusions, swollen motor axons, intranuclear inclusion bodies and the loss of GABA-containing neurons [1-4]. These diseases prevalently diagnosed mid-late life and apparently diagnosed as “pre-clinical” stage that is developing extensive pathological changes in the brain. Systematic treatments are emerging effective towards the reverse and/or forestall the onset and/or progress of the diseases [4, 5].

Most CNS disorders result from the abnormalities in the processing of proteins and defective processing causes the accumulation of specific neuronal proteins: amyloid ß (Aß)- and tau-proteins of Alzheimer’s disease (AD); α-synuclein of Parkinson’s disease (PD); Huntingtin (HTT) protein of Huntington’s disease (HD); Superoxide dismutase-1 (SOD-1) of Amyotrophic lateral sclerosis (ALS) and Ataxin of Spinocerebellar ataxia (SCA), to mention few. These abnormal processing of neuronal proteins can entail misfolding of the native proteins, altered post-translational modification of newly synthesized proteins, abnormal proteolytic cleavage, anomalous gene splicing, improper expression, or diminished clearance of degraded proteins [6-7]. Because these filamentous aggregates display the ultrastructural and tinctorial properties of amyloid, these diseases can be grouped together as brain amyloidoses [5,8] (Figure 1.1).

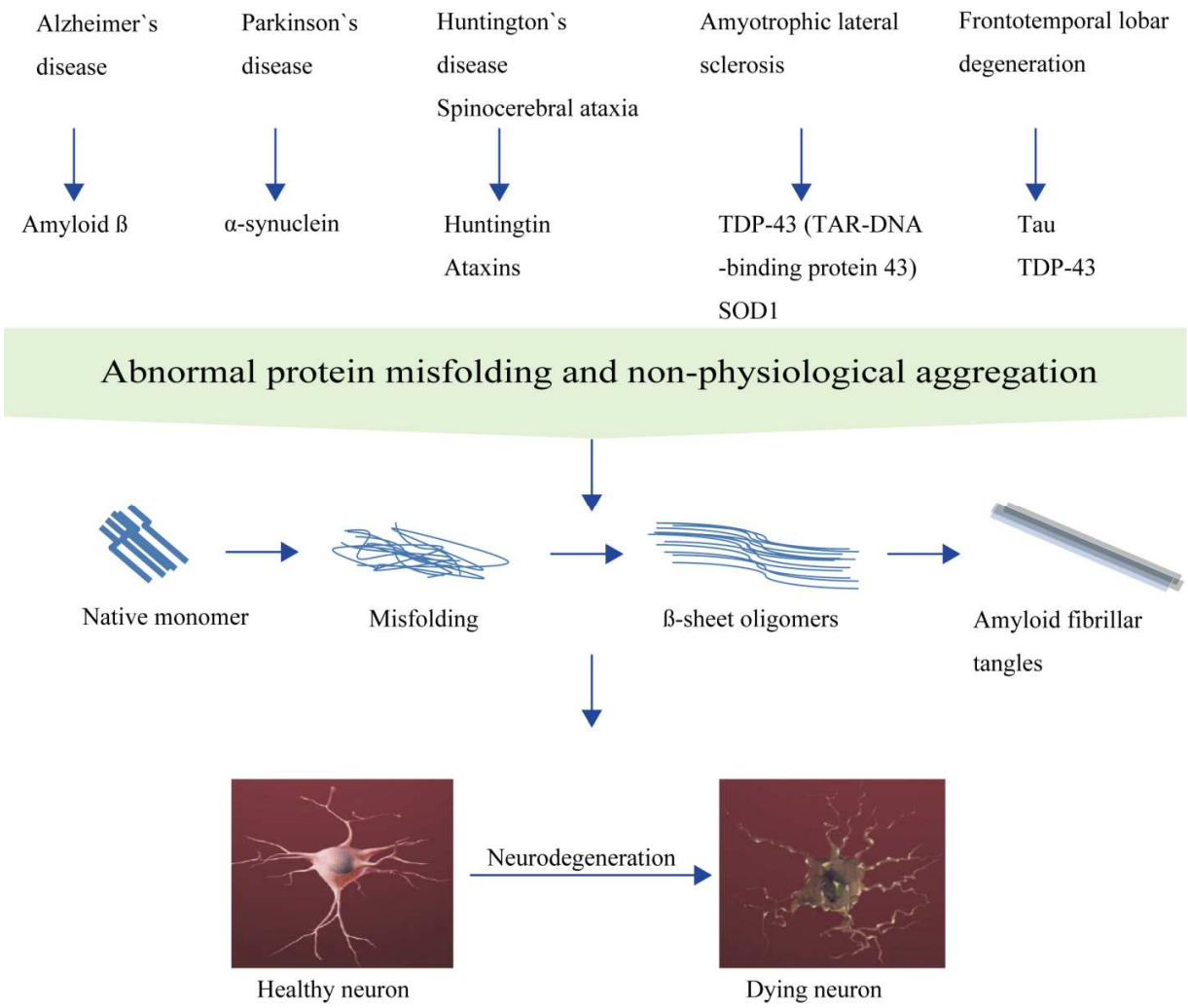

Figure 1.1. Protein misfolding and aggregation are the common molecular pathogenesis of neurodegenerative diseases.

1.1.1. Alzheimer's Disease

Alzheimer's disease (AD) is the most common devastating and late-onset neurodegenerative disorder. AD is characterized by a progressive neuronal loss accompanied by loss of memory, mood changes, problems with communication and reasoning. This devastating disorder can be early onset genetic cases (familial AD) and vast majority of late onset sporadic forms that are caused by several factors such as estrogen, anti-inflammatory drugs, cerebrovascular diseases, oxidants, and metals; however, the processes by which the factors may influence disease development in the sporadic cases are still poorly understood. Regardless, studies suggested that it is likely to be multifactorial including genetic predisposition, protein trafficking and turnover, glycosphingolipids (GSL) abnormalities, and impairment of neurotrophin signaling [9,10].

Moreover, morphological evidences in Alzheimer's disease showed that selective neuronal degeneration in human brain is region specific [11-13]. The brain with AD has an abundance of two abnormal structures - amyloid plaques and neurofibrillary tangles - that are made of misfolded proteins. This is especially true in certain regions of the brain that are important in memory. The other main feature of AD is the loss of connections between cells that leads to diminished cell function and cell death [14,15]. Amyloid beta (Aß) is the major constituents of the fibrils composing senile plaques and vascular amyloid deposits. Scientists have been striving to clearly demonstrate the mechanism of Aß production from amyloid precursor proteins (APP) processing by the harmful pathway, in which APP is cleaved by a ß-secretase yielding sAPPß and amyloidogenic fragment A4CT (the soluble sAPPß isoform, which extends from the Aß amino terminus to the carboxyl terminus of APP) and subsequent cleavage

of A4CT within its transmembrane region by gama-secretase generating the Aß (1-40) and Aß (1-42/43). The clinically important Aß that deposits as amyloid in AD brain is most likely has been produced locally and also appears to occur in all cells and tissues that can be detectable in plasma and cerebrospinal fluids [10,18,19].

Recently there has been evidenced that tau oligomer's, which form before paired helical filaments (PHFs) and neurofibrillary tangles (NFTs), could be the structure mediating neurodegeneration even before the fibrillary tau is deposited [20]. Soluble aggregates (i.e., Aß and α-synuclein) have been implicated as the primary toxic species in many degenerative diseases [21]. Several studies have shown aberrant glycosylation of proteins in APP, tau and the two proteases responsible for Aß production also have roles in protein glycosylation [22]. In addition, bisecting GlcNAc delays ß-site APP cleaving enzyme 1 (BACE1, aka ß-secretase) degradation leading to Aß production, which is the hallmark of AD [23]. Since relatively unexplored topic, AD total glycome analysis of the targeted areas of amyloid deposits, the brain, serum and CSF deserves more attention for the development of improved biomarkers and treatment methods.

1.1.2. Parkinson's Disease

Parkinson's disease (PD) is characterized by tremor at rest, bradykinesia, postural and autonomic instability and shuffling. It is the second most progressive CNS disorder after AD and the most frequent subcortical degenerative disease. The core pathology of PD affects the dopamine producing neurons of the substantia nigra (SN) of the midbrain and other

monoaminergic neurons in the brain stem [3,24-26]. As a result, PD correlates with degeneration of the dopaminergic nigrostriatal pathway and dopamine depletion in the striatum. The vast majorities of PD cases are sporadic [27-29] and probably caused by interaction of environmental and genetic factors [30].

PD is a synucleinopathy; and the most pathological hallmark of adult onset PD is fibrils made of insoluble polymers of alpha synuclein deposited in the neuronal body forming round lamellated eosinophilic cytoplasmic inclusions, the Lewy bodies (LBs), often near the nucleus. Lewy bodies are densest in the substantia nigra but can also be present in monoaminergic, cerebral cortices and other neurons. Alpha synuclein is also deposited in neuronal processes (Lewy neurites), in astrocytes and oligodendroglial cells. A major constituent of Lewy bodies is aggregated alpha-synuclein protein. As a result, all goes with the degeneration of dopaminergic nigrostriatal pathway, dopamine depletion in the striatum, neuronal degeneration and death. Moreover, the presence of alpha-synuclein in cortical Lewy bodies would be indispensable to maximize the diagnosis of AD with insufficient numbers of plaques and neurofibrillary tangels for those suffering from dementia [31].

Furthermore, dopamine (DA) metabolism is the main source of reactive oxygen species in DA cells, and also DA is may be responsible for DA cell degeneration. The cytosolic levels of DA depend on its synthesis and DA transport, in which the later is performed by dopamine transporter (DAT). The glycosylated DAT form transports DA more efficiently than the non-glycosylated form suggesting DAT glycosylation is involved in the differential vulnerability of midbrain DA cells in PD [32]. Taken together, the deposition of abnormal proteins and neuronal death triggers aberrant glycosylation or vice versa, and study of total glycome expression levels

is required to expand our knowledge of the disease process in order to find complimentary or alternative treatment strategies.

1.1.3. Huntington's Disease

Huntington's disease (HD), one of the trinucleate repeat disorders, nosologically classified as the presence of neuronal intranuclear inclusions (NIIs), dystrophic neuritis (DNs), the loss of GABA-containing neurons in the neostriatum and, subsequently, in the cerebellar cortex [33]. The HD mutation is dominant and almost completely penetrant [2]. The increased numbers of CAG repeats in the HD gene are expressed as an elongated huntingtin (HTT) protein with 40 to 150 polyglutamine (polyQ) residues (CAG ranges for normal individuals are 9-35). The huntingtin, the function of which is unknown, is a 350 KDa protein encoded by the HD gene (initially labeled as IT15) [1,2,33,34]. It is associated with proteinaceous deposits that are found in patients' brain of which aggregated polyQ is a major component [35]. The disease is caused by an abnormal elongation of a CAG repeat sequence in exon 1 of the HD gene [36], which is sufficient to cause a progressive neurological phenotype in transgenic mice [37]. HD is an autosomal, dominantly inherited, and progressive neurodegenerative disorder and, accordingly, the hallmark for fatal genetic diseases [38-42].

Mechanistically, the mutant huntingtin protein produced by an increase in the number of CAG repeats in the *HD* gene is cleaved to fragments that retain increased number of glutamine residues. These fragments are conjugated with ubiquitin and carried to the proteasome complex. Subsequent cleavage is incomplete, and components of both huntingtin and the proteasome are

translocated to the nucleus where aggregates form, and resulting in neuronal intranuclear inclusions (NIIs). In nucleus, HTT acts to induce apoptosis but death does not correlate with the formation of NIIs [43].

1.2. Glycosylation/Aberrant Glycosylation

Glycosylation is the most prevalent post-translational modification (PTM) of proteins in higher organisms essential to modulate a wide range of protein and lipid functions within or on extracellular surfaces of the cell. Protein glycosylation is either *N*-linked (GlcNAcβ1-Asn linkage with a minimal amino acid sequence of Asn-X-Ser/Thr, where X ≠ Pro) or *O*-linked (where GalNAc is added to Ser or Thr), and GSLs are synthesized by a sequential transfer of sugar residues to a ceramide lipid anchor (Figure 1.2). Interestingly, all share pivotal roles such as cellular differentiation, adhesion, immunity, signal transduction and growth control [44-46]. However, there is no comprehensive glycomics focusing on mammalian brain glycoconjugates towards the discovery of neurodegenerative biomarkers while a few *N*- and *O*-glycans specific to rat brain glycoproteins have been reported [47-49].

The atrophy of the neurons due to pediatric and adulthood diseases of the central nervous system leads to aberrant glycosylation and the biosynthesis pattern of the available glycans is altered. Aberrant glycosylation, in turn, impairs neurite growth and fasiculation, synapse formation and stabilization, and also causes psychomotor difficulties, mental retardation and other neuropathological symptoms that are highlighted by congenital disorders of glycosylation (CDG) [50]. Understanding the glycosylation pattern of *N*-, *O*-, and glycosphingolipids (GSL)-

glycans, which is affected by either genetic or environmental cellular stressors, is a promising step towards an easy prognosis of disease progression. Either serum or cerebrospinal fluids (CSF) specimens from humans with neurodegenerative and aging diseases are valid candidates for biomarker detection [50-52].

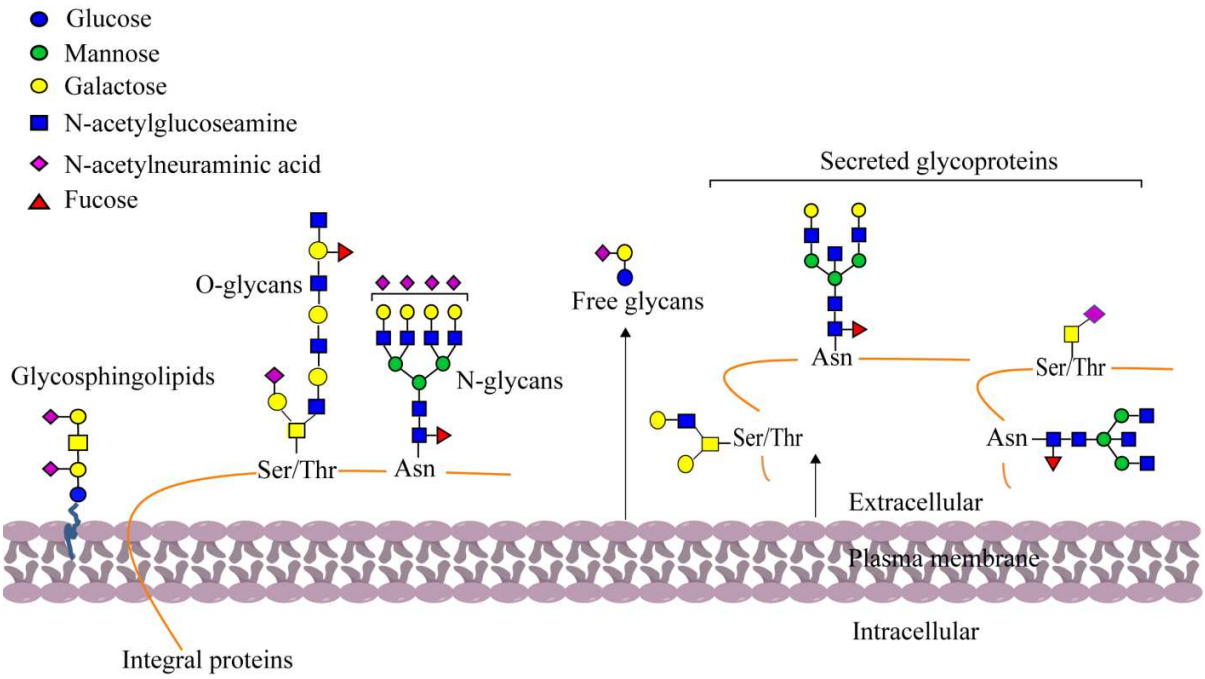

Figure 1.2. Basic core structures of *N*-, *O*-, and *GSL*-glycans.

1.3. Total Glycomics

Glycomics is the systems-level study of the glycan repertoires or glycomes, which comprise the entire set of glycans produced in a single organism [53]. It has been an attractive area of research in the postgenome era emerging as a new paradigm for biomarker discovery [54-

58]. However, the stereochemical and structural diversity of monosaccharides, the heterogeneous or highly complicated glycan structures of glycoproteins (microheterogeneity), the multivalent nature of glycan-protein interactions [58,59], and the lack of a direct genetic code for glycan complex modification (the non-template dependent biosynthesis of glycans) [60-62] are the challenges that scientists are faced with. As the most structurally and functionally diverse class of molecules in nature to undergo versatile protein modifications, glycoconjuagtes play a key role in tracing the cellular glycosylation patterns of multifunctional proteins [63] as well as finding potential glyco-biomarkers in the field of drug discovery [64,65].

Many efforts to identify glycosylation defects in cases of CDG, in conserved oligomeric Golgi (COG)-deficient patients, and in the increasing prevalence of age and age-related diseases have been made over the years. These include the study of glycoform characterization of serum, plasma and CSF using ESI-MS, affinity chromatography, and 2-DE followed by MS/MALDI-MS/DNA sequencer adapted-fluorophore assisted carbohydrate electrophoresis (DSA-FACE) and HILIC-HPLC [47]. Moreover, glycosylation changes in non-invasive bodily fluids, inter alia, serum, urine, plasma glycomes and on individual glycoproteins have been identified as promising biomarkers for the detection of prostate cancer [59], hepatocarcinoma cancer (HCC) and cirrhosis of the liver [66,67], pancreatic cancer [68], ulcerative colitis [69], and bladder cancer [70]. Measuring the degree of alteration of specific glycans in serum/plasma or whole blood has helped to provide a novel, non-invasive method for determining prognoses in cases of cancer and the existence of specific altered glyco-phenotypes, which might represent risk factors for the sequela of certain diseases [71-76]. Most serum proteins are synthesized in the liver, and any glycosylation changes in serum of total *glycoforms* are the direct result of an alteration of the liver or β-lymphocyte pathophysiology. Huntingtin protein targeting experiments have also been

performed to understand the pathogenesis of neurodegenerative diseases [2,36]. Since oligosaccharides attached to the proteins play significant roles in tissue development and maintenance, the brain tissue of human and transgenic mice provides additional systems for such studies [36,77]. Besides brain, serum is preferred as of an easy diagnosis for the discovery of novel disease specific biological markers with high sensitivity and specificity. In addition, researchers are rely on CSF for AD biological diagnosis [78,79]. All these encouraged the writer to target those specimens as source of biological markers in neurodegenerative diseases.

As a first initiative, I have estimated the glycan composition and quantified the total glycomes (*N*-, *O*-, GSL-glycans) expression levels in brain tissue, serum, and CSF of neurodegenerative diseases (AD, PD, and HD) via glycoblotting [79-81] assisted sample preparation, i.e., glycan enrichment, combined with MALDI-TOF/MS analysis. Glycoblotting-assisted sample preparation is an easy, expedite and one-pot solid phase process to obtain perfectly purified and labeled glycans. This technique circumvents the “bottlenecks” of time-consuming and imprecise purification processes used in more authentic methods. In addition, glycome analyses using glycoblotting is advantageous over genomics and proteomics (which are rich in line type information) because it ensures multiple, more reliable or stable information and more importantly indispensable to assess the disease progression with rapid, early and parallel diagnosis. Therefore, total glycomics employing glycoblotting is a superior tool for profiling typical glycans and quantifying their expression levels in human or model mice, of targeted brain regions, serum and CSF towards the discovery of novel disease biomarkers (Figure 1.3).

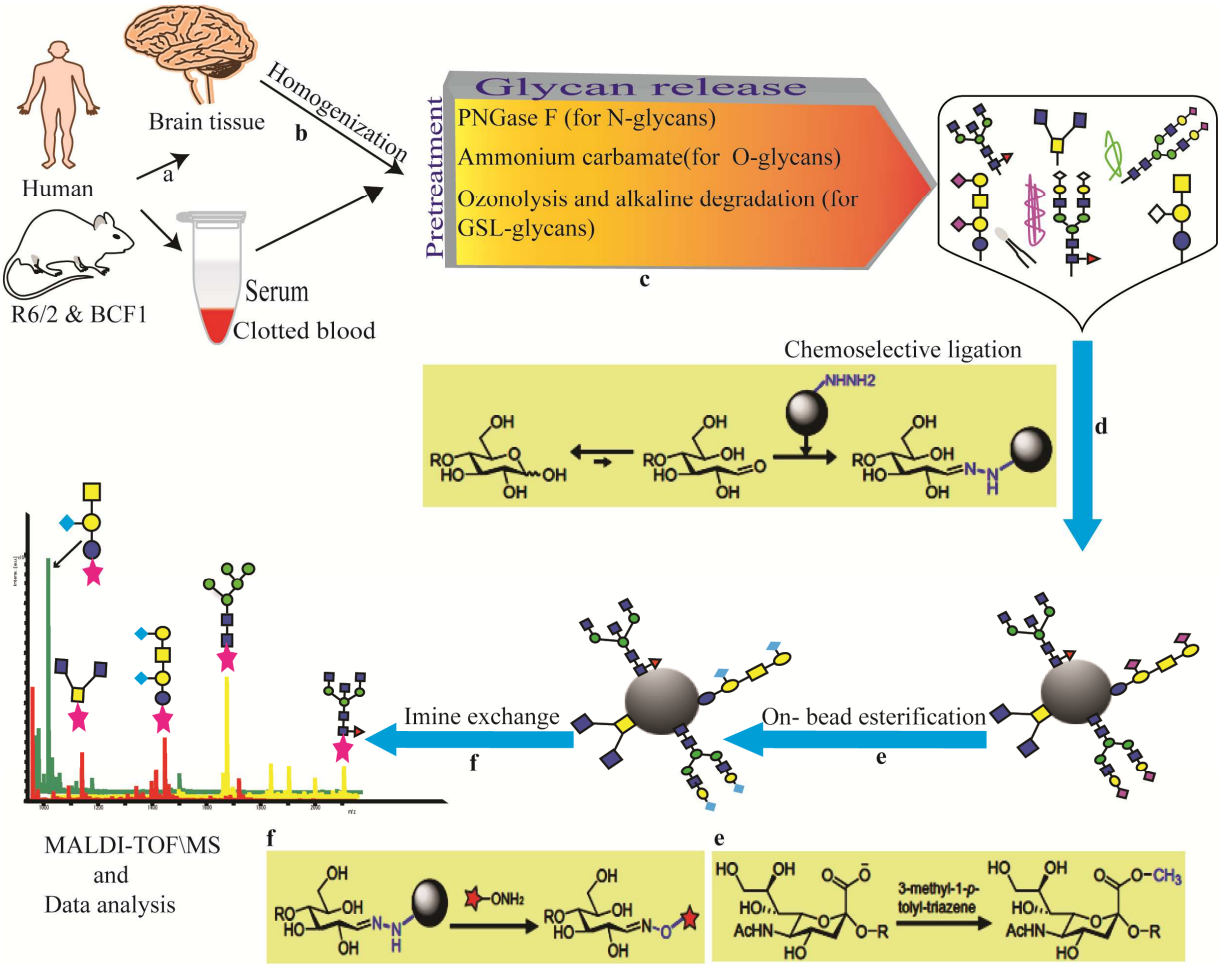

Figure 1.3. Schematic diagram of total glycomics. (a) Dissection and perfusion (in case of 12-week-old mice). (b) Homogenization of human and mice brain tissues. (c) Trypsin digestion, followed by PNGase F and ammonium carbamate cleavage of *N*- and *O*-glycans, respectively; chloroform/methanol extraction and native GSL-glycans cleavage by ozonolysis and subsequent fragmentation by alkaline treatment in the case of oligosaccharides from GSLs. (d) Chemoselective capturing of reducing oligosaccharides on BlotGlyco® beads. (e) On-bead methyl esterification. (f) Derivatization, glycan release, and Finally, MALDI-TOF/MS analysis of either aoWR or BOA labeled *N*-, *O*-, or *GSL*-glycans.

Glycoblotting [79-81] is a standardized technology in high throughput glycomics. It was developed in our laboratory to facilitate the glycan enrichment process of highly complicated mixtures such as bodily fluids, cells, tissues, and organs of both human and knock-out mice. The purpose of this enrichment process was to assess the *N*-, *O*-, and *GSL*-glycans expression levels of PTMs in various human diseases when compared with those normal subjects. This new operational method has been applied to large scale structural and functional analysis of protein glycosylation [82-84], diseases related to glycan biomarker exploration [67-70,86], and to reveal the trends and complex patterns of glycans diverse taxonomic groups of different bird species [87]. MS based glycome analysis is a rapid and sensitive strategy to carry out both fundamental studies of glycan biological activities and to identify potential disease markers [88]. Achievements stemming from a multitude of samples studies have encouraged the author to extend efforts to estimate the structural composition and the total glycome expression levels in neurodegenerative diseases via glycoblotting-assisted MALDI-TOF/MS and avidin-biotin lectin staining (for mouse brain tissue) [89]. I was able to observe a difference in structure and in the amount of glycomes between AD, PD, HD and the normal/control groups. As the leading of the neurodegenerative diseases, the total glycomics of AD, PD and HD can serve as a blueprint to profile the glycomes of either environmentally or genetically based CNS dementia/disorders. Such an achievement would be a great step towards the discovery of new glyco-biomarkers for this particular class of diseases.

1.4. Aim of the Thesis

The field of glycomics is expanding at a stunning pace; however, still challenged by the "bottlenecks" of the current glycomics, such as time-consuming and imprecise glycan purification processes used in more authentic methods. In addition, there is no comprehensive glycome analyses of neurodegenerative diseases reported yet. To fulfill the high demand of disease specific glycan markers, the writer targets glycoblotting-assisted sample preparation and MALDI-TOF/MS analysis to estimate the composition and quantify the expression levels of the total glycomes: *N*-, *O*-, *GSL*-glycans from human and mice brain tissue, serum and CSF samples of AD, PD, and HD. This relatively new technique is an easy, expedite, and one-spot solid phase process to obtain purified and labeled glycan based on solid/liquid separation.

In chapter 2, I will discuss about the presumptive composition and expression levels of *N*-glycans of neurodegenerative diseases and suggest novel glyco-biomarkers. Chapter 3 will cover about *O*-glycans, particularly mucin types. In Chapter 4, the author will discuss in detail about the estimated composition and amount of GSL-glycans levels in neurodegenerative diseases. Chapter 5 covers the concluding remarks of the whole research, more importantly, emphasize glyco-biomarkers as the promising candidates in the field of drug discovery and neuroscience.

1.5. References

[1] N.W. Kowall, R.J. Ferrante, J.B. Martin. Patterns of cell loss in Huntington's disease, Trends Neurosci 10 (1987) 24 – 29.

[2] J.B. Martin, Molecular basis of the neurodegenerative disorders, N. Engl. J. Med. 340 (1999) 1970 – 1980.

[3] C.A. Ross, M.A. Poirier, Protein aggregation and neurodegenerative disease, Nat Med. 10 (2004) S10 – S17.

[4] M.S. Forman, J.Q. Trojanowski, V.M. Lee, Neurodegenerative diseases: a decade of discoveries paves the way for therapeutic breakthroughs, Nat Med 10 (2004) 1055 – 63.

[5] D.M. Skovronsky, V.M. Lee, J.Q. Trojanowski, Neurodegenerative diseases: new concepts of pathogenesis and their therapeutic implications. Annu Rev Pathol 1 (2006) 151 – 170.

[6] S.B. Prusiner, M.D. Shattuck lecture: Neurodegenerative diseases and prions, N Engl J Med 344 (2001) 1516 – 1526.

[7] M. Shi, W. Michael Caudle, Jing Zhang. Biomarker Discovery in Neurodegenerative Diseases: A Proteomic Approach, Neurobiol Dis. 35 (2009) 157 – 164.

[8] L.C. Serpell, J.M. Smith, Direct visualization of the β-sheet structure of synthetic Alzheimer's amyloid, J Mol Biol. 299 (2000) 225 – 231.

[9] T. Mutoh, Y. Hirabayashi, T. Mihara, M. Ueda, H. Koga, A. Ueda, T. Kokura, and H. Yamamoto, Role of glycosphingolipids and therapeutic perspectives on Alzheimer's disease, CNS Neurol. Disord. Drug Targets. 5 (2010) 375 – 380.

[10] Q.X. Li, S.J. Fuller, K. Beyreuther, C.L. Master, The amyloid precursor protein of Alzheimer's disease in human brain and blood, J Leukoc Biol. 66 (1999) 567 – 574.

[11] D.L. Price, P.J. Whitehouse, R.G. Struble, A.W. C'lark, J.T. Coyle, M.R. De Long, J.C. Hedreen, Basal Forebrain Chohnergic Systems in Alzhelmer's Disease and Related Dementias, Neurosci Commun 1 (1982) 84 – 92.

[12] T. Arendt, V. Bigl, A. Arendt, A. Tennstedt, Loss of neurons in the nucleus basalis of Meynert in Alzheimer's disease, paralysis agitans and Korsakoff's disease, Acta Neuropath 61 (1983) 101 – 108.

[13] M.J. Ball, Neuronal loss, neurofibrillary tangles and granulovacuolar degeneration in the hippocampus with ageing and dementia, Acta Neuropath 37 (1977) 111 – 118.

[14] D.J. Selkoe, Normal and abnormal biology of the ß-amyyloid precursor protein, Annu. Rev. Neurosci. 17 (1994) 489 – 517.

[15] L.L. Iversen, R.J. Mortishire-Smith, S.J. Pollack, M.S. Shearman, The toxicity in vitro of beta-amyloid protein, Biochem. J. 311 (1995) 1 – 16.

[16] S.J. Fuller, E. Storey, Q.X. Li, A.L. Smith, K. Beyreuther, C.L. Masters, Intracellular production of ßA4 amyloid of Alzheimer’s disease: modulation by phosphoramidon and lack of coupling to the secretion of the amyloid precursor, Biochem. 34 (1995) 8091 – 8098.

[17] Q.-X. Li, S. Whyte, J.E. Tanner, G. Evin, K. Beyreuther, C.L. Masters,Secretion of Alzheimer’s disease Ab amyloid peptide by activated human platelets, Lab. Invest. 78 (1998) 461 – 469.

[18] P. Seubert, C. Vigo-Pelfrey, F. Esch, M. Lee, H. Dovey, D. Davis, S. Sinha, M. Schlossmacher, J. Whaley, C. Swindleshurst, R. McCormack, R. Wolfert, D. Selkoe, I. Lieberburg, D. Schenk, Isolation and quantification of soluble Alzheimer’s ß-peptide from biological fluids, Nature 359 (1992) 325 – 327.

[19] N. Suzuki, T.T. Cheung, X.D. Cai, A. Odaka, L. Otvos, C. Jr., Eckman, T.E. Golde, S.G. Younkin, An increased percentage of long amyloid ß protein secreted by familial amyloid b protein precursor (bAPP717) mutants, Science 264 (1994) 1336 – 13401.

[20] M.D. Cárdenas-Aguayo, L. Gómez-Virgilio , S. DeRosa, M.A. Meraz-Ríos, The Role of Tau oligomers in the onset of Alzheimer's disease neuropathology, ACS Chem. Neurosci. 5 (2014) 1178 – 1191.

[21] C. Haass, D.J. Selkoe, Soluble protein oligomers in neurodegeneration: lessons from the Alzheimer's amyloid ß-peptide, Nat. Rev. Mol. Cell Biol. 8 (2007) 101 – 112.

[22] S. Schedin-Weiss, B. Winblad, L.O. Tjernberg, The role of protein glycosylation in Alzheimer's disease, FEBS J. 281 (2014) 46 – 62.

[23] Y. Kizuka, S. Kitazume, R. Fujinawa, T. Saito, N. Iwata, T.C. Saido , M. Nakano, Y. Yamaguchi, Y. Hashimoto, M. Staufenbiel, H. Hatsuta, S. Murayama, H. Manya, T. Endo, N. Taniguchi, An aberrant sugar modification of BACE1 block its lysosomal targeting in Alzheimer's disease, EMBO Mol Med 7 (2015) 175 – 189.

[24] A.E. Lang, A.M. Lozano, Parkinson's disease. Second of two parts, N. Engl. J. Med. 339 (1998) 1130 – 1143.

[25] A.E. Lang, A.M. Lozano, Parkinson's disease. First of two parts, N. Engl. J. Med. 339 (1998) 1044 – 1053.

[26] L.S. Forno, Neuropathology of Parkinson's disease, J. Neuropathol. Exp. Neurol. 55 (1996) 259 – 272.

[27] T. Gasser, Genetics of Parkinson's disease, J. Neurol. 248 (2001) 833-840 in: C.A. Ross, M.A. Poirier, Protein aggregation and neurodegenerative disease, Nat Med. 10 (2004) S10 – S17.

[28] R.L. Nussbaum, M.H. Polymeropoulos, Genetics of Parkinson's disease, Hum. Mol. Genet. 6 (1997) 1687 – 1691.

[29] C.M. Tanner, R. Ottman, S.M. Goldman SM, J. Ellenberg, P. Chan, R. Mayeux, J.W. Langston, Parkinson disease in twins: an etiologic study, JAMA. 281 (1999) 341 – 346.

[30] T. M. Dawson, V.L. Dawsin, Rare genetic mutations shed light on the pathogenesis of Parkinson's disease, J. Clin. Invest 111 (2003) 145 – 151.

[31] A.D. Roses, Apolipoprotein E and Alzheimer's disease. The tip of the susceptibility iceberg, Ann. NY Acad. Sci. 855 (1998) 738 – 743.

[32] D. Afonso-Oramas, I. Cruz-Muros, D. Alvarez de la Rosa, P. Abreu, T. Giráldez, J. Castro-Hernández, J. Salas-Hernández, J.L. Lanciego, M. Rodríguez, T. González-Hernández, Dopamine transported glycosylation correlates with the vulnerability of midbrain dopaminergic cells in Parkinson's disease, Neurobiol Dis. 36 (2009) 494 – 508.

[33] M. DiFiglia, E. Sapp, K. O. Chase, S. W. Davies, G. P. Bates, J. P. Vonsattel, N. Aronin, Aggregation of huntingtin in neuronal intranuclear inclusions and dystrophic neurites in brain, Science 277 (1997) 1990 – 1993.

[34] A. H. Sharp, S. J. Loev, G. Schilling, S. H. Li, X. J. Li, J. Bao, M. V. Wagster, J. A. Kotzuk, J. P. Steiner, A. Lo, Widespread expression of Huntington's disease gene (IT15) protein product, Neuron 14 (1995) 1065 – 1074.

[35] G. Bates, Huntingtin aggregation and toxicity in Huntington's disease, Lancet 361 (2003) 1642 – 1644.

[36] S. H. Li, X. J. Li, Huntingtin - protein interactions and the pathogenesis of Huntington's disease, Trends Genet. 20 (2004) 146 – 154.

[37] L. Mangiarini, K. Sathasivam, M. Seller, B. Cozens, A. Harper, C. Hetherington, M. Lawton, Y. Trottier, H. Lehrach, S. W. Davies, G. P. Bates, Exon 1 of the HD gene with an expanded CAG repeat is sufficient to cause a progressive neurological phenotype in transgenic mice, Cell 87 (1996) 493 – 506.

[38] The Huntington's Disease Collaborative Research Group, A novel gene containing a trinucleotide repeat that is expanded and unstable on Huntington's disease chromosomes, Cell 72 (1993) 971 – 983.

[39] C. M. Ambrose, M. P. Duyao, G. Barnes, G. P. Bates, C. S. Lin, J. Srinidhi, S. Baxendale, H. Hummerich, H. Lehrach, M. Altherr, J. Wasmuth, A. Buckler, D. Church, D. Housman, M. Berks, G. Micklem, R. Durbin, A. Dodge, A. Read, J. Gusella, M.E. MacDonald, Structure and expression of the Huntington's disease gene: evidence against simple inactivation due to an expanded CAG repeat, Somat Cell Mol Genet. 20 (1994) 27 – 38.

[40] L. M. Morales, J. Estévez, H. Suárez, R. Villalobos, L. Chacín de Bonilla, E. Bonilla, Nutritional evaluation of Huntington disease patients, Am J Clin Nutr. 50 (1989) 145 – 150.

[41] A. Trejo, M. C. Boll, M. E. Alonso, A. Ochoa, L. Velasquez, Use of oral nutritional supplements in patients with Huntington's disease, Nutrition 21 (2005) 889 – 894.

[42] P. S. Harper, Huntington's disease, W. B. Saunders, London, 1991.

[43] F. Saudou, S. Finkbeiner, D. Devys, M.E. Greenberg, Huntingtin acts in the nucleus to induce Apoptosis but death does not correlate with the formation of Intranuclear Inclusions, Cell 95 (1998) 55 – 66.

[44] J. L. Price, D. L. Powers, E. T. Powers, J. W. Kelly, Glycosylation of the enhanced aromatic sequon is similarly stabilizing in three distinct reverse turn contexts, Proc Natl Acad Sci U S A 108 (2011) 14127 – 14132.

[45] R. Kleene, M. Schachner, Glycans and neural cell interactions, Nat Rev Neurosci. 5 (2004) 195 – 208.

[46] S.-I. Hakomori, Y. Zhang, Glycosphingolipid antigens and cancer therapy, Chem. Biol. 4 (1997) 97 – 104.

[47] Y. J. Chen, D. R. Wing, G. R. Guile, R. A. Dwek, D. J. Harvey, S. Zamze, Neutral *N*-glycans in adult rat brain tissue - complete characterization reveals fucosylated hybrid and complex structures, Eur. J. Biochem. 251(1998) 691 – 703.

[48] S. Zamze, D. J. Harvey, Y. J. Chen, G. R. Guile, R. A. Dwek, D. R. Wing, Sialylated *N*-glycans in adult rat brain tissue – awidespread distribution of disialylated antennae in complex and hybrid structures, Eur. J. Biochem. 258 (1998) 243 – 270.

[49] W. Chai, C. T. Yuen, H. Kogelberg, R. A. Carruthers, R. U. Margolis, T. Feizi, A. M. Lawson, High prevalence of 2-mono- and 2, 6-disubstituted manol-terminating sequences among *O*-glycans released from brain glycopeptides by reductive alkaline hydrolysis, Eur. J. Biochem. 263 (1999) 879 – 888.

[50] R. Barone, L. Sturiale, A. Palmigiano, M. Zappia, D. Garozzo, Glycomics of pediatric and adulthood diseases of the central nervous system, J Proteomics 75 (2012) 5123 – 5139.

[51] C. C. Chen, S. Engelborghs, S. Dewaele, N. Le Bastard, J. J. Martin, V. Vanhooren, C. Libert, P. P. De Deyn, Altered serum glycomics in Alzheimer's disease: A potential blood biomarker? Rejuvenation Res. 13 (2010) 439 – 444.

[52] V. Vanhooren, S. Dewaele, C. Libert, S. Engelborghs, P. P. De Deyn, O. Toussaint, F. Debacq-Chainiaux, M. Poulain, Y. Glupczynski, C. Franceschi, K. Jaspers, I. van der Pluijm, J. Hoeijmakers, C. C. Chen, Serum N-glycan profile shift during human aging, Exp Gerontol. 45 (2010) 738 – 743.

[53] S. J. North, S. Chalabi, M. Sutton-Smith, A. Dell, S. M. Haslam, Mouse and Human Glycomes, in Hand book of glycomics (Eds.: R. D. Cummings, J. M. Pierce), Academic Press, New York, 2009, pp. 263 – 327.

[54] A. K. Callesen, J. S. Madsen, W. Vach, T. A. Kruse, O. Mogensen, O. N. Jensen, Serum protein profiling by solid phase extraction and mass spectrometry: A future diagnostics tool? Proteomics 9 (2009) 1428 – 1441.

[55] K. L. Abbott, K. Aoki, J.-M. Lim, M. Porterfield, R. Johnson, R. M. O'Regan, L. Wells, M. Tiemeyer, M. Pierce, Targeted glycoproteomic identification of biomarkers for human breast carcinoma, J. Proteome Res. 7 (2008) 1470 – 1480.

[56] S. Srivastava, Move over proteomics, here comes glycomics, J. Proteome Res. 7 (2008) 1799.

[57] N. H. Packer, C.-W. Von der Lieth, K. F. Aoki-Kinoshita, C. B. Lebrilla, J. C. Paulson, R. Raman, P. Rudd, R. Sasisekharan, N. Taniguchi, W. S. York, Frontiers in glycomics:

Bioinformatics and biomarkers in disease. An NIH White Paper prepared from discussions by the focus groups at a workshop on the NIH campus, Proteomics 8 (2008) 8 – 20.

[58] P. Gagneux, A. Varki, Evolutionary considerations in relating oligosaccharide diversity to biological function, Glycobiology 9 (1999) 747 – 755.

[59] J. N. Arnold, R. Saldova, U. M. A. Hamid, P. M. Rudd, Evaluation of the serum N-linked glycome for the diagnosis of cancer and chronic inflammation, Proteomics 8 (2008) 3284−3293.

[60] S. A. Brooks, M. V. Dwek, U. Schumacher, Functional and Molecular Glycobiology, BIOS Scientific Publishers Limited, Oxford, U.K., 2002.

[61] H. Lis, N. Sharon, Protein glycosylation: Structural and functional aspects, Eur. J. Biochem. 218 (1993) 1 – 27.

[62] K. Lakshmi, K. M. Lara, Glycomics analysis: an array of technology, ACS Chem. Biol. *4* (2009) 715 – 732.

[63] A. Varki, J.B. Lowe, Biological roles of glycans, in Essential of Glycobiology (Eds. A. Varki, R.D. Cummings, J.D. Esko, H.H. Freeze, P. Stanley, C.R. Bertozzi, G.W. Hart, and M.E. Etzler, 2nd ed.), Cold Spring Habor Laboratory Press, Cold Spring Harbor, New York, 2009, pp. 75 – 88.

[64] R. Kannagi, N. A. Cochran, F. Ishigami, S. Hakomori, P. W. Andrews, B. B. Knowles, D. Solter, Stage-specific embryonic antigens (SSEA-3 and -4) are epitopes of a unique globo-series gangliosides isolated from human teratocarcinoma cells, EMBO J. 2 (1983) 2355 – 2361.

[65] J. B. Lee, J. M. Kim, S. J. Kim, J. H. Park, S. H. Hong, S. I. Roh, M. K. Kim, H. S. Yoon, Comparative characteristics of three human embryonic stem cell lines, Mol Cells. 19 (2005) 31 – 38.

[66] X.-E. Liu, L. Desmyter, C.-F. Gao, W. Laroy, S. Dewaele, V. Vanhooren , L. Wang, H. Zhuang, N. Callewaer, C. Libert, R. Contreras, C. Chen, N-glycomics changes in Hepatocellular carcinoma patients with liver cirrhosis induced by hepatitis B virus, Hepatology 46 (2007) 1426 – 1435.

[67] T. Kamiyama, H. Yokoo, J. Furukawa, M. Kurogochi, T. Togashi, N. Miura, K. Nakanishi, H. Kamachi, T. Kakisaka, Y. Tsuruga, A. Taketomi, S-I. Nishimura, S. Todo, Identification of novel serum biomarkers of hepatocellular carcinoma using glycomic analysis, Hepatology 57 (2013) 2314 – 2325.

[68] K. Nouso, M. Amano, K. Miyahara, M. Y. Ito, K. Miyahara, Y. Morimoto, H. Kato, K. Tsutsumi, T. Tomoda, N. Yamamoto, S. Nakamura, S. Kobayashi, K. Kuwaki, H. Hagihara, H. Onishi, Y. Miyake, F. Ikeda, H. Shiraha, A. Takaki, T. Nakahara, S-I. Nishimura, K. Yamamoto, Clinical utility of high-throughput glycome analysis in patients with pancreatic cancer, J. Gastroenterology 48 (2013) 1171 – 1179.

[69] K. Miyahara, K. Nouso, S. Saito, S. Hiraoka, K. Harada, S. Takahashi, Y. Morimoto, S. Kobayashi, F. Ikeda, Y. Miyake, H. Shiraha, A. Takaki, M. Amano, S.-I Nishimura, K. Yamamoto, Serum glycan markers for evaluation of disease activity and prediction of clinical course in patients with ulcerative colitis, PLOS ONE 8 (2013) e74861.

[70] M. Takeuchi, M. Amano, H. Kitamura, T. Tsukamoto, N. Masumori, K. Hirose, T. Ohashi, S-I. Nishimura, *N*- and *O*-glycome analysis of serum and urine from bladder cancer patients

using a high-throughput glycoblotting method, Journal of Glycomics & Lipidomics 3 (2013)108.

[71] J. Bones, S. Mittermayr, N. O'Donoghue, A. Guttman, P. M. Rudd, Ultra performance liquid chromatographic profiling of serum *N*-glycans for fast and efficient identification of cancer associated alterations in glycosylation, Anal Chem. 82 (2010) 10208 – 10215.

[72] A. Pierce, R. Saldova, U. M. Abd Hamid, J. L. Abrahams, E. W. McDermott, D. Evoy, M. J. Duffy, P. M. Rudd, Levels of specific glycans significantly distinguish lymph node-positive from lymph node-negative breast cancer patients, Glycobiology 20 (2010) 1283 – 1288.

[73] A. Knezevic, O. Gornik, O. Polasek, M. Pucic, I. Redzic, M. Novokmet, P. M. Rudd, A. F. Wright, H. Campbell, I. Rudan, G. Lauc, Effects of aging, body mass index, plasma lipid profiles, and smoking on human plasma *N*-glycans, Glycobiology 20 (2010) 959 – 969.

[74] M. Pucic, S. Pinto, M. Novokmet, A. Knezevic, O. Gornik, O. Polasek, L. Vlahovicek, W. Wang, P. M. Rudd, A. F. Wright, H. Campbell, I. Rudan, G. Lauc, Common aberrations from the normal human plasma *N*-glycan profile, Glycobiology 20 (2010) 970 – 975.

[75] R. Saldova, Y. Fan, J. M. Fitzpatrick, R. W. Watson, P. M. Rudd, Core fucosylation and alpha2-3 sialylation in serum *N*-glycome is significantly increased in prostate cancer comparing to benign prostate hyperplasia, Glycobiology 21 (2011) 195 – 205.

[76]. Y. J. Chen, D. R. Wing, G. R. Guile, R. A. Dwek, D. J. Harvey, S. Zamze, Neutral *N*-glycans in adult rat brain tissue - complete characterization reveals fucosylated hybrid and complex structures, Eur. J. Biochem. 251(1998) 691 – 703.

[77] G.M. McKhann, D.S. Knopman, H. Chertkow, B.T. Hyman, C.R. Jack Jr, C.H. Kawas, W.E. Klunk, W.J. Koroshetz, J.J. Manly, R. Mayeux, R.C. Mohs, J.C. Morris, M.N. Rossor, P.

Scheltens, M.C. Carrillo, B. Thies, S. Weintraub, C.H. Phelps, The diagnosis of dementia due to Alzheimer's disease: recommendations from the National Institute on Aging-Alzheimer's Association workgroups on diagnostic guidelines for Alzheimer's disease, Alzheimers Dement. 7(2011) 263 – 269.

[78] S. Lehmann, A. Gabelle, C. Paquet, Can we rely on of ratios of cerebrospinal fluid biomarkers for AD biological diagnosis? DOI: http://dx.doi.org/10.1016/j.jalz.2014.09.003. Alzheimer's Dementia (2014) 1-2 Published online: November 15, 2014.

[79] S.-I. Nishimura, K. kiikura, M. Kurogochi, T. Masushita, M. Fumoto, H. Hinou, R. kamitani, H. Nakagawa, K. Deguchi, N. Miura, K. Monde, H. Konde, High-throughput protein glycomics: Combined use of chemoselective glycoblotting and MALDI-TOF/TOF mass spectroscopy, Angewu.Chem. Int.Ed. 44 (2005) 91 – 96.

[80] Y. Miura, M. Hato, Y. Shinohara, H. Kuramoto, J.-i. Furukawa, M. Kurogochi, H. Shimaoka, M. Tada, K. Nakanishi, M. Ozaki, S. Todo, S.-I. Nishimura, BlotGlycoABC™, an integrated glycoblotting technique for rapid and large scale clinical glycomics, Mol. Cell. Proteomics 7 (2008) 370 – 377.

[81] J.-i. Furukawa, Y. Shinohara, H. Kuramoto, Y. Miura, H. Shimaoka, M. Kurogochi,M. Nakano, S.-I. Nishimura, Comprehensive approach to structural and functional glycomics based on chemoselective glycoblotting and sequential tag conversion, Anal. Chem. 80 (2008) 1094 – 1101.

[82] Y. Kita, Y. Miura, J.-i. Furukawa, M. Nakano, Y. Shinohara, M. Ohno, A. Takimoto, S.-I. Nishimura, Quantitative glycomics of human whole serum glycoprotein based on the standardized protocol for librating *N*-glycans, Mol. Cell. Proteomics 6 (2007) 1437 – 1445.

[83] M. Amano, M. Yamaguchi, Y. Takegawa, T. Yamashita, M. Terashima, J.-i. Furukawa, Y. Miura, Y. Shinohara, N. Iwasaki, A. Minami, S.-I. Nishimura, Threshold in in stage-specific embryonic glycotypes uncovered by a full portrait of dynamic *N*- glycan expression during cell proliferation, Mol. Cell. Proteomics 9 (2010) 523 – 537.

[84] Y. Miura, K. Kato, Y. Takegawa, M. Kurogochi, J.-i. Furukawa, Y. Shinohara, N. Nagahori, M. Amano, H. Hinou, S.-I. Nishimura, Glycoblotting – assisted O- glycomics: Ammonium carbamate allows for highly efficient release from glycoproteins, Anal. Chem. 82 (2010) 10021 – 10029.

[85] N. Nagahori, M. Abe, S.-I. Nishimura, Structural and functional glycosphingolipids by glycoblotting with aminonooxy-funcionalized gold nanaoparticles, Biochemistry 48 (2009) 583 – 594.

[86] S. Hatakeyama, M. Amano, Y. Tobisawa, T. Yoneyama, N. Tsuchiya, T. Habuchi, S-I. Nishimura, C. Ohyama, Serum *N*-glycan alteration associated with renal cell carcinoma detected by high-throughput glycan analysis, J. Urol. 191 (2014) 805 – 831.

[87] K. Hirose, M. Amano, R. Hashimoto, Y.C. Lee, S.-I. Nishimura, Insight into glycan diversity and evolutionary lineage based on comparative Avio-N-glycomics and sialic acid analysis of 88 Egg Whites of Galloanserae, Biochemistry 50 (2011) 4757 – 4774.

[88] H. J. An, S.R. Kronewitter, M.L. de Leoz, C. B. Lebrilla, Glycomics and disease markers, Curr Opin Chem Biol. 13 (2009) 601 – 607.

[89] S. A. Brooks, D. M. Hall, Lectin histochemistry to detect altered glycosylation in cells and tissues, Methods Mol Biol. 878 (2012) 31 – 50.

Chapter 2

N-Glycomics of Neurodegenerative Diseases

2.1. Introduction

The glycosylation process is the most prevalent form of post-translational modifications of proteins in more highly evolved organisms. *N*-glycosylation is the attachment of an oligosaccharide chain via the amide group of an Asn residue present in the tripeptide consensus sequence – Asn-X-Thr/Ser (where X can be any amino acid except Pro). Each glycosylated site may contain many different glycan structures, viz., oligomannose, in which only mannose residues are attached to the core (Manα1-6(Manα1-3)Manß1-4GlcNAcß1-4GlcNAcß1-Asn-X-Ser/Thr); complex, in which "antenna" initiated by *N*-acetylglucosaminetransferases (GlcNAcTs) are attached to the core; and hybrid, in which only mannose residues are attached to the Manα1-6 arm of the core and one or two antennae are on the Manα1-3 arm [1,2] (Figure 2.1).

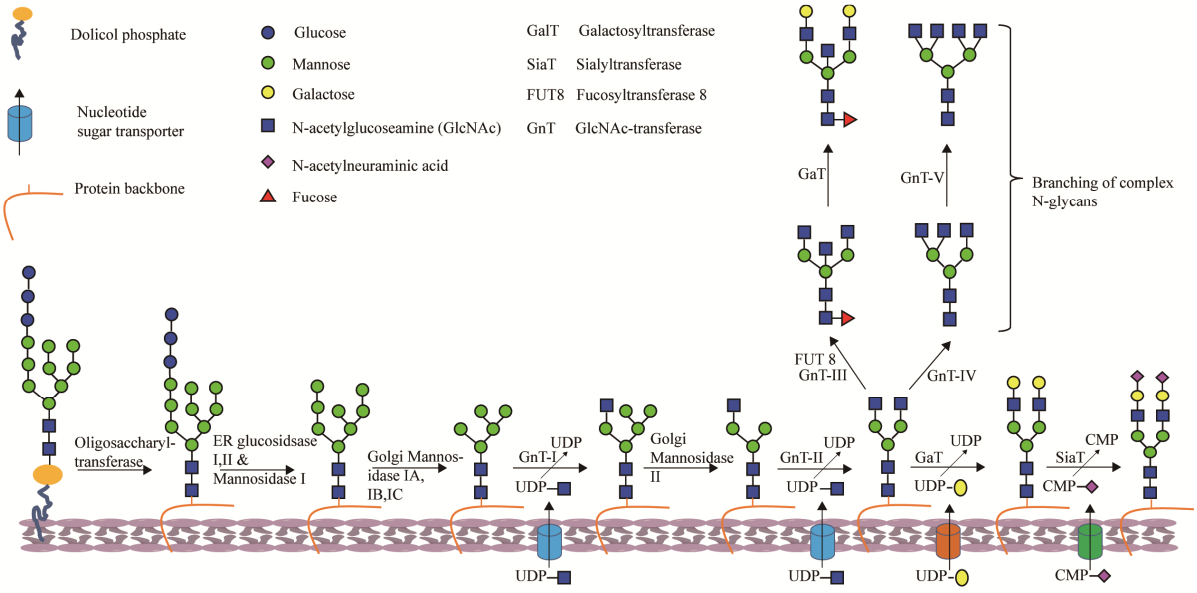

Figure 2.1. *N*-glycan processing in endoplasmic reticulum and Golgi apparatus.

Both chemical and enzymatic methods can be used for the release of *N*-glycans. An hydrous hydrazine can release unreduced *N*-linked glycans from glycoproteins. This approach suffers from the loss of information relating to the protein since the peptide bonds are destroyed; the acyl groups are cleaved from the *N*-acylamino sugars and sialic acids, calling for the reacetylation step, assuming that the sialic acid residues were originally acetylated; and small amount of *O*-acetyl substitution during the reacetylation step. As a result, it's preferable to apply enzymatic methods for the release of *N*-glycans. The most popular one is peptide *N*-glycosidase F (PNGase F), which cleaves the intact glycan chains as glycosylamine and readily converted into reducing glycans. With few exceptions (*N*-glycans with certain modifications of the *N*-glycan core found only in slime molds, plants, insects, and parasites), PNGase F releases practically all protein-bound *N*-linked carbohydrates except those with fucose attached to the 3 position of the Asn-linked GlcNAc residue [3]. Human and mice N-glycomes are not only play roles for communication of cell-cell, cell-antigen and cell-protein/hormones but also differentiate site-specific glycosylation [4].

Glycomics, as defined in chapter 1, is the comprehensive study of all of the carbohydrate structures produced by a defined system. This can be performed at the whole organism or an individual cell or tissue type. In chapter 2, I discuss about *N*-glycan analysis of the brain tissues, sera and CSF of neurodegenerative diseases. Strategically, I designed *N*-glycomics comprising extraction of glycoproteins of the brain tissues, sera and CSF. Briefly, acetone precipitated proteins (in case of brain homogenates and CSF) and sera were solubilized, reduced and alkylated. Preparation of tryptic digested glycopeptides facilitates the release of *N*-glycans by means of PNGase F digestion. The *N*-glycans released applied to glycoblotting process [5-7],

viz., released glycans were selectively captured onto high density hydrazide beads (BlotGlyco® H) for highly efficient purification of oligosaccharide, on-bead methyl esterification to stabilized sialic acid(s) for the simultaneous qunatitation of neutral and sialylated oligosaccharides by MALDI-TOF/MS, and the oliogosaccharides were finally recovered as BOA or aoWR derivatives via imine exchange that enabled high sensitive and quantitative analysis by MALDI-TOF/MS.

For MALDI-TOF/MS analysis, the sample is co-crystallized with a 1:1 ratio to a low molecular weight matrix which absorbs at the wave length of the laser. The energy of the laser is first absorbed by the matrix molecules. Stimulated matrix molecules transfer their excess energy to the sample molecules and become ionized. For this reason, MALDI is a soft ionization method that produces predominantly molecular ions from the released glycans with little or no fragmentation. Consequently, MALDI-TOF/MS is the pre-eminent technique for screening complex mixtures of glycans from biological extracts, thereby revealing the types of glycans present [3]. The results of which were used to select target ions for further analysis by tandem TOF/TOF analysis, affording sequences that are informative about fragment ions, providing information concerning structural features, sequence positions and branching patterns (Figure 2.2). However, it should also be noted that, since MS-based analyses can provide only possible *N*-glycans by estimating sugar compositions predicted using known *N*-glycome database, further NMR-based structural characterization using synthetic standards may be necessary to determine precise structures with respect to stereochemistry and branching positions in the glycoside linkages.

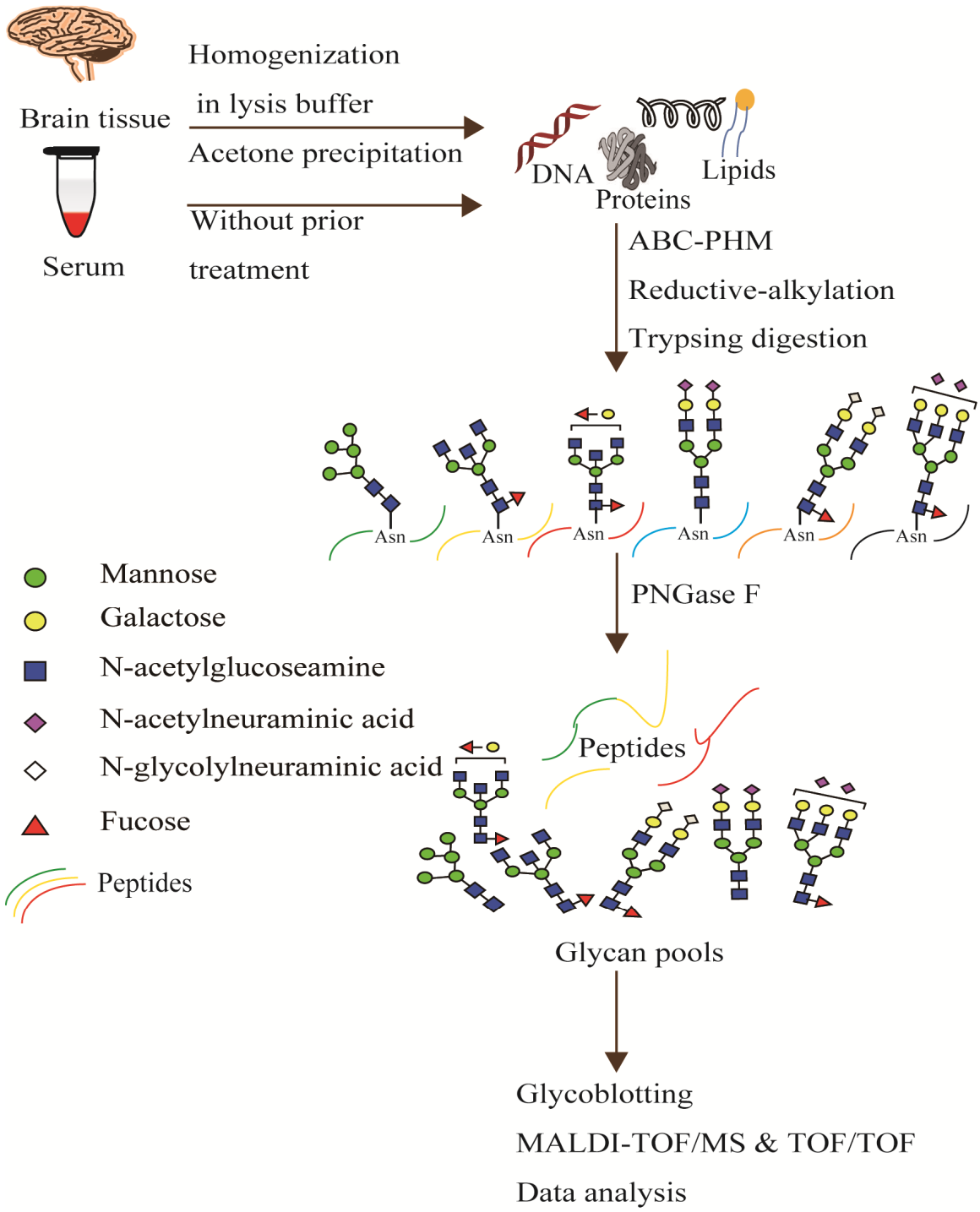

Figure 2.2. Schematic representation of *N*-glycomics.

2.2. Results

2.2.1. Brain Tissue *N*-Glycan Analysis of HD Transgenic and WT Mice

Using glycoblotting-based sample preparation combined with MALDI-TOF/MS analysis of brain total glycomes of HD transgenic (R6/2) and WT mice (BCF1), I could efficiently estimate the types of *N*-glycan moieties. As a preliminary trial, I first analyzed the whole brain (20 mg randomly taken) of perfused and unperfused BCF1 mice to assess the dominant glycans present in the brain, enabling to established an in-house database, and to exclude the possible impingement of *N*-glycans from serum. While perfused males BCF1 (BCF1 ♂) and unperfused males BCF1 (BCF1 ♂) were found to have 240.71 ± 53.22 and 20.45 ± 7.26 pmoles, respectively, perfused females BCF1 (BCF1 ♀) and unperfused females BCF1 (BCF1 ♀) were found to have 591.07 ± 141.67 and 173.54 ± 39.45 pmoles, respectively ($p < 0.01$ for male and $p < 0.05$ for female mice). I have found significant difference in the amount of *N*-glycans in the perfused compared to the unperfused mouse brain tissues. Only trace amount of terminal sialic acid containing *N*-glycans were found in perfused mice as compared to the unperfused mice. Surprisingly, total *N*-glycan expression levels were found to be higher in female BCF1 mice as compared to males in both perfused and unperfused groups when the glycoblotting protocol was used directly for whole brain tissues in which the striatum and cortex had not been separated. I also found that the *N*-glycans intra-mice deviation was reduced in perfused mice relative to those of the unperfused mice As a result, I decided to select the perfused mouse brain tissues for total glycomics HD transgenic and control group mice.

I have estimated 75 and 78 *N*-glycans in the striatum and the cortex, respectively, in which 67 of those were common between the two. There were 9 striatum-specific [Peak no. 48, 52, 56, 63, 69, 74,78, 83 & 84] and 11 cortex-specific [Peak no. 45, 47, 58, 72, 77, 80, 81, 82, 85, 86, 87] *N*-glycans. All 61 peaks in the striatum (80.3%) and 64 peaks in the cortex (82.1%) were reported in the GlycosuitDB (http://www.glycosuitdb.expassy.org/results) as summarized in Table 2.1. I determined, using database sample sources, that more than 85% of those *N*-glycans were sourced from the brain of the *M. Musculus* and *R. norvegicus* species.

A.

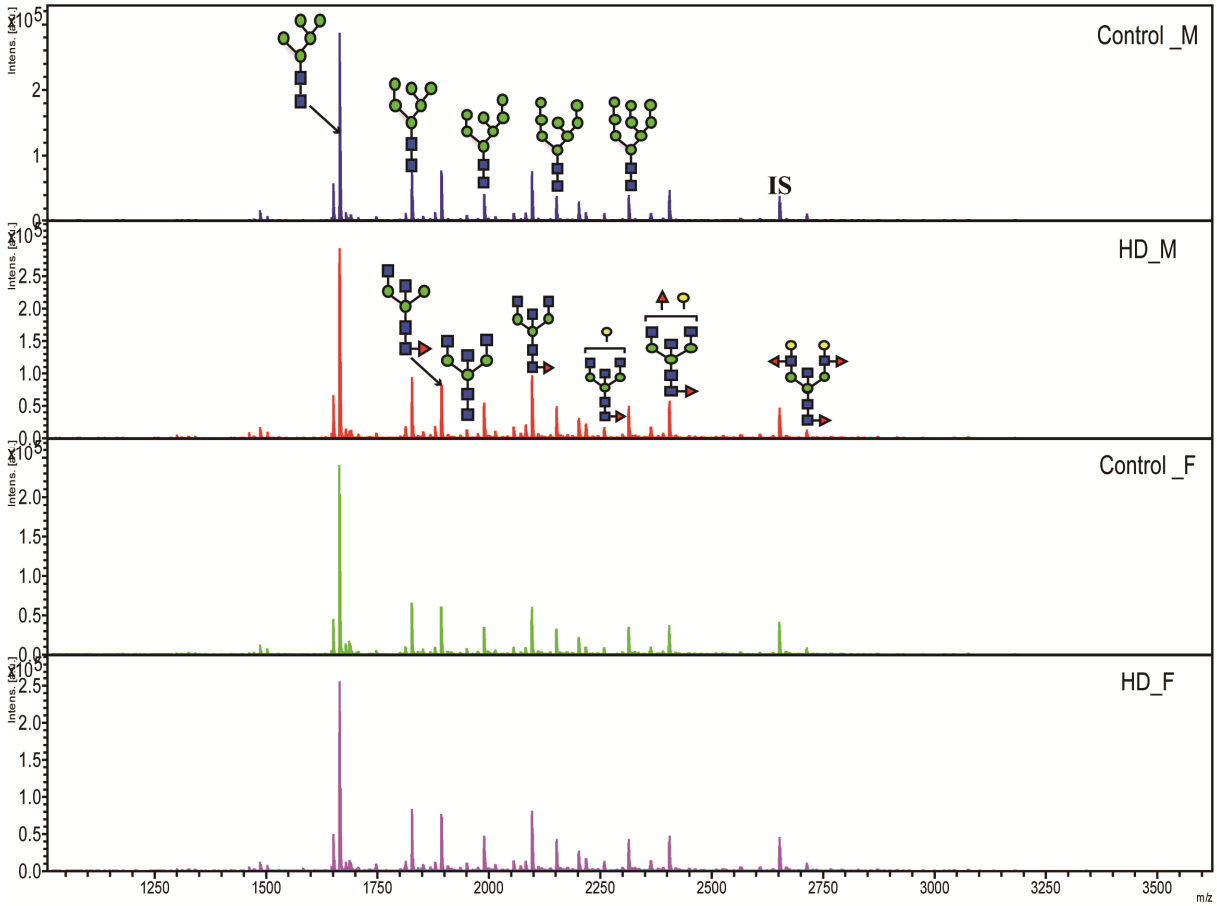

B.

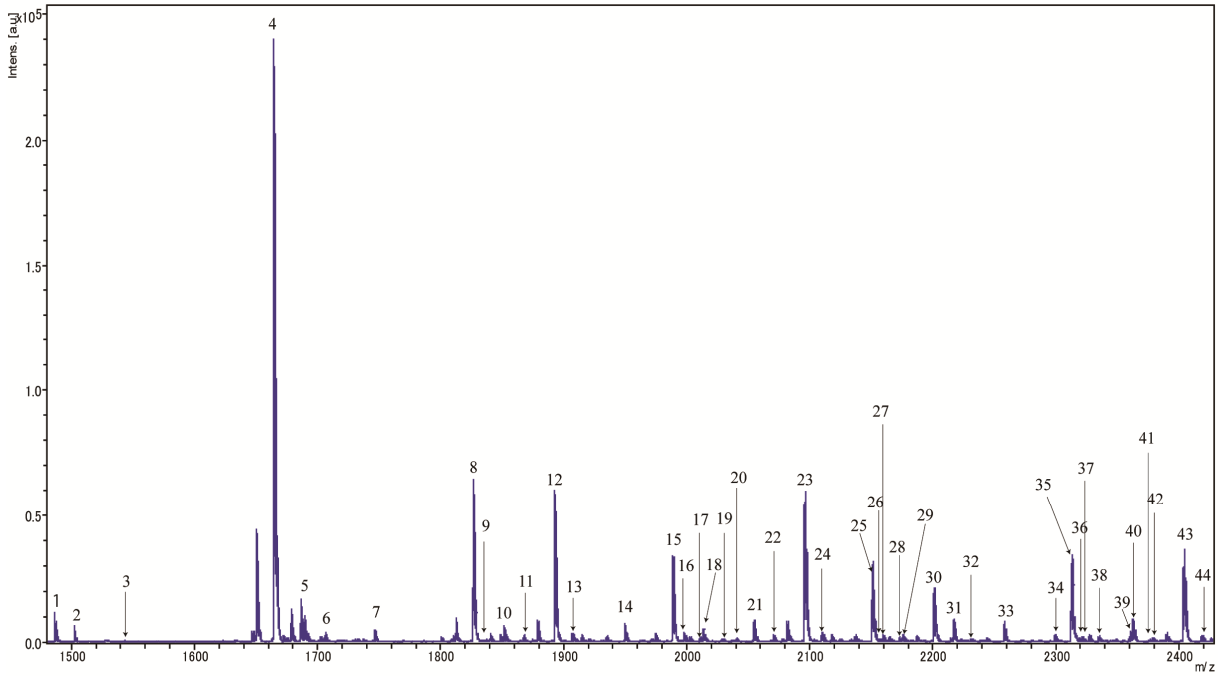

C.

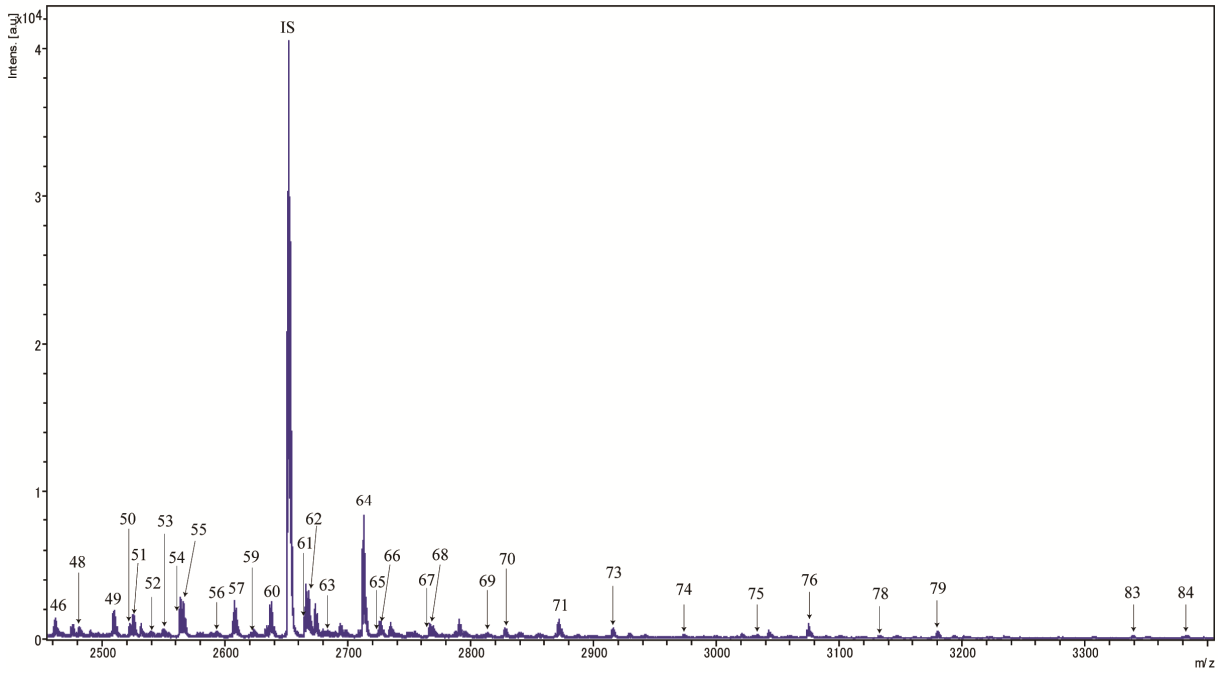

Figure 2.3. Representative MALDI-TOF/MS spectra of striatum *N*-glycans of HD transgenic and WT mice (IS indicates A2amide used as an internal standard, and n = 3 and N = 2 where n and N are number of the mouse and the experiment, respectively. M, male; F, female). B and C are shown the peak numbers in representative spectra of striatum *N*-glycans of HD transgenic and WT mice. Since 11 peaks [Peak no. 45, 47, 58, 72, 77, 80, 81, 82, 85, 86, and 87] were cortex specific and did not include them in the striatum spectra while all common *N*-glycans in striatum and cortex were assigned. Glycan cartoons were constructed using the standard Consortium for Functional nomenclature, i.e., blue square, *N*-acetylglucosamine; red triangle, fucose; green circle, mannose; and yellow circle, galactose.

Table 2.1. Estimated composition of *N*-glycans from striatum, cortex and serum of R6/2 and BCF1. These peaks are common to both the disease and control groups in this study. GlcNAc, *N*-acetylglucosamine; Man, Mannose; Deoxyhexose, fucose; HexNAc, *N*-acetylhexosamine (*N*-acetylglucosamine or *N*-acetylgalactosamine depends on the description); Hex, hexose (Mannose, glucose and galactose depend of the description); NeuAc, *N*-acetylneuraminic acid; and NeuGc, *N*-glycolylneuraminic acid. The asterisk (*) shows peak number 16 and 23 containing NeuGc that are detected only in serum, not in brain tissues.

Brain and serum Common *N*- glycans		Brain	Serum
Composition	ExPasy MW	Peak no.	Peak no.
(HexNAc)1 + (Man)3 (GlcNAc)2	1095.40	3	1
(Hex)2 + (Man)3 (GlcNAc)2	1216.42	4	2
(HexNAc)1 (Deoxyhexose)1 + (Man)3 (GlcNAc)2	1241.45	5	3
(Hex)1 (HexNAc)1 + (Man)3 (GlcNAc)2	1257.45	6	4
(Hex)3 + (Man)3 (GlcNAc)2	1378.48	8	5
(Hex)2 (HexNAc)1 + (Man)3 (GlcNAc)2	1419.50	11	6
(HexNAc)2 (Deoxyhexose)1 + (Man)3 (GlcNAc)2	1444.53	12	7
(Hex)1 (HexNAc)2 + (Man)3 (GlcNAc)2	1460.53	13	8
(Hex)4 + (Man)3 (GlcNAc)2	1540.53	15	9
(Hex)1 (HexNAc)1 (NeuAc)1 + (Man)3 (GlcNAc)2	1548.54	17	10
(Hex)1 (HexNAc)2 (Deoxyhexose)1 + (Man)3 (GlcNAc)2	1606.59	21	12
(Hex)2 (HexNAc)2 + (Man)3 (GlcNAc)2	1622.58	22	13
(HexNAc)3 (Deoxyhexose)1 + (Man)3 (GlcNAc)2	1647.61	23	14
(Hex)5 + (Man)3 (GlcNAc)2	1702.58	25	15
(Hex)2 (HexNAc)1 (NeuAc)1 + (Man)3 (GlcNAc)2	1710.60	28	16*
(Hex)1 (HexNAc)1 (Deoxyhexose)1 (NeuGc)1 + (Man)3 (GlcNAc)2	1710.60		
(Hex)2 (HexNAc)2 (Deoxyhexose)1 + (Man)3 (GlcNAc)2	1768.64	31	19
(Hex)1 (HexNAc)3 (Deoxyhexose)1 + (Man)3 (GlcNAc)2	1809.67	33	20
(Hex)6 + (Man)3 (GlcNAc)2	1864.63	35	21
(Hex)2 (HexNAc)2 (NeuAc)1 + (Man)3 (GlcNAc)2	1913.68	41	23*
(Hex)1 (HexNAc)2 (Deoxyhexose)1 (NeuGc)1 + (Man)3 (GlcNAc)2	1913.68		
(Hex)1 (HexNAc)3 (Deoxyhexose)2 + (Man)3 (GlcNAc)2	1955.72	43	25
(Hex)2 (HexNAc)3 (Deoxyhexose)1 + (Man)3 (GlcNAc)2	1971.72	44	26
(HexNAc)4 (Deoxyhexose)2 + (Man)3 (GlcNAc)2	1996.75	45	27
(Hex)1 (HexNAc)4 (Deoxyhexose)1 + (Man)3 (GlcNAc)2	2012.75	46	28
(Hex)2 (HexNAc)2 (Deoxyhexose)1 (NeuAc)1 + (Man)3 (GlcNAc)2	2059.73	50	30
(Hex)3 (HexNAc)2 (NeuAc)1 + (Man)3 (GlcNAc)2	2075.73	52	31
(Hex)1 (HexNAc)3 (Deoxyhexose)3 + (Man)3 (GlcNAc)2	2101.78	53	32
(Hex)1 (HexNAc)4 (Deoxyhexose)2 + (Man)3 (GlcNAc)2	2158.80	57	34
(Hex)1 (HexNAc)4 (NeuAc)1 + (Man)3 (GlcNAc)2	2157.78	58	35
(Hex)2 (HexNAc)4 (Deoxyhexose)1 + (Man)3 (GlcNAc)2	2174.80	59	36
(Hex)2 (HexNAc)2 (Deoxyhexose)2 (NeuAc)1 + (Man)3 (GlcNAc)2	2205.79	62	37
(Hex)3 (HexNAc)2 (Deoxyhexose)1 (NeuAc)1 + (Man)3 (GlcNAc)2	2221.79	63	39
(Hex)2 (HexNAc)2 (Deoxyhexose)1 (NeuAc)2 + (Man)3 (GlcNAc)2	2350.83	70	46
(Hex)3 (HexNAc)4 (Deoxyhexose)3 (NeuAc)1 + (Man)3 (GlcNAc)2	2920.06	84	53

Brain specific *N*- glycans		Brain	
Composition	ExPasy MW	m/z	Peak no.
(Deoxyhexose)1 + (Man)3 (GlcNAc)2	1038.38	1486.6	1
(Hex)1 + (Man)3 (GlcNAc)2	1054.37	1502.6	2
(HexNAc)2 + (Man)3 (GlcNAc)2	1298.48	1746.7	7
(HexNAc)1 (Deoxyhexose)2 + (Man)3 (GlcNAc)2	1387.51	1835.8	9
(Hex)1 (HexNAc)1 (Deoxyhexose)1 + (Man)3 (GlcNAc)2	1403.51	1851.7	10
(HexNAc)3 + (Man)3 (GlcNAc)2	1501.56	1949.8	14
(Hex)1 (HexNAc)1 (Deoxyhexose)2 + (Man)3 (GlcNAc)2	1549.57	1997.8	16
(Hex)2 (HexNAc)1 (Deoxyhexose)1 + (Man)3 (GlcNAc)2	1565.56	2013.8	18
(Hex)3 (HexNAc)1 + (Man)3 (GlcNAc)2	1581.56	2029.8	19
(HexNAc)2 (Deoxyhexose)2 + (Man)3 (GlcNAc)2	1590.59	2038.8	20
(Hex)1 (HexNAc)3 + (Man)3 (GlcNAc)2	1663.61	2111.8	24
(Hex)1 (HexNAc)1 (Deoxyhexose)1 (NeuAc)1 + (Man)3 (GlcNAc)2	1694.60	2156.9	26
(Hex)3 (HexNAc)1 (Deoxyhexose)1 + (Man)3 (GlcNAc)2	1727.61	2175.9	29
(Hex)1 (HexNAc)2 (Deoxyhexose)2 + (Man)3 (GlcNAc)2	1752.64	2200.9	30
(Hex)3 (HexNAc)2 + (Man)3 (GlcNAc)2	1784.63	2232.9	32
(HexNAc)4 (Deoxyhexose)1 + (Man)3 (GlcNAc)2	1850.69	2298.9	34
(Hex)2 (HexNAc)1 (Deoxyhexose)1 (NeuAc)1 + (Man)3 (GlcNAc)2	1856.66	2318.9	36
(Hex)3 (HexNAc)1 (Deoxyhexose)2 + (Man)3 (GlcNAc)2	1873.67	2321.9	37
(Hex)3 (HexNAc)1 (NeuAc)1 + (Man)3 (GlcNAc)2	1872.65	2334.9	38
(Hex)1 (HexNAc)2 (Deoxyhexose)1 (NeuAc)1 + (Man)3 (GlcNAc)2	1897.68	2359.9	39
(Hex)2 (HexNAc)2 (Deoxyhexose)2 + (Man)3 (GlcNAc)2	1914.70	2362.9	40
(Hex)3 (HexNAc)2 (Deoxyhexose)1 + (Man)3 (GlcNAc)2	1930.69	2378.9	42
(Hex)7 + (Man)3 (GlcNAc)2	2026.69	2474.9	47
(Hex)3 (HexNAc)1 (Deoxyhexose)1 (NeuAc)1 + (Man)3 (GlcNAc)2	2018.71	2481.0	48
(Hex)2 (HexNAc)2 (Deoxyhexose)3 + (Man)3 (GlcNAc)2	2060.76	2509.0	49
(Hex)3 (HexNAc)2 (Deoxyhexose)2 + (Man)3 (GlcNAc)2	2076.75	2525.0	51
(Hex)1 (HexNAc)3 (Deoxyhexose)1 (NeuAc)1 + (Man)3 (GlcNAc)2	2100.76	2563.0	54
(Hex)2 (HexNAc)3 (Deoxyhexose)2 + (Man)3 (GlcNAc)2	2117.78	2566.0	55
(HexNAc)4 (Deoxyhexose)3 + (Man)3 (GlcNAc)2	2142.81	2591.0	56
(Hex)8 + (Man)3 (GlcNAc)2	2188.74	2637.0	60
(Hex)1 (HexNAc)5 (Deoxyhexose)1 + (Man)3 (GlcNAc)2	2215.82	2664.1	61
(Hex)2 (HexNAc)3 (Deoxyhexose)3 + (Man)3 (GlcNAc)2	2263.83	2712.1	64
(Hex)2 (HexNAc)3 (Deoxyhexose)1 (NeuAc)1 + (Man)3 (GlcNAc)2	2262.81	2725.1	65
(Hex)3 (HexNAc)3 (Deoxyhexose)2 + (Man)3 (GlcNAc)2	2279.83	2728.1	66
(Hex)1 (HexNAc)4 (Deoxyhexose)1 (NeuAc)1 + (Man)3 (GlcNAc)2	2303.84	2766.1	67
(Hex)2 (HexNAc)4 (Deoxyhexose)2 + (Man)3 (GlcNAc)2	2320.86	2769.1	68
(Hex)2 (HexNAc)2 (Deoxyhexose)3 (NeuAc)1 + (Man)3 (GlcNAc)2	2351.85	2814.1	69
(Hex)2 (HexNAc)3 (Deoxyhexose)2 (NeuAc)1 + (Man)3 (GlcNAc)2	2408.87	2871.1	71
(Hex)3 (HexNAc)3 (Deoxyhexose)3 + (Man)3 (GlcNAc)2	2425.89	2874.1	72
(Hex)2 (HexNAc)4 (Deoxyhexose)3 + (Man)3 (GlcNAc)2	2466.91	2915.2	73
(Hex)2 (HexNAc)2 (Deoxyhexose)2 (NeuAc)2 + (Man)3 (GlcNAc)2	2496.89	2973.2	74
(Hex)2 (HexNAc)3 (Deoxyhexose)1 (NeuAc)2 + (Man)3 (GlcNAc)2	2553.91	3030.2	75
(Hex)2 (HexNAc)4 (Deoxyhexose)2 (NeuAc)1 + (Man)3 (GlcNAc)2	2611.95	3074.2	76
(Hex)3 (HexNAc)4 (Deoxyhexose)3 + (Man)3 (GlcNAc)2	2628.97	3077.2	77
(Hex)2 (HexNAc)2 (Deoxyhexose)1 (NeuAc)3 + (Man)3 (GlcNAc)2	2641.93	3132.2	78
(Hex)3 (HexNAc)3 (Deoxyhexose)3 (NeuAc)1 + (Man)3 (GlcNAc)2	2716.98	3179.2	79

Brain specific *N*- glycans		Brain	
Composition	ExPasy MW	m/z	Peak no.
(Hex)3 (HexNAc)3 (Deoxyhexose)1 (NeuAc)2 + (Man)3 (GlcNAc)2	2715.96	3192.2	80
(Hex)2 (HexNAc)4 (Deoxyhexose)1 (NeuAc)2 + (Man)3 (GlcNAc)2	2756.99	3233.3	81
(Hex)2 (HexNAc)5 (Deoxyhexose)2 (NeuAc)1 + (Man)3 (GlcNAc)2	2815.03	3277.3	82
(Hex)3 (HexNAc)3 (Deoxyhexose)2 (NeuAc)2 + (Man)3 (GlcNAc)2	2862.02	3338.3	83
(Hex)3 (HexNAc)3 (Deoxyhexose)1 (NeuAc)3 + (Man)3 (GlcNAc)2	3007.06	3497.3	85
(Hex)4 (HexNAc)4 (Deoxyhexose)3 (NeuAc)2 + (Man)3 (GlcNAc)2	3373.21	3849.5	86
(Hex)4 (HexNAc)4 (Deoxyhexose)2 (NeuAc)3 + (Man)3 (GlcNAc)2	3518.25	4008.5	87

Serum specific *N*- glycans		Serum	
Composition	ExPasy MW	m/z	Peak no.
(Hex)1 (HexNAc)1 (NeuGc)1 + (Man)3 (GlcNAc)2	1564.54	1724.6	11
(Hex)2 (HexNAc)1 (NeuGc)1 + (Man)3 (GlcNAc)2	1726.59	1886.7	17
(Hex)1 (HexNAc)2 (NeuAc)1 + (Man)3 (GlcNAc)2	1751.62	1911.7	18
(HexNAc)5 + (Man)3 (GlcNAc)2	1907.71	2053.6	22
(Hex)2 (HexNAc)2 (NeuGc)1 + (Man)3 (GlcNAc)2	1929.67	2089.8	24
(Hex)2 (HexNAc)4 + (Man)3 (GlcNAc)2	2028.74	2174.7	29
(Hex)2 (HexNAc)2 (Deoxyhexose)1 (NeuGc)1 + (Man)3 (GlcNAc)2	2075.73	2235.8	31
(Hex)2 (HexNAc)3 (NeuAc)1 + (Man)3 (GlcNAc)2	2116.76	2276.8	33
(Hex)2 (HexNAc)2 (NeuAc)2 + (Man)3 (GlcNAc)2	2204.77	2378.8	38
(Hex)2 (HexNAc)2 (Deoxyhexose)2 (NeuGc)1 + (Man)3 (GlcNAc)2	2221.79	2381.9	39
(Hex)2 (HexNAc)2 (NeuAc)1 (NeuGc)1 + (Man)3 (GlcNAc)2	2220.77	2394.8	40
(Hex)4 (HexNAc)2 (NeuAc)1 + (Man)3 (GlcNAc)2	2237.78	2397.9	41
(Hex)3 (HexNAc)2 (Deoxyhexose)1 (NeuGc)1 + (Man)3 (GlcNAc)2	2237.78	2397.9	
(Hex)2 (HexNAc)2 (NeuGc)2 + (Man)3 (GlcNAc)2	2236.76	2410.9	42
(Hex)3 (HexNAc)3 (NeuAc)1 + (Man)3 (GlcNAc)2	2278.81	2438.9	43
(Hex)2 (HexNAc)3 (Deoxyhexose)1 (NeuGc)1 + (Man)3 (GlcNAc)2	2278.81	2438.9	
(Hex)2 (HexNAc)4 (NeuAc)1 + (Man)3 (GlcNAc)2	2319.84	2479.9	44
(Hex)4 (HexNAc)4 + (Man)3 (GlcNAc)2	2352.85	2498.9	45
(Hex)2 (HexNAc)2 (Deoxyhexose)1 (NeuAc)1 (NeuGc)1 + (Man)3 (GlcNAc)2	2366.83	2540.9	47
(Hex)2 (HexNAc)2 (Deoxyhexose)1 (NeuGc)2 + (Man)3 (GlcNAc)2	2382.82	2556.9	48
(Hex)3 (HexNAc)3 (Deoxyhexose)1 (NeuAc)1 + (Man)3 (GlcNAc)2	2424.87	2585.0	49
(Hex)3 (HexNAc)3 (NeuAc)1 (NeuGc)1 + (Man)3 (GlcNAc)2	2585.90	2760.0	50
(Hex)3 (HexNAc)4 (Deoxyhexose)1 (NeuAc)1 + (Man)3 (GlcNAc)2	2627.95	2788.1	51
(Hex)2 (HexNAc)2 (Deoxyhexose)3 (NeuAc)2 + (Man)3 (GlcNAc)2	2642.95	2817.0	52
(Hex)3 (HexNAc)3 (NeuGc)3 + (Man)3 (GlcNAc)2	2908.98	3097.1	54
(Hex)3 (HexNAc)3 (Deoxyhexose)1 (NeuAc)2 (NeuGc)1 + (Man)3 (GlcNAc)2	3023.05	3211.1	55
(Hex)3 (HexNAc)3 (Deoxyhexose)1 (NeuGc)3 + (Man)3 (GlcNAc)2	3055.04	3243.2	56
(Hex)5 (HexNAc)4 (NeuAc)2 + (Man)3 (GlcNAc)2	3097.09	3271.3	57
(Hex)6 (HexNAc)5 (Deoxyhexose)1 (NeuAc)2 + (Man)3 (GlcNAc)2	3608.28	3782.4	58
(Hex)5 (HexNAc)5 (Deoxyhexose)2 (NeuAc)1 (NeuGc)1 + (Man)3 (GlcNAc)2	3608.28	3782.4	
(Hex)4 (HexNAc)5 (Deoxyhexose)3 (NeuGc)2 + (Man)3 (GlcNAc)2	3608.28	3782.4	

From MALDI-TOF/MS analysis, I was able to estimate high mannose and complex types of *N*-glycans with the latter existing in bi-, tri-, and tetra-antennary forms, most of which are highly core-fucosylated and have bisecting-GlcNAc (Figure 2.3). Even though quantitatively small in the whole brain, sialylated *N*-glycans were also present with high amount in the cortex than in the striatum. Although Lewis^x (Le^x) and sialyl Lewis^x (sLe^x) structures should be considered from the compositional analysis, further structural characterization is needed to confirm the existence of these specific antigenic oligosacchardies. While terminal GalNAc (peak # 34, 45, 53, 56, 61, 68) also seem to exist, there was no direct evidence for the presence of NeuGc in HD transgenic and WT mice in the present sudy. I performed all glycomics experiments independently and at least two times. The molecular weights and estimated compositions of *N*-glycans of the brain tissue (striatum and cortex) and serum of the HD model and its control mice were tabulated in Table 2.1.

For quantitative analysis, the area of *N*-glycans detected in MS were normalized with a known concentration of IS (20 pmoles of A2amide, namely non-natural amidated A2 prepared originally in our laboratory). There were no significant differences in *N*-glycan expression levels in the striatum and cortex of HD transgenic and control group mice (Table 2.2). However, the groups differ with respect to a few *N*-glycans that were specific to brain regions and gender.

Table 2.2. Total glycome (pmole ± SD) of HD transgenic and control group mice based on protein concentration (100 µg proteins for *N*- and *O*-glycans and 100 µg protein equivalent of *GSL*-glycans) and 20 µL of digested serum of each sample.

		Control		HD	
Total glycomes	Sample	BCF1_♂	BCF1_♀	R6/2_♂	R6/2_♀
N - glycomes	Striatum	426.44 ± 4.98	404.71 ± 18.5	401.64 ± 15.48	379.99 ± 36.28
	Cortex	253.77 ± 58.73	241.32 ± 51.05	255.86 ± 29.62	264.15 ± 51.65
	Serum	306.65 ± 11.35	250.83 ± 10.98	246.90 ± 26.13	233.15 ± 34.62
O -glycomes	Striatum	247.83 ± 88.75	208.69 ± 82.94	354.33 ± 194.47	170.42 ± 81.36
	Cortex	148.10 ± 99.42	158.91 ± 66.72	170.83 ± 104.46	114.68 ± 36.35
	Serum	6.48 ± 3.63	3.60 ± 2.23	1.84 ± 0.53	2.21 ± 0.75
GSL -glycomes	Striatum	267.55 ± 35.53	436.93 ± 130.22	942.35 ± 124.96	472.72 ± 127.61
	Cortex	1433.72 ± 192.02	1110.77 ± 377.88	1185.54 ± 261.57	1839.34 ± 383.31
	Serum	325.84 ± 35.44	242.26 ± 58.10	198.78 ± 36.98	154.10 ± 49.87

2.2.1.1. Glycotyping Analysis of Brain Tissue *N*-Glycans

To facilitate the glycome profiling analysis and their changes between HD transgenic and control group mice, we applied the glycotyping (relative ratio of *N*-glycan types) analysis approach [8,9]. Here, I focused on the high mannose, fucosylated, bisecting and antennary types of complex *N*-glycan moieties. Typically, I found high mannose (>50%), core fucosylated (>28%), bisecting-GlcNAc (>35%) and biantennary (>32%) as major types of *N*-glycans in the striatum and cortex of R6/2 and BCF1 of both sexes. While the high mannose types were

decreased, those of core fucosylated, bisecting-GlcNAc and biantennary types of *N*-glycans were increased in the R6/2 compared to the BCF1, albeit these number statistically insignificant (Table 2.3). Using TOF/TOF analysis, possible major glycoforms were high mannose, core-fucosylated, biantennary and bisecting-GlcNAc types of *N*-glycans (Figure 2.4). Moreover, hybrid and complex types *N*-glycans with bisecting GlcNAc show unfragmented HexHexNAc and $Hex_2HexNAc_2$ (peak no. 7, 12, 14, 21, 23, 30) under the laser irradiation during the TOF/TOF analysis. This result might indicate that the bisecting-GlcNAc residue both found in the hybrid and complex type *N*-glycans contribute significantly to the stability of these *N*-glycans under high energy laser irradiation in the TOF/TOF fragmentation processes. Interestingly, it was also demonstrated that Golgi alpha-mannosidase, one of the key exoglycosidases in a general biosynthetic pathway of the hybrid and complex type *N*-glycans, cannot remove non-reducing Man residues of the key intermediates in the presence of the neighboring bisecting-GlcNAc residue [10]. It seems likely that interaction of this GlcNAc with outer-chain sugar residues as well as steric effect might be critical for such unique resistance observed both in the TOF/TOF and enzymatic fragmentation experiments.

A.

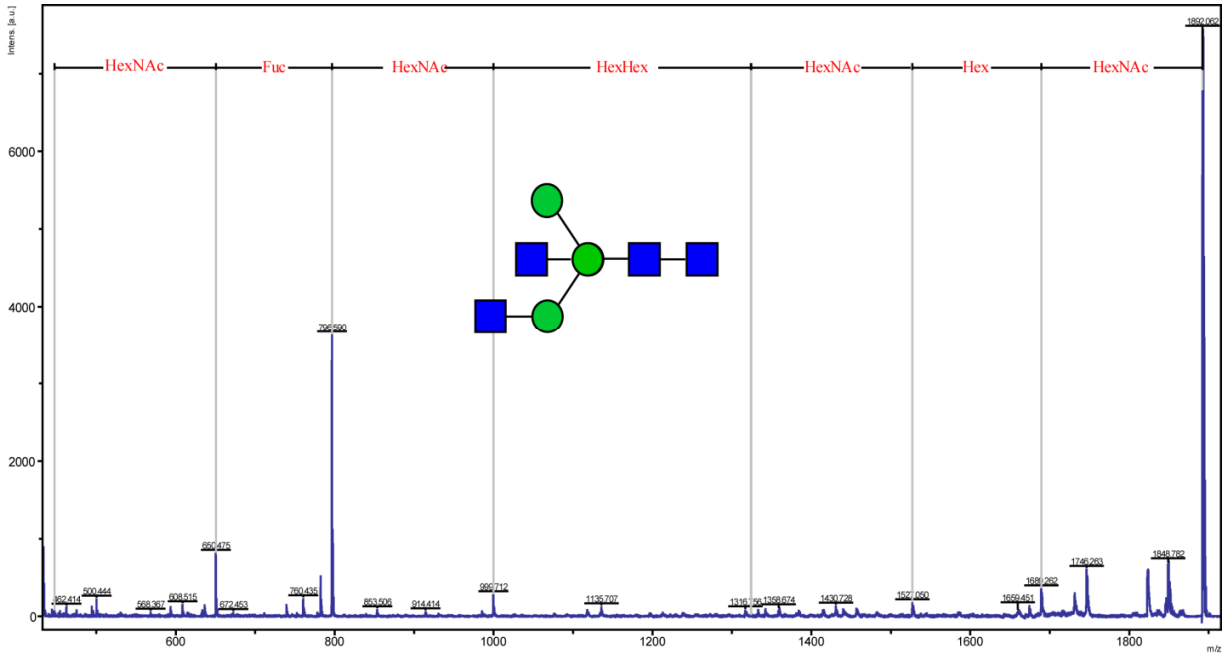
HexNAc
Fuc
HexNAc
HexHex
HexNAc
Hex
HexNAc
Intens. [a.u.]
m/z

B.

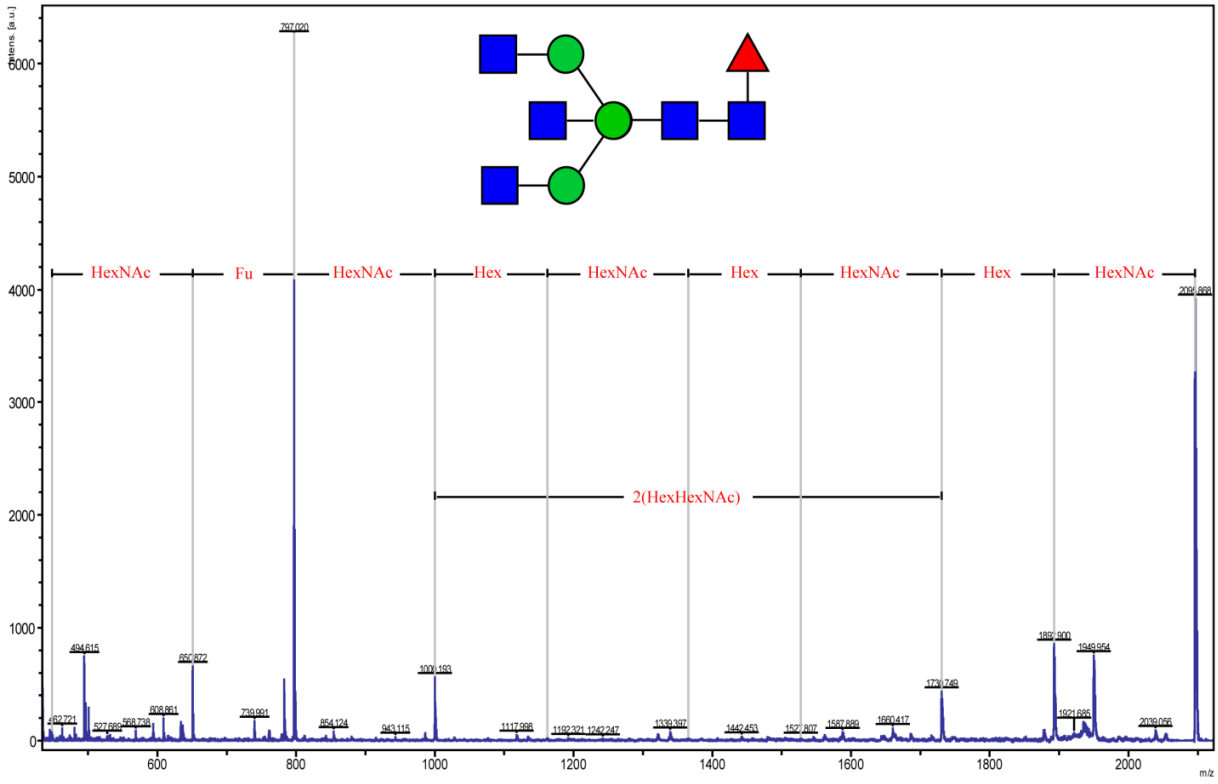
HexNAc
Fu
HexNAc
Hex
HexNAc
Hex
HexNAc
Hex
HexNAc
2(HexHexNAc)
Intens. [a.u.]
m/z

C.

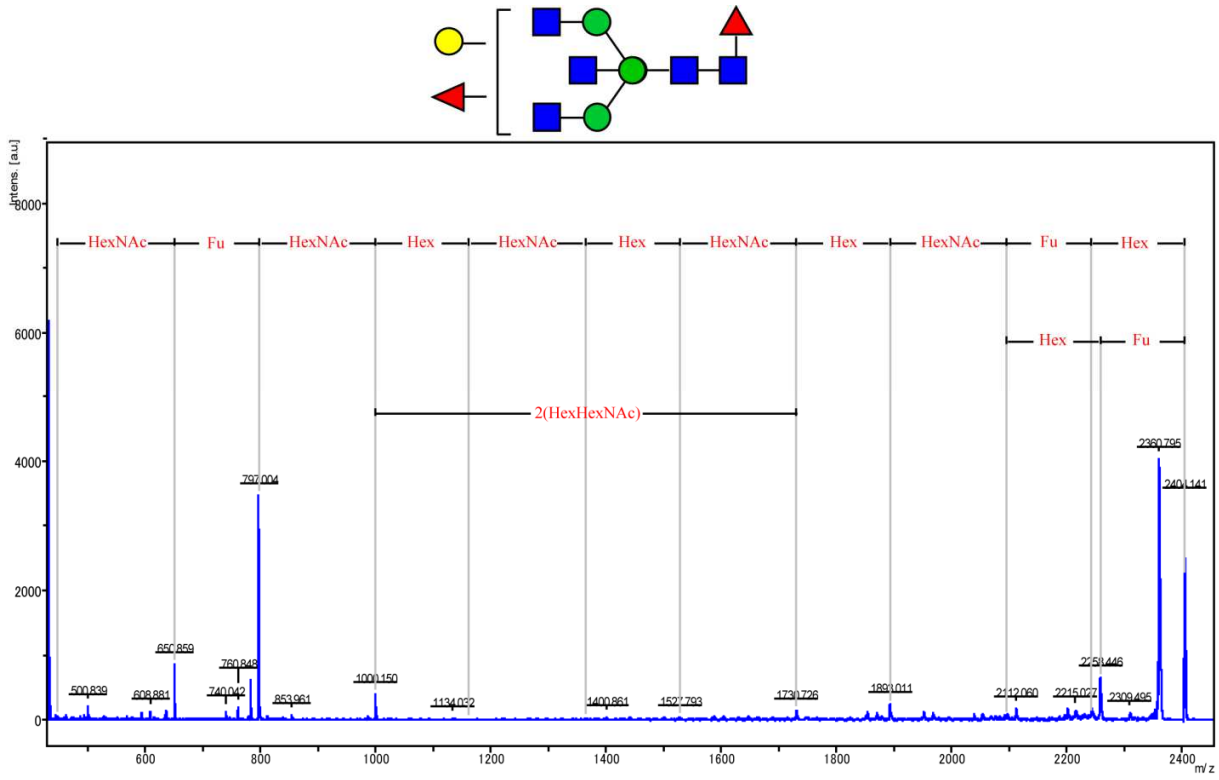

Figure 2.4. TOF/TOF Analysis of selective *N*- glycans in brain of both HD model mice and WT. A) m/z 1892.046, B) m/z 2095.075, and C) 2404.059. Glycan cartoons were constructed using the standard Consortium for Functional nomenclature, i.e., blue square, *N*-acetylglucosamine; red triangle, fucose; green circle, mannose; yellow circle, galactose.

Table 2.3. Glycotyping analysis (in %) of *N*-glycans of HD transgenic and WT mice.

		Striatum					Cortex			
Glycotype	No. peaks	BCF1_♂	BCF1_♀	R6/2_♂	R6/2_♀	No. peaks	BCF1_♂	BCF1_♀	R6/2_♂	R6/2_♀
High Mannose	7	53.9	56.0	49.6	49.8	7	51.4	50.3	48.3	49.3
Mono-Fucose	28	28.1	27.4	31.6	30.4	28	28.4	28.5	30.1	30.1
Di-Fucose	16	13.2	12.2	13.5	14.0	19	15.0	15.2	15.7	14.8
Tri-Fucose	9	1.6	1.2	1.4	1.7	8	1.9	2.0	2.1	1.8
Mono-Sialic acid	20	2.2	1.2	2.7	1.9	19	2.4	2.6	2.5	1.9
Di-Sialic acid	4	0.2	0.0	0.1	0.1	5	0.2	0.2	0.2	0.1
Bisect-GlcNAc	24	35.5	34.4	38.0	37.9	23	34.8	35.3	37.0	36.3
Bi-antennary	35	27.9	26.1	31.3	31.6	29	31.6	32.1	34.8	33.5
Tri-antennary	8	1.0	0.5	1.1	1.1	12	1.4	1.5	1.9	1.4
Tetra-antennary	2	0.2	0.2	0.3	0.4	6	0.4	0.4	0.5	0.5

2.2.1.2. Avidin-Biotin Complex Lectin Staining of Brain Tissue Sections

I applied avidin conjugated lectins specific to high mannose (ConA), core-fucosylated (LCH/LCA), bisecting-GlcNAc (PHA-E_4), LacNAc (DSA), terminal sialic acid (SNA) and non-sialylated T-antigen (PNA) to study the localization of glycoconjugates in brain tissue. Around the nucleus, I was able to observe the less intensely stained regions of the striatum and cortex of R6/2 by ConA (highly pronounced in male R6/2), the striatum of R6/2 ♂ and cortex of R6/2 ♀ by LCA, and both the striatum and cortex of R6/2 ♀ by PHA-E_4 as compared to those of WT mice. In addition, SNA and PNA staining both in the striatum and cortex confirmed the presence of the terminal sialic acid and *O*-glycans, respectively. In general, there were slight differences in the staining intensity with the lectins in the brain sections of HD transgenic and WT mice dependent on the total amount of *N*-glycans expression levels. However, the results stained by means of LCA and PHA-E4 did not support the specific glycoform alterations suggested by the

comprehensive glycomics described above, while the ConA staining clearly indicated significant changes found in *N*-glycan analysis (Figure 2.5). Conventional PAS approach appeared to give non-specific staining in all brain regions.

ConA BCF1♂ Around nucleus

100x striatum / cortex | 400x cortex | 400x striatum

+++ ++

ConA R6/2♂

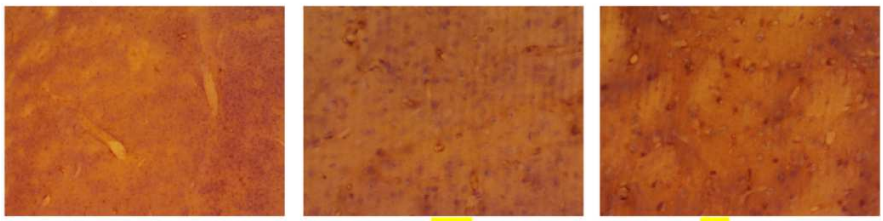

++ +

100x striatum / cortex | 400x cortex | 400x striatum

ConA BCF1♀

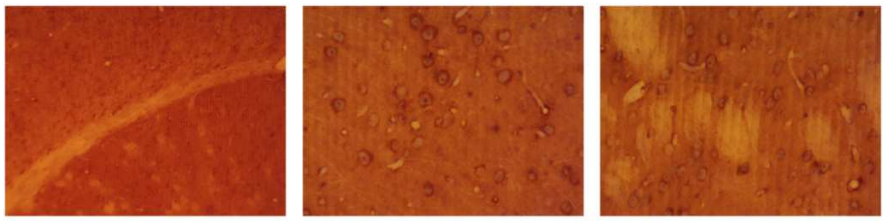

100x striatum / cortex | 400x cortex | 400x striatum

+++ ++

ConA R6/2♀

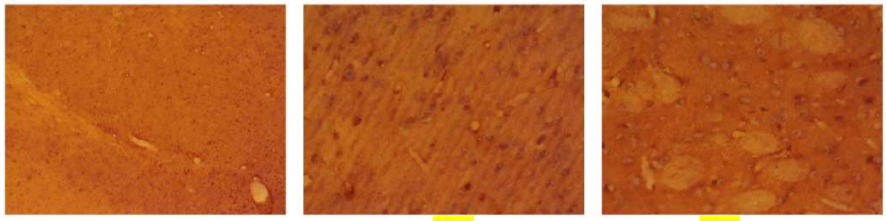

++ ++

100x striatum / cortex | 400x cortex | 400x striatum

LCA BCF1♂

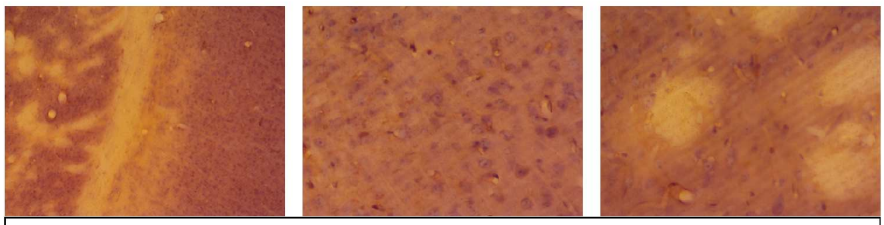

100x striatum / cortex	400x cortex	400x striatum
	++	++

LCA R6/2♂

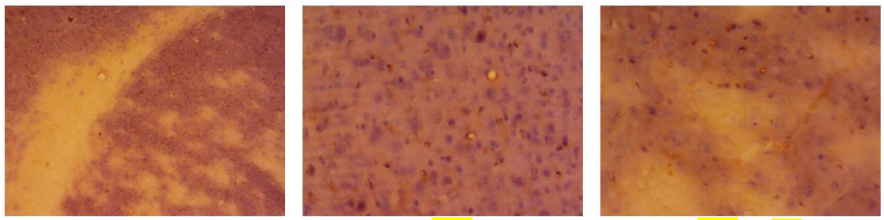

100x striatum / cortex	400x cortex	400x striatum
	++	++ → +

LCA BCF1♀

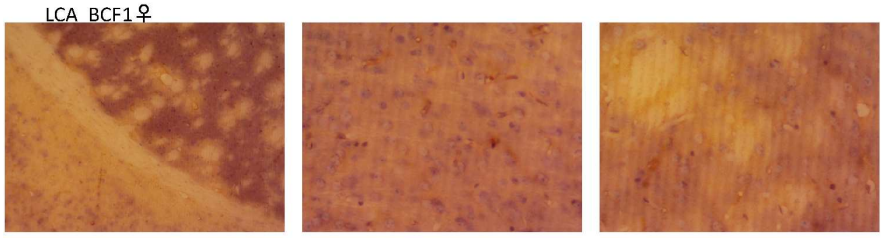

100x striatum / cortex	400x cortex	400x striatum
	++	++

LCA R6/2♀

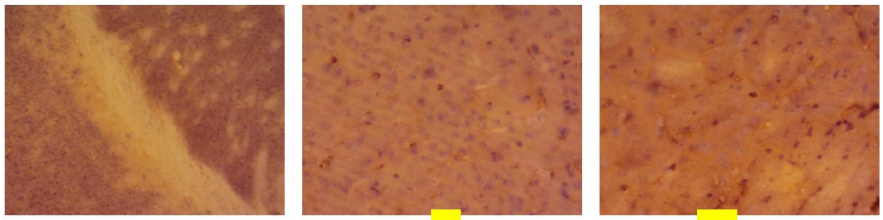

100x striatum / cortex	400x cortex	400x striatum
	+	++

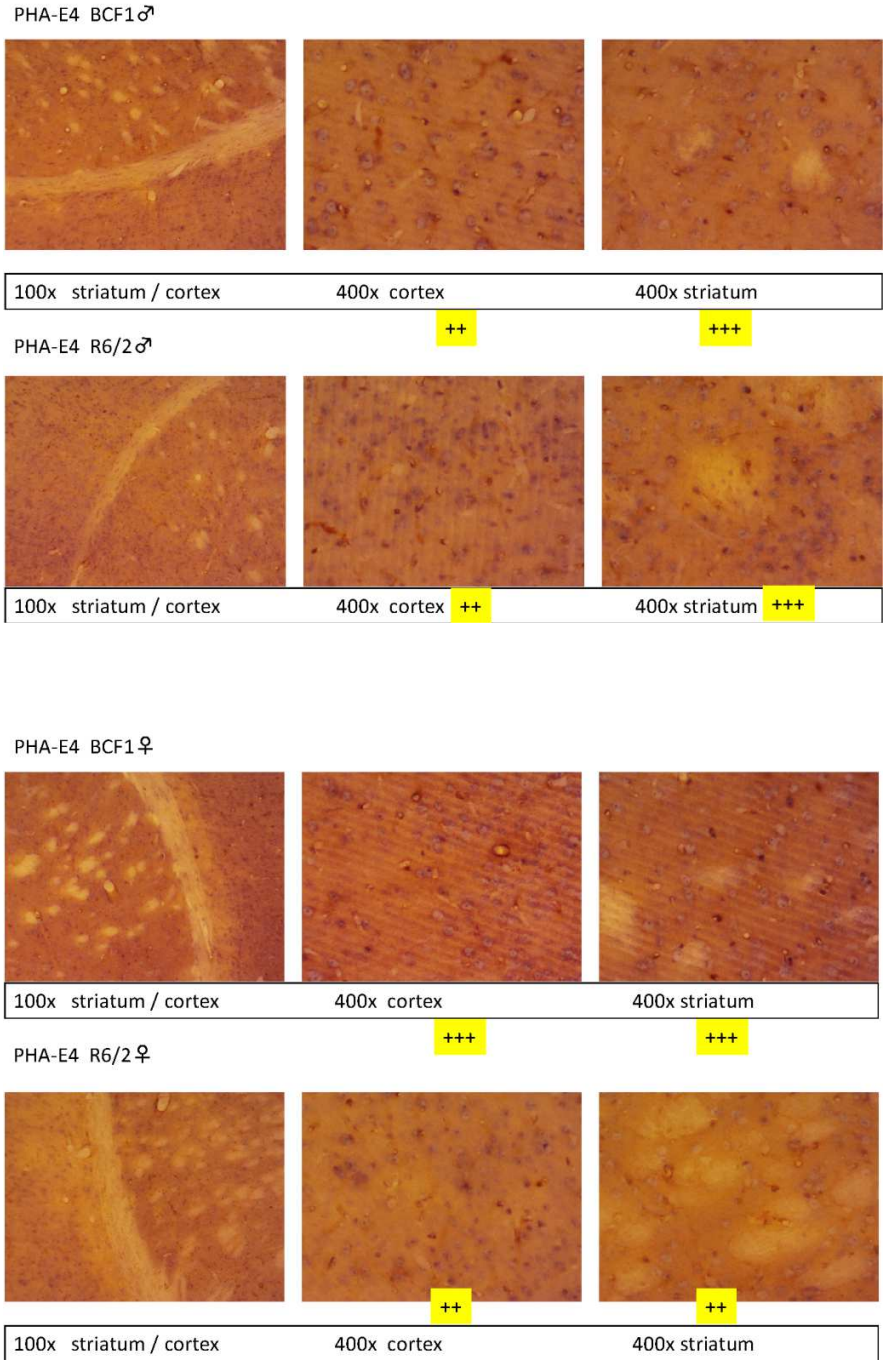

Figure 2.5. Lectin staining of striatum and cortex of R6/2 and BCF1 mice (each Avidin - conjugated lectins are specified on each slide). The signs indicated: +++, very strong stain; ++, strong stain; +, weak stain.

2.2.2. Serum *N*-Glycan Analysis of HD Transgenic and WT Mice

Towards the discovery of a potential glyco-biomarker for an easy diagnosis and therapy, I extended efforts to profile and quantify *N*-glycans from the sera of HD transgenic and WT mice (n=5, N=2, where n and N are the number of samples and experiments, respectively). As estimated, 58 (plus 8 with same m/z with different composition) *N*-glycans were found in serum, 51 peaks (85%) of which *N*-glycans were reported in the GlycosuitDB (http://www.glycosuitdb.expassy.org/results). All of the peaks (m/z) specific to serum and common with brain *N*-glycans composition are shown in Table 2.1 and peak numbers are shown in Figure 2.6 A and B.

A.

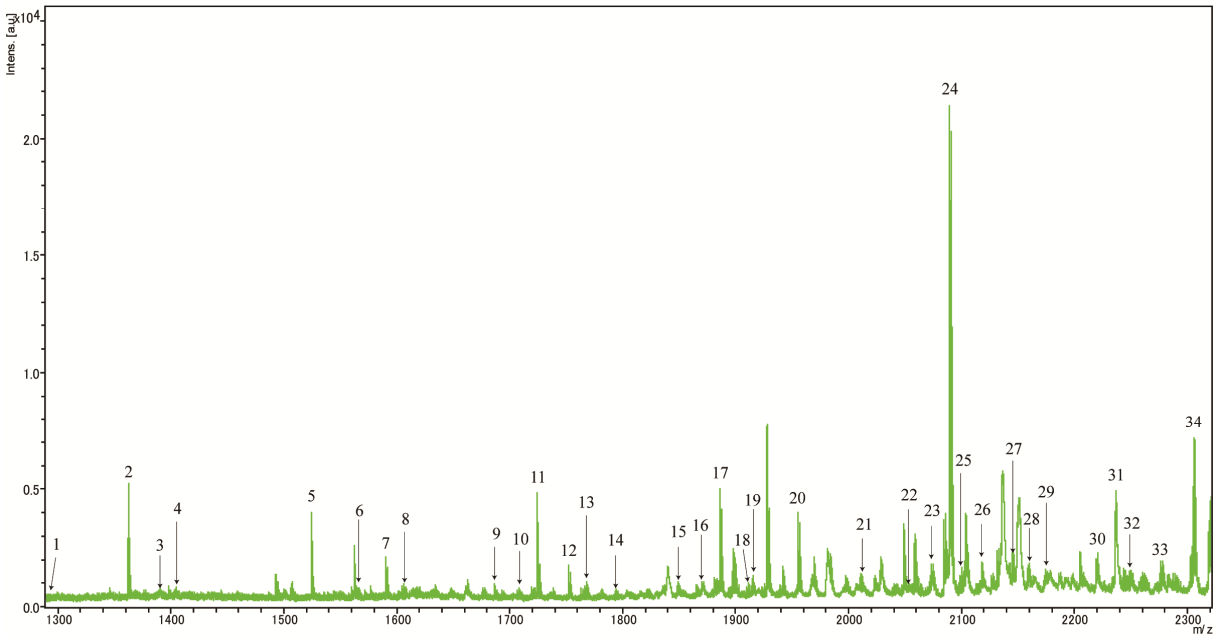

B.

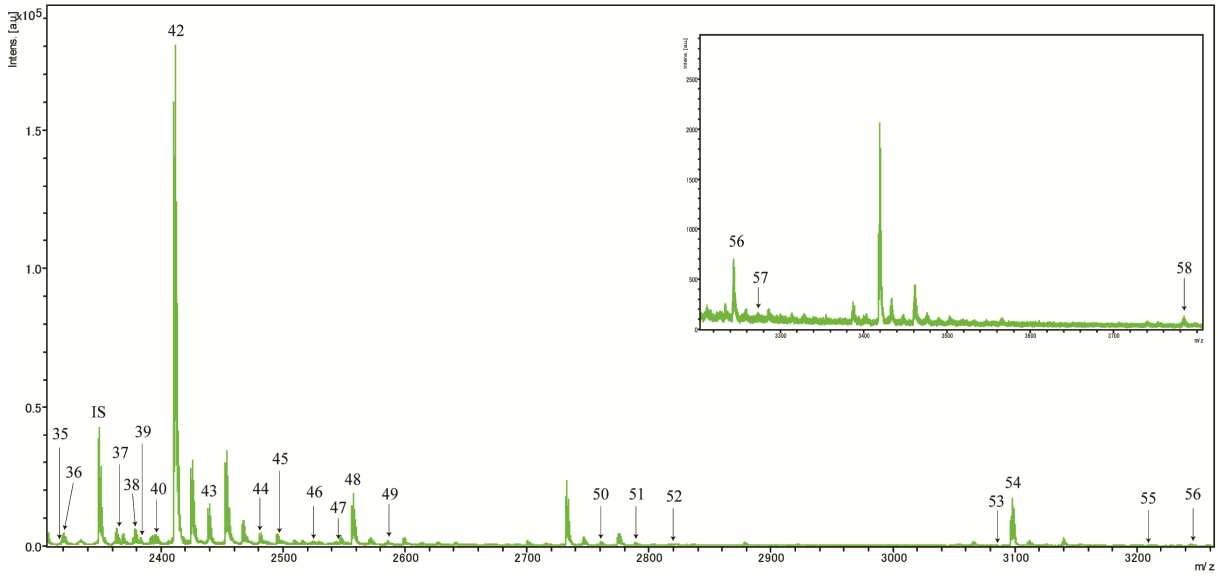
Intens. [a.u.]
x10^5
1.5
1.0
0.5
0.0
IS
35
36
37
38
39
40
42
43
44
45
46
47
48
49
50
51
52
53
54
55
56
2400
2500
2600
2700
2800
2900
3000
3100
3200
m/z
56
57
58

C.

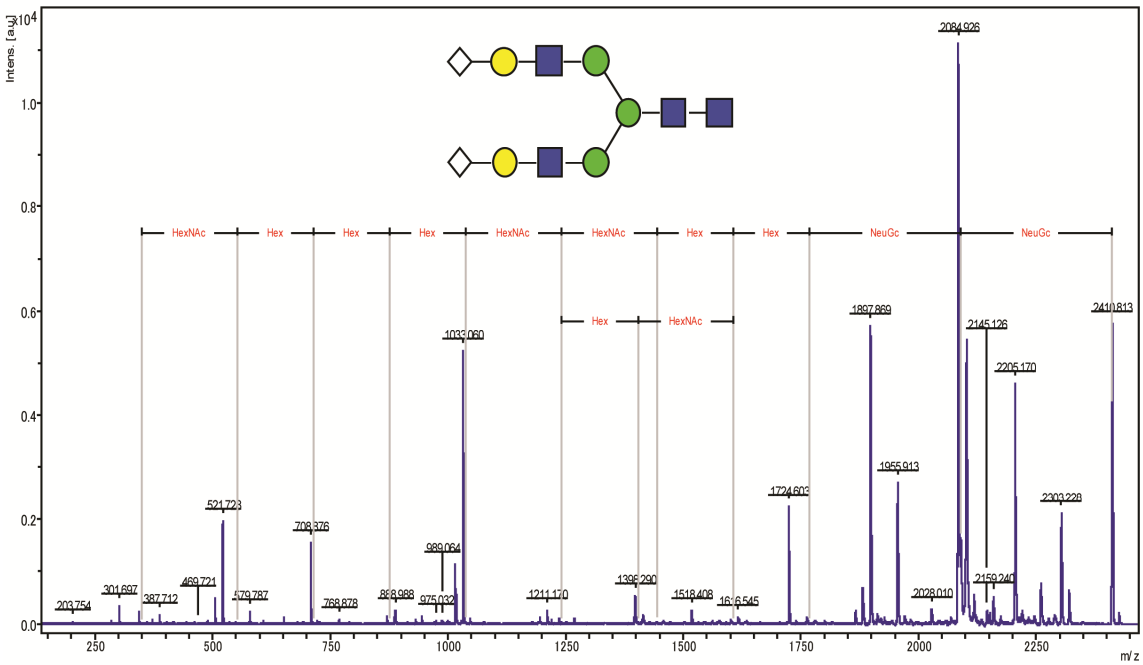
Intens. [a.u.]
x10^4
1.0
0.8
0.6
0.4
0.2
0.0
HexNAc
Hex
Hex
Hex
HexNAc
HexNAc
Hex
Hex
NeuGc
NeuGc
Hex
HexNAc
2084.926
1897.869
2411.813
2145.126
2205.170
1955.913
1724.609
2303.228
2159.240
2028.010
1033.060
989.064
975.032
1396.290
1518.408
1211.170
1616.545
868.988
768.878
708.376
521.723
469.721
387.712
301.697
203.754
250
500
750
1000
1250
1500
1750
2000
2250
m/z

Figure 2.6. A and B) Representative MALDI-TOF/MS spectra of serum *N*-glycans shown each peak numbers (compositioin shown in Table 2.1) of HD transgenic and WT mice (IS indicates A2amide used as an internal standard, and n = 5 and N = 2 where n and N are number of the mouse and the experiment, respectively). C) TOF/TOF analysis of the major peak in serum *N*-glycan analysis (peak# 47, m/z 2410.86). Glycan cartoons were constructed using the standard Consortium for Functional nomenclature, i.e., blue square, *N*-acetylglucosamine; red triangle, fucose; green circle, mannose; yellow circle, galactose; and white diamond, *N*-glycolylneuraminic acid.

Quantitatively, the amount of *N*-glycans released from the serum of R6/2 and BCF1 were shown in Table 2.4. *N*-glycans decreased in male and female HD transgenic mouse (with the female decrease being slightly less pronounced) as compared to the WT mice. I have selected few peaks that show a significant difference in *N*-glycan expression levels between HD transgenic and WT mice (Table 2.4). The largest peak in the serum *N*-glycan level (peak no. 42) was higher in the control group than in HD transgenic mice, and the peak of the core-fucosylated form of this glycan (peak no. 48) was higher for the HD transgenic mice. I specified peak no. 42 using TOF/TOF analysis (Figure 2.6). From glycotyping analysis, I have estimated that core-fucosylated *N*-glycans were higher in R6/2 than the control group mice (increased from 12.1 to 38.6% in male and 29.9 to 43.8% in female mice, Figure 2.7). Moreover, high levels of disialic acid (majority of *N*-glycolylneuraminic acid) containing biantennary type *N*-glycans were found in the HD transgenic and WT mice. However, the levels of high mannose and bisecting type *N*-glycans were small compared to those in the striatum and cortex of the same experimental mice.

Table 2.4. Selected peaks of *N*-glycans (pmole ± SD) from 10 μL serum of HD transgenic and control group mice. Glycan cartoons were constructed using the standard Consortium for Functional nomenclature, i.e., blue square, *N*-acetylglucosamine; red triangle, fucose; green circle, mannose; yellow circle, galactose; purple diamond, *N*-acetylneuraminic acid; and white diamond, *N*-glycolylneuraminic acid.

		Control		HD		
Peak No.	m/z	BCF1_♂	BCF1_♀	R6/2_♂	R6/2_♀	Structure
24	2089.75	16.62 ± 0.84	10.04 ± 1.09	8.85 ± 1.11	8.27 ± 0.96	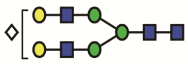
42	2410.06	205.83 ± 17.73	120.28 ± 6.50	98.80 ± 8.15	82.06 ± 9.14	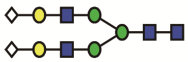
48	2556.93	16.85 ± 2.96	43.90 ± 3.23	63.21 ± 12.63	69.00 ± 13.48	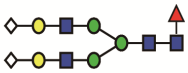
49	2584.98	0.68 ± 0.26	2.02 ± 0.86	3.29 ± 1.37	4.24 ± 1.66	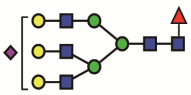
54	3097.12	13.89 ± 2.44	7.40 ± 0.93	5.29 ± 1.52	3.99 ± 0.98	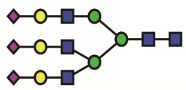

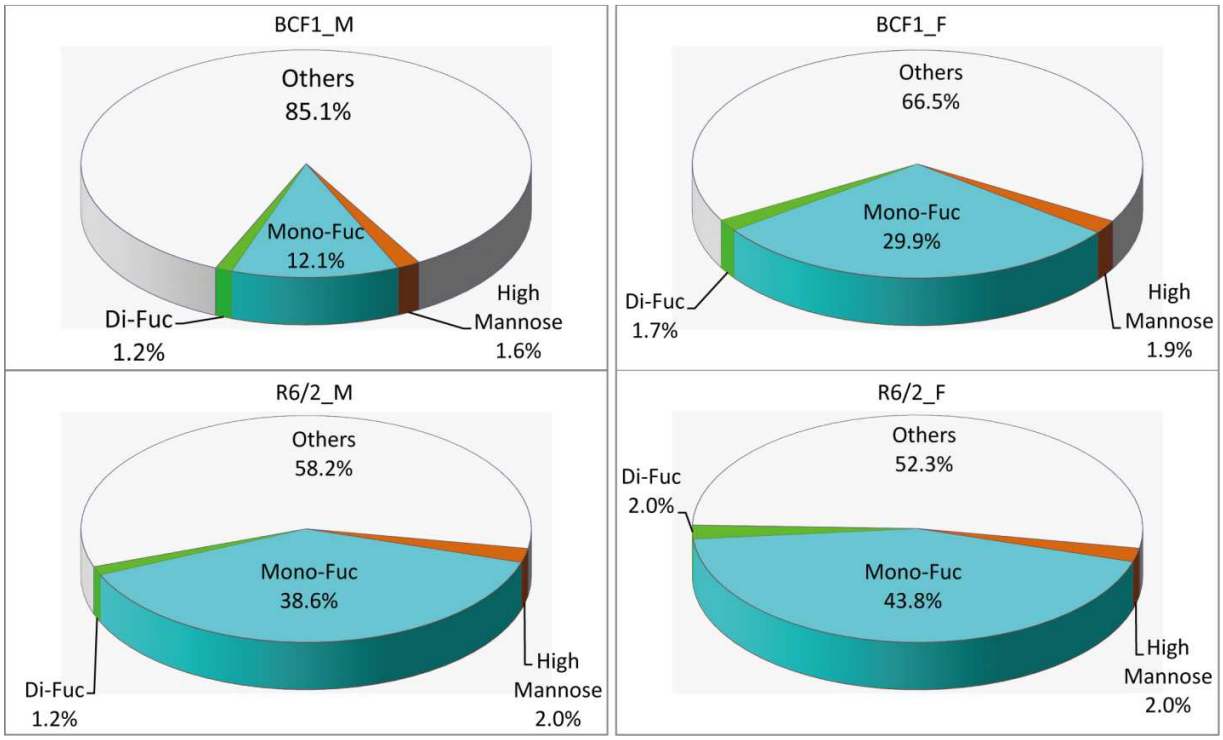

Figure 2.7. Glycotyping analysis of fucosylated *N*-glycans from serum R6/2 and BCF1 (Mono-Fuc, core-fucose; Di-Fuc, di-fucose; others, *N*-glycan types except mentioned; M, male; and F, female).

2.2.2. *N*-Glycan Analysis of AD, PD, HD and Normal Subjects

2.2.2.1. Human Brain Tissue *N*-Glycan Analysis

I have estimated the composition of 40 *N*-glycans that are common to both genders and classified as high mannose, hybrid and complex types of *N*-glycans. The later contain proximal fucose and bisecting-GlcNAc (Figure 2.8 and Table 2.5). Quantitatively, the amount of *N*-glycans in frontal cortices of AD, PD and HD were found in decreased levels than the Normal subjects of both sexes ($p<0.05$). In parietal cortex, *N*-glycans were increased in male PD and decreased in female HD ($p<0.05$, Table 2.6). In temporal cortex, *N*-glycans were in increased levels in male AD while there is no any significant difference in the rest part of the cortices.

A.

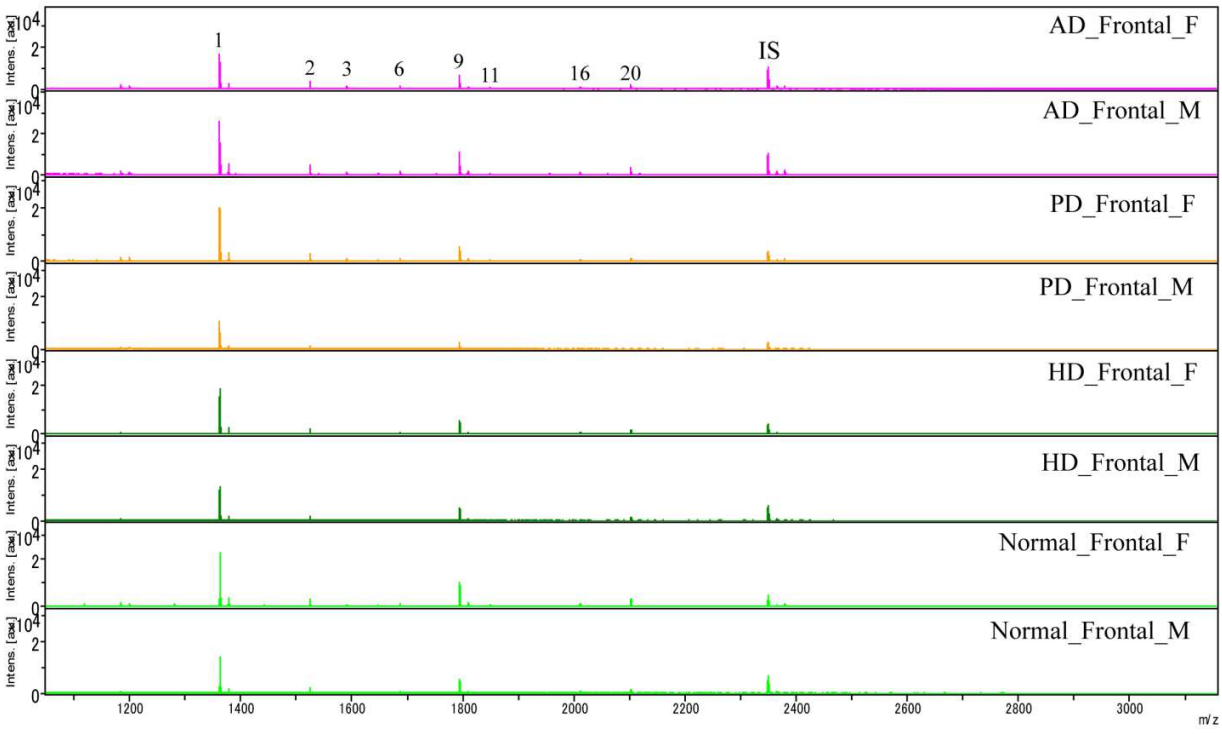

B.

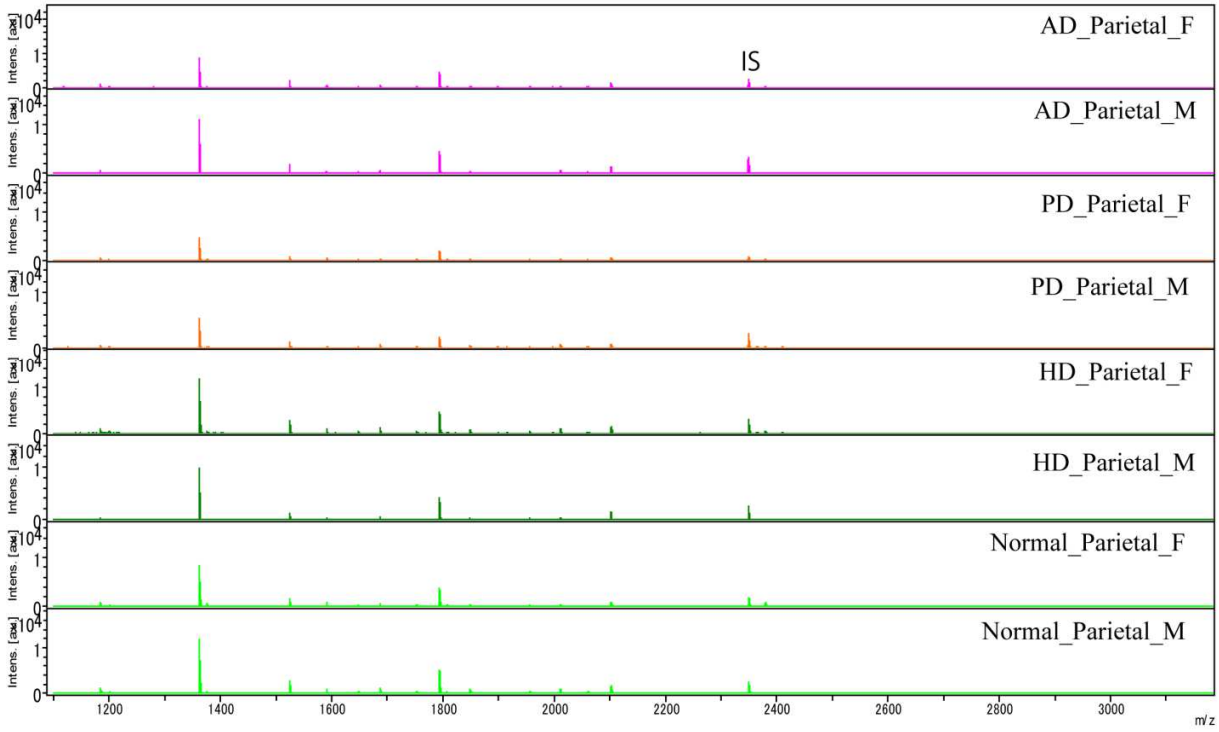
AD_Parietal_F
IS
AD_Parietal_M
PD_Parietal_F
PD_Parietal_M
HD_Parietal_F
HD_Parietal_M
Normal_Parietal_F
Normal_Parietal_M
Intens. [a.u.]
1200
1400
1600
1800
2000
2200
2400
2600
2800
3000
m/z

C.

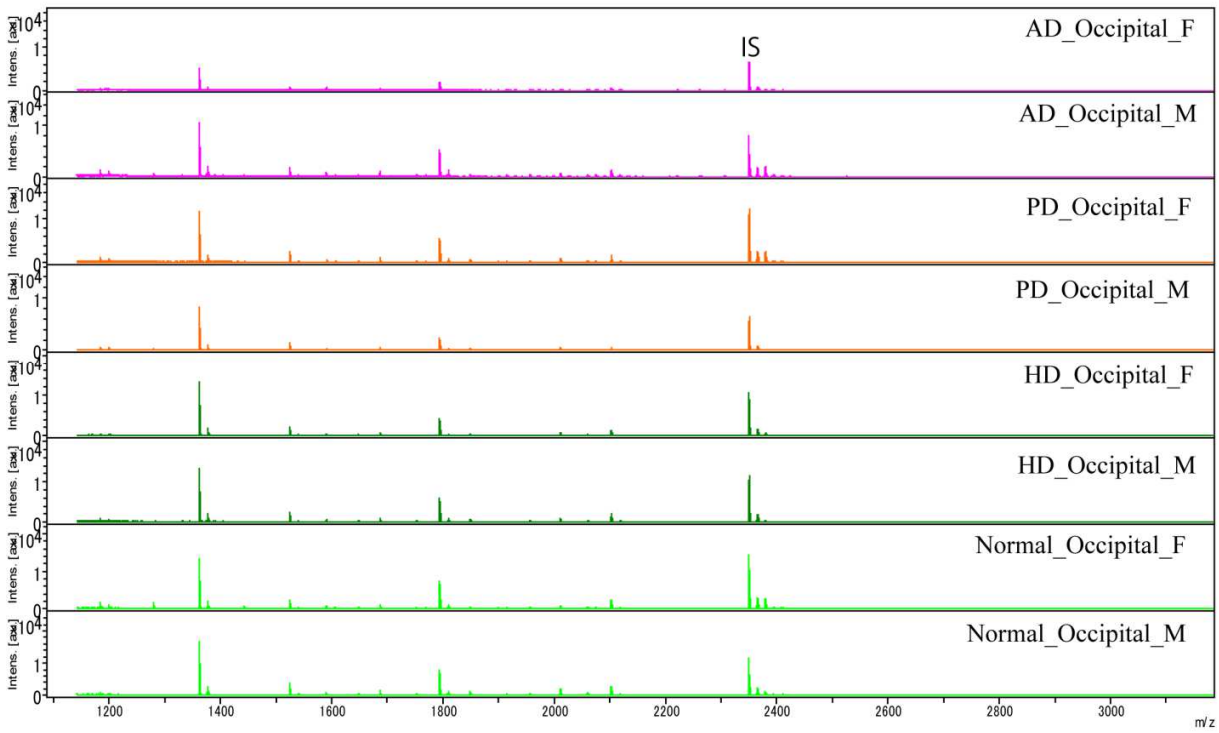
AD_Occipital_F
IS
AD_Occipital_M
PD_Occipital_F
PD_Occipital_M
HD_Occipital_F
HD_Occipital_M
Normal_Occipital_F
Normal_Occipital_M
Intens. [a.u.]
1200
1400
1600
1800
2000
2200
2400
2600
2800
3000
m/z

D.

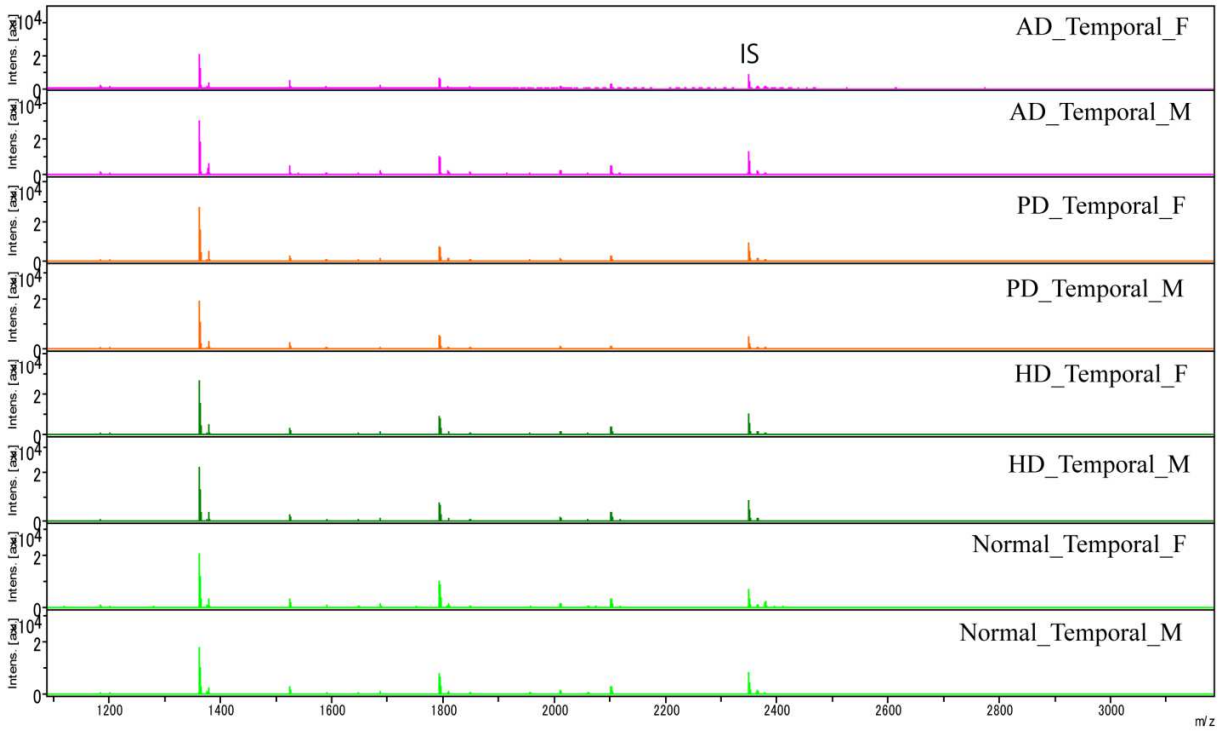

Figure 2.8. Representative MALDI-TOF/MS spectra of human brain tissue *N*-glycans. A) Frontal cortex, B) Parietal cortex, C) Occipital cortex, and D) Temporal cortex (AD, Alzheimer's disease; PD, Parkinson's disease; HD, Huntington's disease; Normal, as control; IS, internal standard; M, male; F, female; and the numbers indicated in the first figure are the peak numbers of the major *N*-glycans).

Table 2.5. Presumptive composition of *N*-glycans in human brain, serum and CSF. GlycanID is the peak numbers of *N*-glycans assigned for each sample. '-' means not detected in that particular sample. GlcNAc, *N*-acetylglucosamine; Man, Mannose; Deoxyhexose, fucose; HexNAc, *N*-acetylhexosamine; Hex, hexose (Mannose or galactose depend of the description); NeuAc, *N*-acetylneuraminic acid; and NeuGc, *N*-glycolylneuraminic acid.

		GlycanID		
Presumptive composition	m/z	Brain	Serum	CSF
(Hex)2 + (Man)3 (GlcNAc)2	1362.47	1	1	1
(HexNAc)2 + (Man)3 (GlcNAc)2	1444.54	-	2	-
(Hex)3 + (Man)3 (GlcNAc)2	1524.53	2	3	2
(Hex)1 (HexNAc)1 (Deoxyhexose)1 + (Man)3 (GlcNAc)2	1549.60	-	4	-
(HexNAc)2 (Deoxyhexose)1 + (Man)3 (GlcNAc)2	1590.60	3	5	3
(Hex)1 (HexNAc)2 + (Man)3 (GlcNAc)2	1606.59	4	6	4
(HexNAc)3 + (Man)3 (GlcNAc)2	1647.61	5	-	5
(Hex)4 + (Man)3 (GlcNAc)2	1686.59	6	7	6
(Hex)1 (HexNAc)1 (NeuAc)1 + (Man)3 (GlcNAc)2	1708.63	-	8	7
(HexNAc)2 (Deoxyhexose)2 + (Man)3 (GlcNAc)2	1736.63	-	9	-
(Hex)1 (HexNAc)2 (Deoxyhexose)1 + (Man)3 (GlcNAc)2	1752.65	7	10	8
(Hex)2 (HexNAc)2 + (Man)3 (GlcNAc)2	1768.63	8	11	9
(HexNAc)3 (Deoxyhexose)1 + (Man)3 (GlcNAc)2	1793.67	9	12	10
(Hex)1 (HexNAc)3 + (Man)3 (GlcNAc)2	1809.66	10	-	11
(Hex)5 + (Man)3 (GlcNAc)2	1848.64	11	13	-
(Hex)1 (HexNAc)1 (Deoxyhexose)1 (NeuAc)1 + (Man)3 (GlcNAc)2	1854.69	-	14	-
(Hex)2 (HexNAc)1 (NeuAc)1 + (Man)3 (GlcNAc)2	1870.68	-	15	-
(Hex)1 (HexNAc)2 (Deoxyhexose)2 + (Man)3 (GlcNAc)2	1898.70	12	-	12
(Hex)1 (HexNAc)2 (NeuAc)1 + (Man)3 (GlcNAc)2	1911.70	-	16	13
(Hex)2 (HexNAc)2 (Deoxyhexose)1 + (Man)3 (GlcNAc)2	1914.70	13	17	14
(HexNAc)3 (Deoxyhexose)2 + (Man)3 (GlcNAc)2	1939.69	-	18	-
(Hex)1 (HexNAc)3 (Deoxyhexose)1 + (Man)3 (GlcNAc)2	1955.73	14	19	15
(Hex)2 (HexNAc)3 + (Man)3 (GlcNAc)2	1971.66	15	-	16
(HexNAc)4 (Deoxyhexose)1 + (Man)3 (GlcNAc)2	1996.93	-	20	-
(Hex)6 + (Man)3 (GlcNAc)2	2010.69	16	21	17
(Hex)3 (HexNAc)1 (NeuAc)1 + (Man)3 (GlcNAc)2	2032.72	-	22	-
(Hex)1 (HexNAc)2 (Deoxyhexose)1 (NeuAc)1 + (Man)3 (GlcNAc)2	2057.73	-	23	18
(Hex)2 (HexNAc)2 (Deoxyhexose)2 + (Man)3 (GlcNAc)2	2060.76	17	-	-
(Hex)2 (HexNAc)2 (NeuAc)1 + (Man)3 (GlcNAc)2	2073.74	18	-	-
(Hex)3 (HexNAc)2 (Deoxyhexose)1 + (Man)3 (GlcNAc)2	2076.75	19	-	-
(Hex)1 (HexNAc)3 (Deoxyhexose)2 + (Man)3 (GlcNAc)2	2101.77	20	25	20

Table 2.5. Continued.

Presumptive composition	m/z	GlycanID		
		Brain	Serum	CSF
(Hex)2 (HexNAc)3 (Deoxyhexose)1 + (Man)3 (GlcNAc)2	2117.75	21	26	21
(HexNAc)4 (Deoxyhexose)2 + (Man)3 (GlcNAc)2	2142.75	-	27	-
(Hex)1 (HexNAc)4 (Deoxyhexose)1 + (Man)3 (GlcNAc)2	2158.78	22	-	22
(Hex)7 + (Man)3 (GlcNAc)2	2172.71	-	28	-
(Hex)1 (HexNAc)2 (Deoxyhexose)2 (NeuAc)1 + (Man)3 (GlcNAc)2	2203.94	-	-	23
(Hex)2 (HexNAc)2 (Deoxyhexose)3 + (Man)3 (GlcNAc)2	2206.81	23	-	24
(Hex)2 (HexNAc)2 (Deoxyhexose)1 (NeuAc)1 + (Man)3 (GlcNAc)2	2219.79	24	29	25
(Hex)3 (HexNAc)2 (Deoxyhexose)2 + (Man)3 (GlcNAc)2	2222.83	25	-	-
(Hex)3 (HexNAc)2 (NeuAc)1 + (Man)3 (GlcNAc)2	2235.80	-	-	26
(Hex)1 (HexNAc)3 (Deoxyhexose)3 + (Man)3 (GlcNAc)2	2247.78	26	30	27
(Hex)1 (HexNAc)3 (Deoxyhexose)1 (NeuAc)1 + (Man)3 (GlcNAc)2	2260.79	27	31	28
(Hex)2 (HexNAc)3 (Deoxyhexose)2 + (Man)3 (GlcNAc)2	2263.83	28	32	-
(Hex)2 (HexNAc)3 (NeuAc)1 + (Man)3 (GlcNAc)2	2276.79	29	33	29
(HexNAc)4 (Deoxyhexose)3 + (Man)3 (GlcNAc)2	2288.77	-	34	30
(Hex)1 (HexNAc)4 (Deoxyhexose)2 + (Man)3 (GlcNAc)2	2304.84	30	-	31
(Hex)2 (HexNAc)4 (Deoxyhexose)1 + (Man)3 (GlcNAc)2	2320.82	31	-	32
(Hex)3 (HexNAc)4 + (Man)3 (GlcNAc)2	2336.81	-	35	33
(Hex)2 (HexNAc)2 (NeuAc)2 + (Man)3 (GlcNAc)2	2378.86	32	36	34
(Hex)1 (HexNAc)3 (Deoxyhexose)2 (NeuAc)1 + (Man)3 (GlcNAc)2	2406.87	33	-	-
(Hex)2 (HexNAc)3 (Deoxyhexose)3 + (Man)3 (GlcNAc)2	2409.90	34	-	35
(Hex)2 (HexNAc)3 (Deoxyhexose)1 (NeuAc)1 + (Man)3 (GlcNAc)2	2422.84	35	37	36
(Hex)3 (HexNAc)3 (NeuAc)1 + (Man)3 (GlcNAc)2	2438.93	-	38	37
(Hex)1 (HexNAc)4 (Deoxyhexose)1 (NeuAc)1 + (Man)3 (GlcNAc)2	2463.88	36	-	38
(Hex)2 (HexNAc)4 (Deoxyhexose)2 + (Man)3 (GlcNAc)2	2466.90	37	-	39
(Hex)3 (HexNAc)4 (Deoxyhexose)1 + (Man)3 (GlcNAc)2	2482.91	-	39	40
(Hex)2 (HexNAc)2 (Deoxyhexose)1 (NeuAc)2 + (Man)3 (GlcNAc)2	2524.90	38	40	41
(Hex)3 (HexNAc)5 + (Man)3 (GlcNAc)2	2539.98	-	-	42
(Hex)2 (HexNAc)3 (NeuAc)2 + (Man)3 (GlcNAc)2	2581.95	-	41	-
(Hex)3 (HexNAc)3 (Deoxyhexose)1 (NeuAc)1 + (Man)3 (GlcNAc)2	2584.92	-	42	43
(Hex)2 (HexNAc)4 (Deoxyhexose)3 + (Man)3 (GlcNAc)2	2612.97	39	-	-
(Hex)2 (HexNAc)3 (Deoxyhexose)1 (NeuAc)2 + (Man)3 (GlcNAc)2	2728.00	-	43	44
(Hex)3 (HexNAc)3 (NeuAc)2 + (Man)3 (GlcNAc)2	2744.01	-	44	45
(Hex)2 (HexNAc)4 (Deoxyhexose)2 (NeuAc)1 + (Man)3 (GlcNAc)2	2772.01	40	-	46
(Hex)3 (HexNAc)3 (Deoxyhexose)1 (NeuAc)2 + (Man)3 (GlcNAc)2	2890.06	-	45	47
(Hex)3 (HexNAc)3 (NeuAc)3 + (Man)3 (GlcNAc)2	3049.11	-	46	48
(Hex)4 (HexNAc)4 (NeuAc)2 + (Man)3 (GlcNAc)2	3109.19	-	47	-
(Hex)3 (HexNAc)3 (Deoxyhexose)1 (NeuAc)3 + (Man)3 (GlcNAc)2	3195.19	-	48	49
(Hex)4 (HexNAc)4 (NeuAc)3 + (Man)3 (GlcNAc)2	3414.31	-	49	-
(Hex)4 (HexNAc)4 (Deoxyhexose)1 (NeuAc)3 + (Man)3 (GlcNAc)2	3560.41	-	50	-
(Hex)4 (HexNAc)4 (NeuAc)4 + (Man)3 (GlcNAc)2	3719.45	-	51	50
(Hex)4 (HexNAc)4 (Deoxyhexose)1 (NeuAc)4 + (Man)3 (GlcNAc)2	3865.56	-	52	-

Table 2.6. Amount of *N*-glycans (pmole ± SD, from 100 µg protein) in human brain cortices AD, PD, HD and Normal subjects (M, male; F, female).

Cerebral cortices	Normal_M	AD_M	PD_M	HD_M
Frontal	218.52 ± 71.89	193.94 ± 78.06	144.79 ± 48.34	168.82 ± 90.37
Parietal	250.95 ± 58.96	344.98 ± 133.49	157.44 ± 83.78	269.62 ± 96.05
Occipital	97.19 ± 39.39	119.66 ± 56.37	68.92 ± 8.75	93.82 ± 40.72
Temporal	138.16 ± 80.49	281.40 ± 147.64	185.69 ± 26.71	217.72 ± 51.79

Cerebral cortices	Normal_F	AD_F	PD_F	HD_F
Frontal	224.88 ± 144.20	153.18 ± 58.23	167.29 ± 64.42	162.46 ± 82.66
Parietal	303.65 ± 68.25	335.74 ± 91.44	292.27 ± 73.59	269.08 ± 56.04
Occipital	73.01 ± 21.69	68.77 ± 26.45	97.26 ± 62.36	52.62 ± 22.03
Temporal	193.76 ± 39.91	239.43 ± 94.00	200.92 ± 57.82	161.48 ± 64.13

From glycotyping analysis, high mannose *N*-glycans were found in increased levels in all diseases compared to the Normal subjects. Except in parietal cortex of female AD and frontal cortex of male HD (which were increased by 2.08% and 1.9%, respectively), core-fucosylated *N*-glycans were in decreased levels in AD, PD, and HD of all sexes. Bisecting GlcNAc was in decreased levels in AD, PD and HD, except in parietal cortex of female AD (that was showed no significant difference) and in frontal cortex of male HD (which was in increased levels). There were not any significant difference in the amount of tri-and tetra-antennary *N*-glycans. Sialic acid is very small (<2 %) in human brain and the result was in accordance with brain tissue of HD transgenic and wild type mice. It can be conclude that the concentration of sialic acid in human and mice brain tissues was found smaller compared to the concentration of other types of *N*-glycans.

2.2.2.2. Human Serum *N*-Glycan Analysis

Serum *N*-glycomics using glycoblotting is a robust, sensitive and importantly quantitative. Moreover, the composition and expression levels of human serum *N*-glycans have been useful for an early detection as well as to assess the progression of many diseases. Targeting that, I have profiled and estimated the compositions of 52 *N*-glycans of different types that are common to both genders (Figure 2.10, Table 2.5). The amount of *N*-glycans were in increased levels in Alzheimer's disease of both sex when compared to the Normal subjects ($p < 0.05$ in male; $p < 0.001$ in female). *N*-glycans were increased and decreased in female and male, respectively, of PD and HD when compared to the Normal subjects, albeit statistically insignificant (Table 2.7).

A.

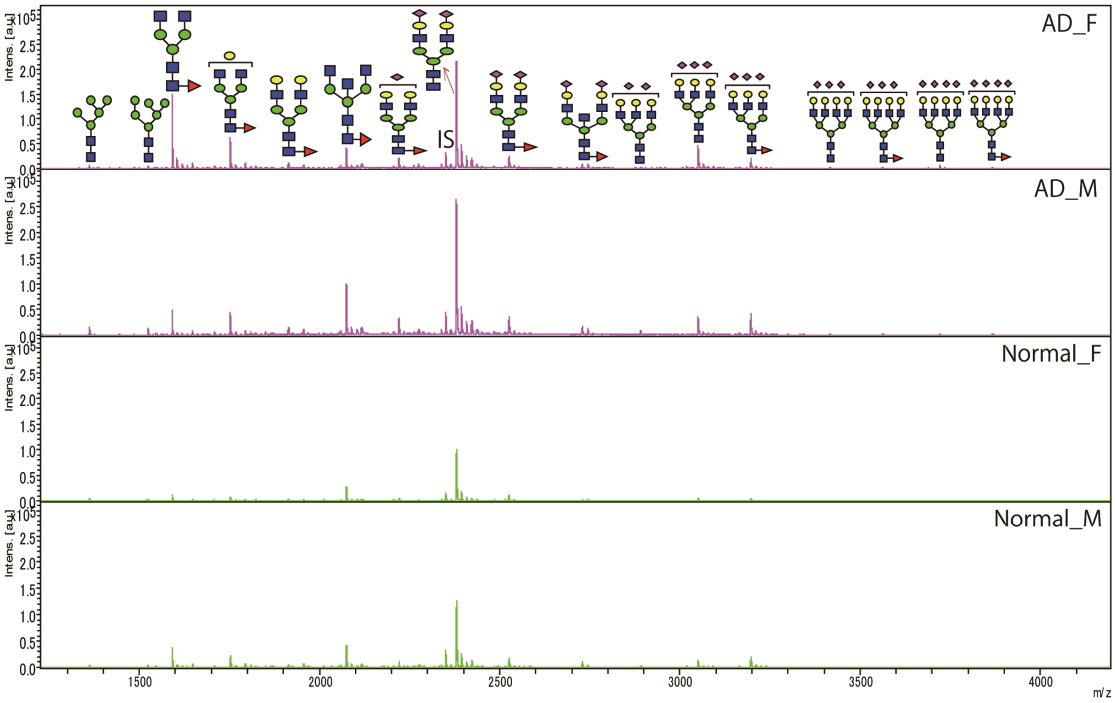
AD_F
IS
AD_M
Normal_F
Normal_M
Intens. [a.u.]
m/z

B.

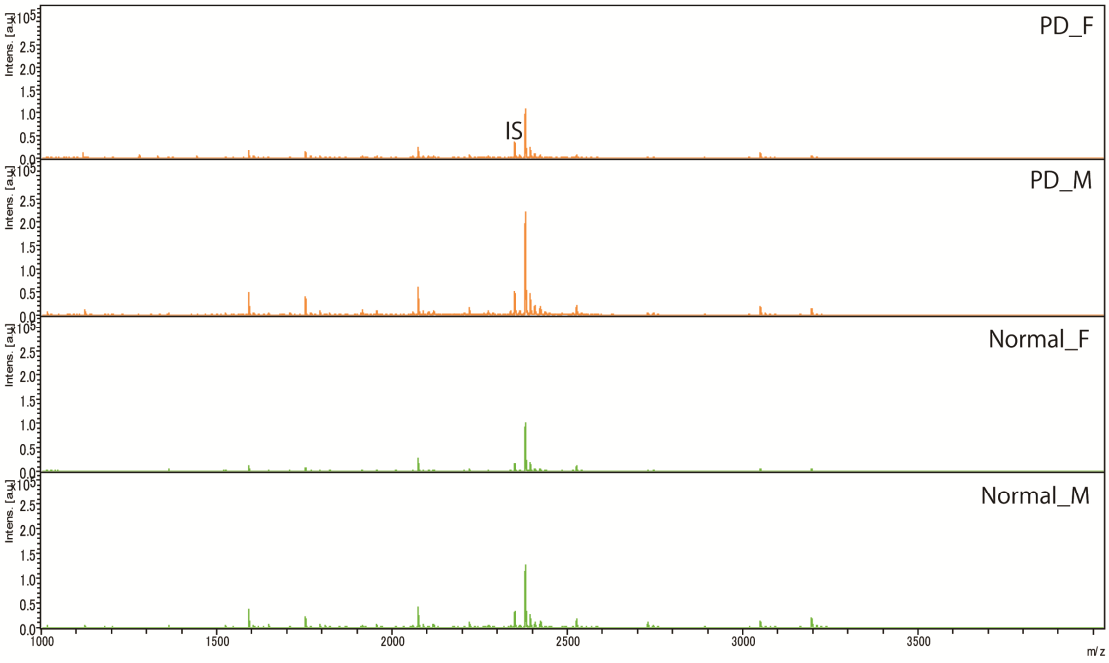
PD_F
IS
PD_M
Normal_F
Normal_M
Intens. [a.u.]
m/z

C.

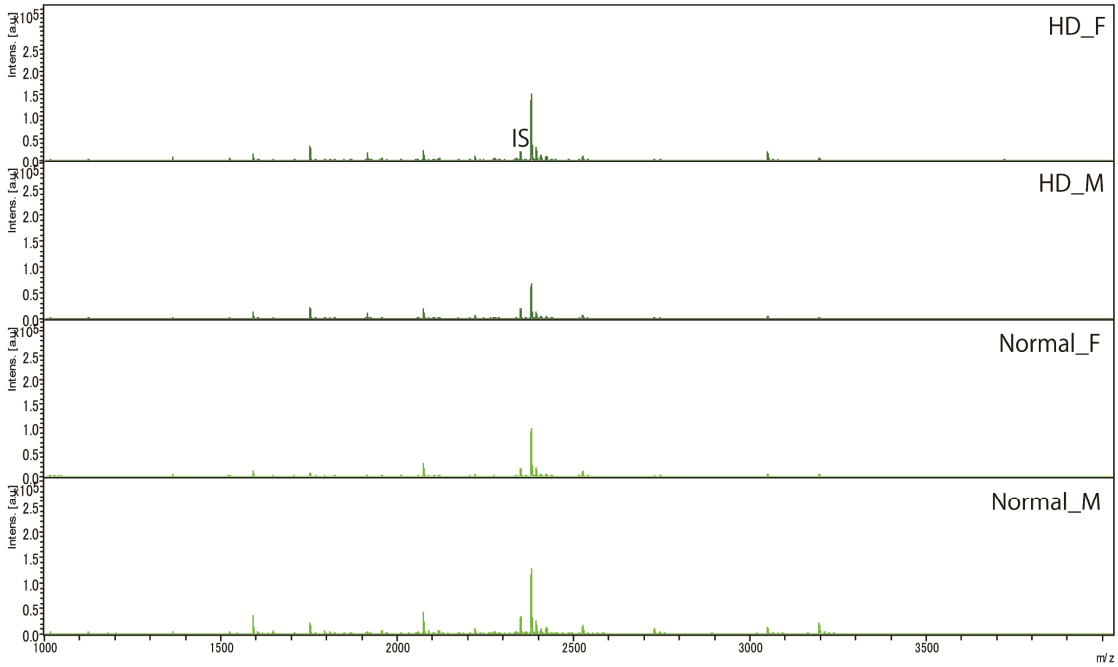

Figure 2.9. MALDI-TOF/MS of human serum *N*-glycans of AD, PD, HD and Normal subjects. Glycan cartoons were constructed using the standard Consortium for Functional nomenclature, i.e., blue square, *N*-acetylglucosamine; red triangle, fucose; green circle, mannose; yellow circle, galactose; purple diamond, sialic acid; M, male; and F, female.

Table 2.7. Amount of *N*-glycans (pmole ± SD) in human serum of neurodegenerative diseases and Normal subjects. M1, M2, and M3 are male samples 1, 2, and 3. F1, F2, and F3 are female samples 1, 2, and 3. Sera sample numbering corresponds to the brain tissue. "–" shows that no sample paired with brain tissue. (Note: *N*-glycans expression levels were different in intra-samples. This is because patients were diagnosed not only neurological but also clinical complications. For example, diabetes Type II, hypertension, kidney failure and heart attack. All of these are sequela of CNS disorders. Moreover, their autolysis time was different. This phenomenon was also observed in case of serum *O*-glycans and *GSL*-glyans analysis in Chapter 3 and 4).

Sample name	M1	M2	M3
Normal	39.12 ± 4.53	404.56 ± 18.55	944.98 ± 264.73
AD	896.39 ± 19.59	731.60 ± 58.45	76.65 ± 6.84
PD	14.35 ± 0.91	434.85 ± 34.71	694.66 ± 12.31
HD	–	57.25 ± 4.78	345.09 ± 9.57

Sample name	F1	F2	F3
Normal	532.33 ± 26.65	145.82 ± 12.71	–
AD	997.02 ± 132.97	979.16 ± 22.83	–
PD	–	704.06 ± 35.54	237.69 ± 9.08
HD	800.68 ± 64.05	–	661.32 ± 42.94

N-glycans expression levels were increased pronouncedly in female neurodegenerative diseases when compared to the Normal subjects, especially in AD (Figure 2.11 A). I calculated specific *N*-glycans which were shown higher disease to Normal ratios, viz., female AD/Normal, female PD/Normal and female HD/Normal (Figure 2.11 B). The major *N*-glycans with higher

expression levels in neurodegenerative diseases compared to the Normal subjects were found biantennary, bisecting and proximal fucosylated *N*-glycans (for example m/z 2117.92 was 17, 10, and 14 times higher in female Alzheimer's, Parkinson's and Huntington's diseases, respectively, Figure 2.11 B).

From glycotyping analysis of human serum *N*-glycans, core fucose containing *N*-glycans were increased in AD of both sexes, male PD and HD compared to the Normal subjects. But di-sialylated *N*-glycans were decreased in those samples. Female PD and HD didn't show any significant difference. There was no direct evidence for the detection of *N*-glycolylneuraminic acid in human serum in this study. Except in male HD, bisecting-GlcNAc was increased in all diseases compared to the controls. Tri-and tetra-antennary *N*-glycans were also increased in AD, in female PD and female HD; however, there were decreased in male HD. Serum *N*-glycans with the core fucose, bisecting-GlcNAc and highly branched *N*-glycans showed a clear-cut difference between Alzheimer's disease and the Normal subjects.

A.

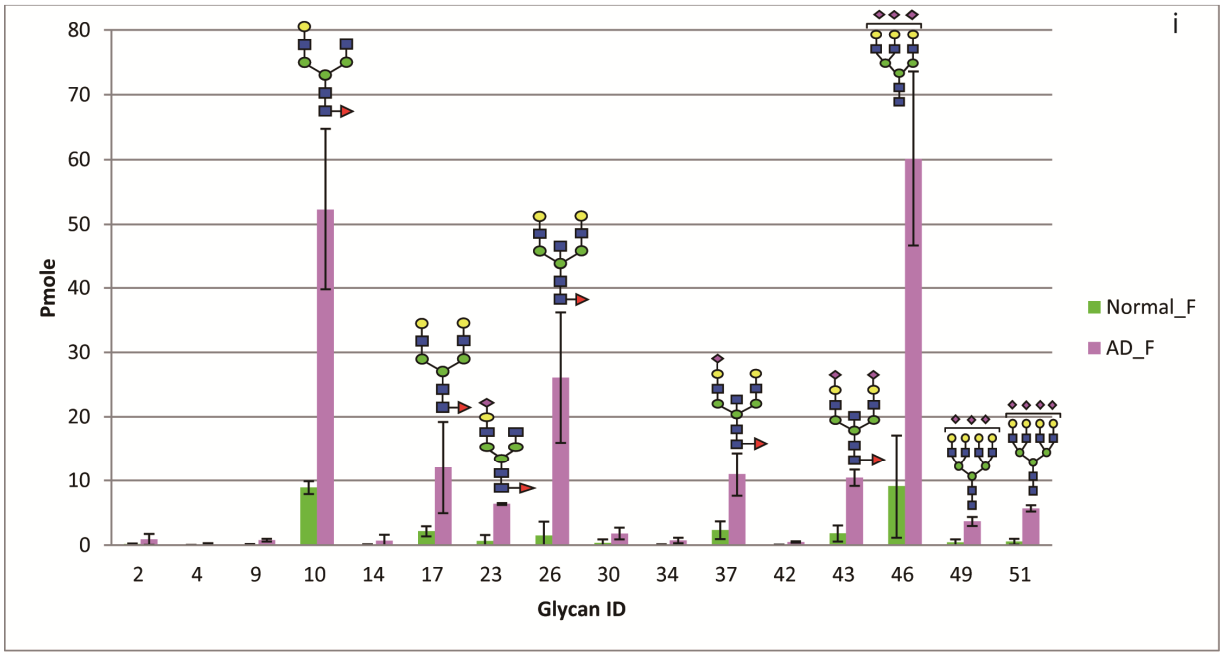
i
Pmole
0
10
20
30
40
50
60
70
80
2
4
9
10
14
17
23
26
30
34
37
42
43
46
49
51
Glycan ID
Normal_F
AD_F

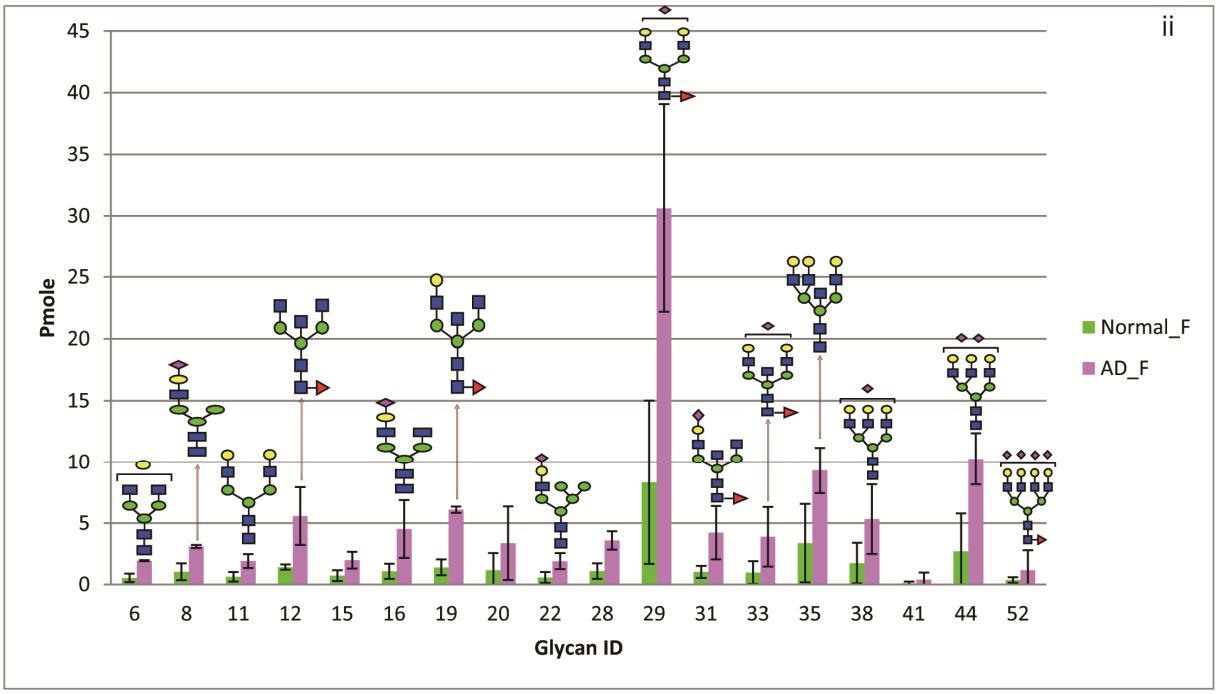
ii
Pmole
0
5
10
15
20
25
30
35
40
45
6
8
11
12
15
16
19
20
22
28
29
31
33
35
38
41
44
52
Glycan ID
Normal_F
AD_F

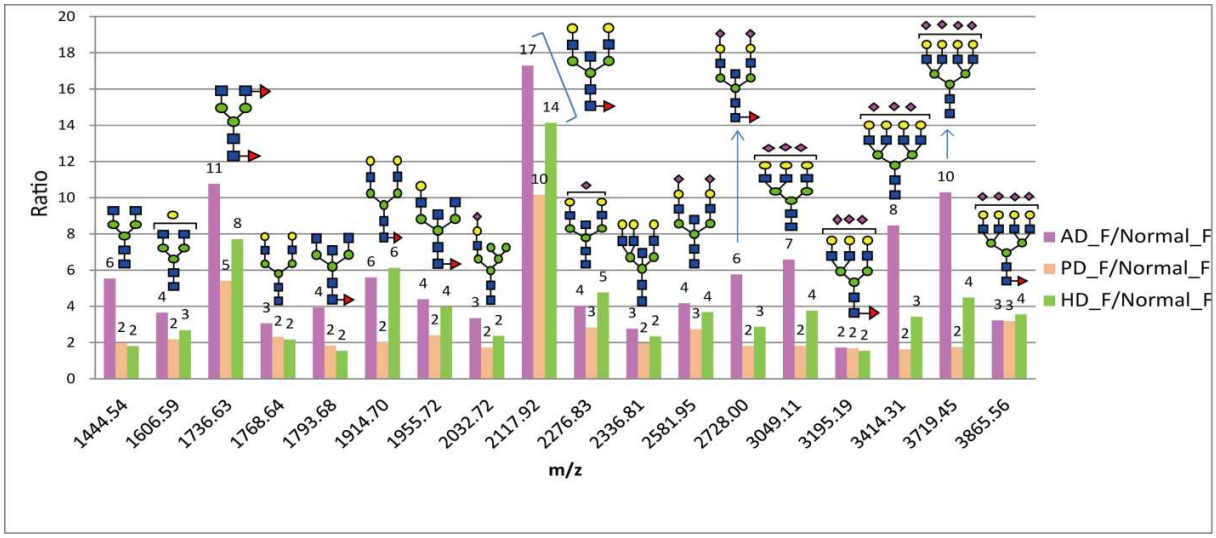

Figure 2.10. *N*-glycan expression levels in female AD, PD and HD compared to their respective controls. A (i) Female AD/Normal ratios ≥ 5, A (ii) Female AD/Normal ≥ 2, B) ratios of specific *N*-glycans of female AD, PD and HD to Normal subjects which are common to AD, PD and HD. AD_F, female AD; PD_F, female PD; HD_F, female HD, and Normal_F, female normal subjects. Glycan cartoons were constructed using the standard Consortium for Functional nomenclature, i.e., blue square, *N*-acetylglucosamine; red triangle, fucose; green circle, mannose; yellow circle, galactose; and purple diamond, sialic acid.

2.2.2.3. Human Cerebrospinal Fluids *N*-Glycan Analysis

Cerebrospinal fluid (CSF) proteomes are produced from the brain, choroid plexus in the brain ventricles originating from the blood, following active and passive transport through the blood brain barrier (BBB), and from drainage of interstitial liquid of the nervous system [18]. Since the CSF compartment is in close anatomical contact with the brain interstitial fluids, where biochemical changes related to chronic neurological diseases (CND) are reflected, CSF is a promising source of biomarkers [19]. Studies had conducted to profile CSF *N*-glycan and investigate biomarkers in leukodystrophies related to ElF2B mutations [20], Idiopathic normal pressure hydrocephalus (iNPH) [21], in intrathecally synthesized CSF proteins for "brain-type" *N*-glycosylation of asialo-transferrin [22] and tenascin-R [23].

In this study, I have estimated the composition of 50 *N*-glycans of all types, which are common to both genders and characterized by large proportions of asialo- and agalacto-chains typically containing core fucose and bisecting GlcNAc (Table 2.5). *N*-glycans expression levels in CSF were significantly increased in AD when compared to the Normal subjects ($p<0.05$, Figure 2.11). Similar to human sera *N*-glycomics, the composition and amount of CSF *N*-glycans differ markedly between genders. The ratios of specific *N*-glycans in neurodegenerative diseases compared to the Normal subjects have shown in Figure 2.12. The expression levels of *N*-glycans were significantly increased in AD compared to the Normal subjects. For example, m/z 1793.67 was increased 10, 2, and 4 times in all male AD, PD, and HD, respectively, compared to the Normal subjects. This particular glycan was also 7 times higher in female AD compared to the Normal subjects. The amounts of glycotypes, specifically core fucose, bisecting-GlcNAc, tri-and

tetra-antennary of *N*-glycans from 100 µg protein of CSF were significantly increased in Alzheimer's disease when compared with the Normal subjects.

A.

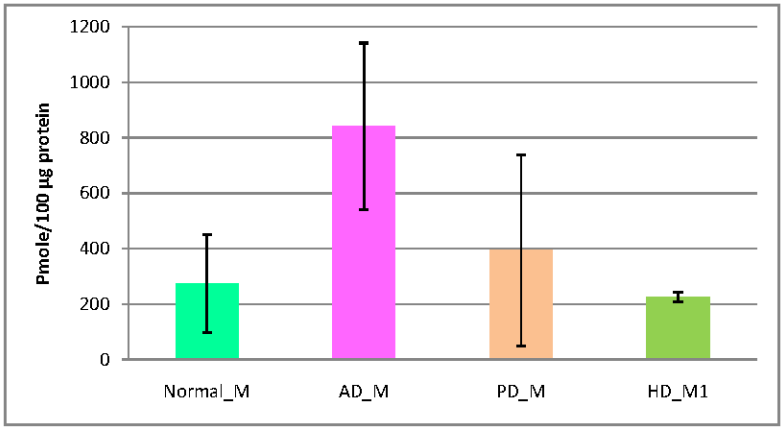

B.

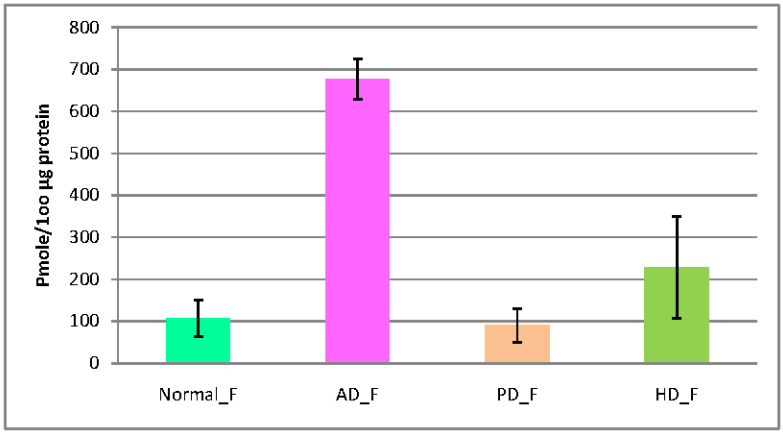

Figure 2.11. Amount of CSF *N*-glycans (pmole ± SD, $p<0.05$ for AD) in A) Male, and B) Female of AD, PD, HD, and the normal subjects (AD, Alzheimer's disease; PD, Parkinson's disease; HD, Huntington' disease; Normal, as control; M, male; and F, female).

A.

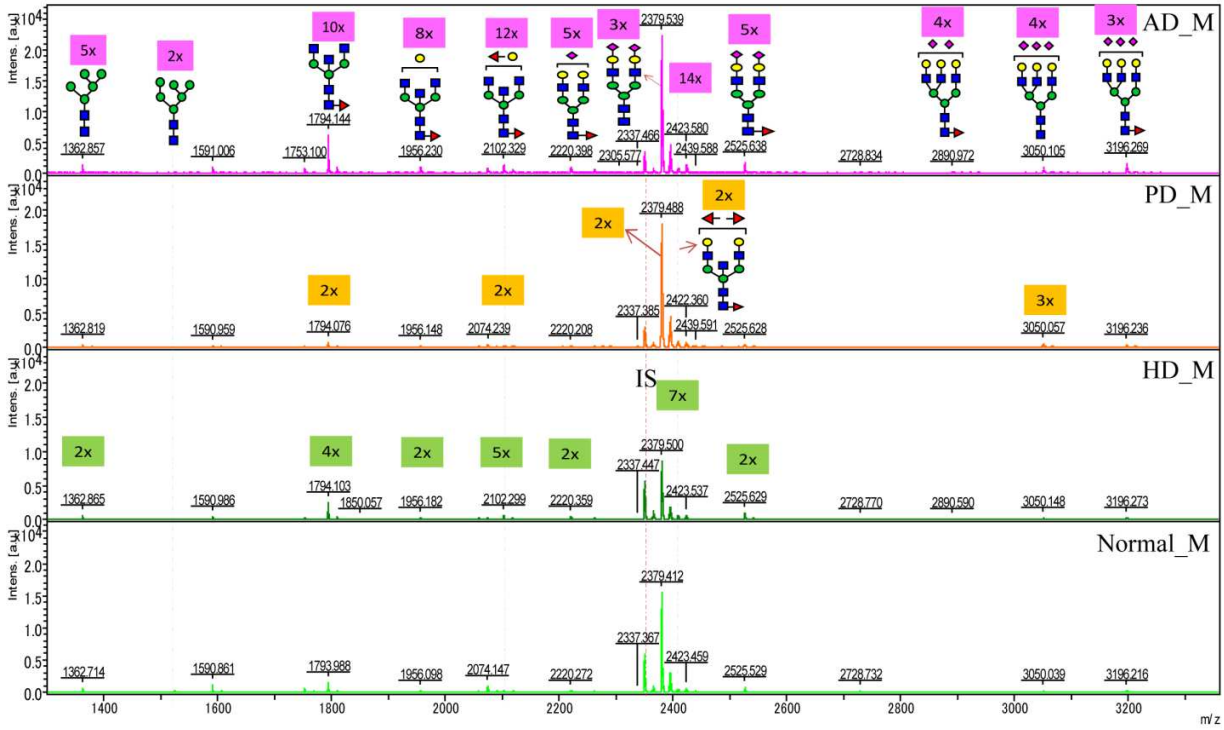
AD_M
PD_M
HD_M
Normal_M
IS
Intens. [a.u.]
m/z
1400
1600
1800
2000
2200
2400
2600
2800
3000
3200

B.

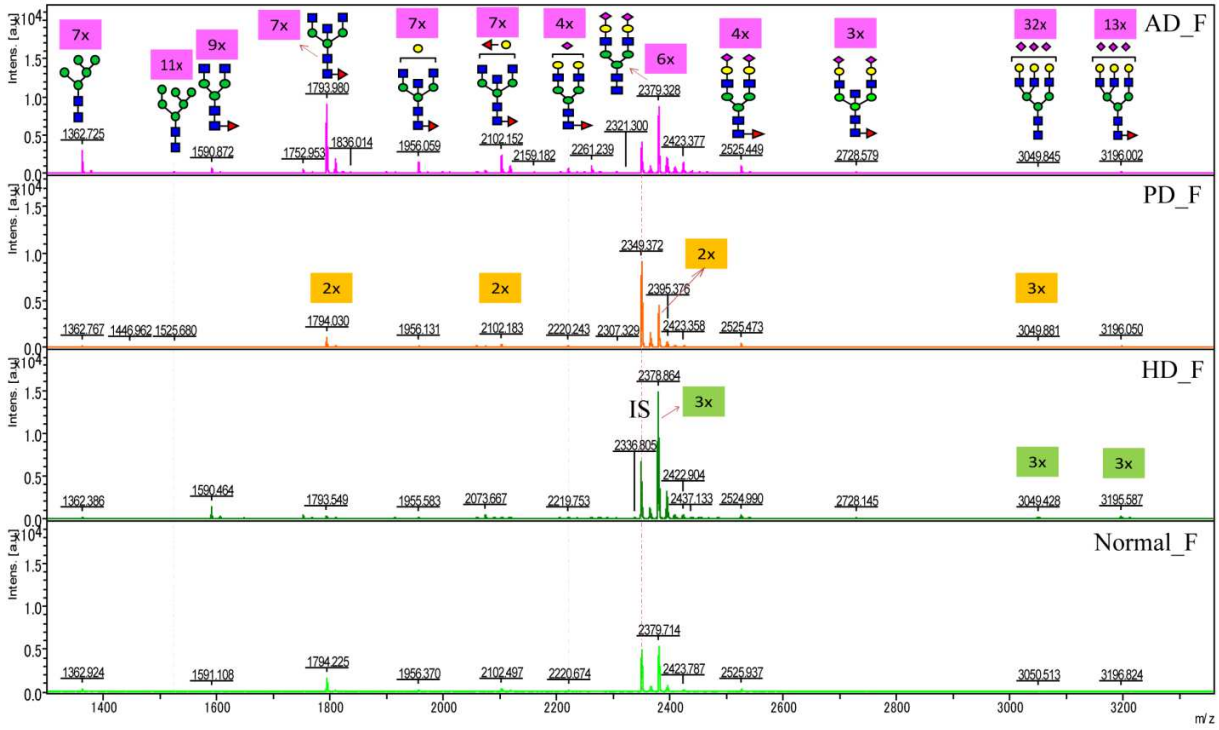

Figure 2.12. MALDI-TOF/MS spectra and ratios of specific human CSF *N*-glycans in AD, PD, and HD compared to the Normal subjects. A) in male, and B) in female, in this study. Glycan cartoons were constructed using the standard Consortium for Functional nomenclature, i.e., blue square, *N*-acetylglucosamine; red triangle, fucose; green circle, mannose; yellow circle, galactose; and purple diamond, sialic acid.

2.2.3. Human Serum *N*-Glycans versus Concentration of Human Immunoglobulin G (IgG)

To find out specific proteins that could be the source for the up-regulation of the specific *N*-glycans in serum and CSF, we have quantified IgG concentration using human IgG ELISA quantitation set (Lot no. E80-1044-29, Bethyl Laboratories, Inc.) based on the manufacturer's protocol. The concentration of human serum *N*-glycans in AD, PD, HD and Normal subjects were shown high positive correlation with the concentration of IgG (r = 0.82, where r is a correlation coefficient); however, lower positive correlation were found in CSF (r = 0.37) (Figure 2.13 A and B). As a result, I strongly suggest that the major serum *N*-glycans were sourced from IgG. Particularly, *N*-glycans containing core-fucosylated, bisecting-GlcNAc and bi-antennary types (Figure 2.13 C).

A.

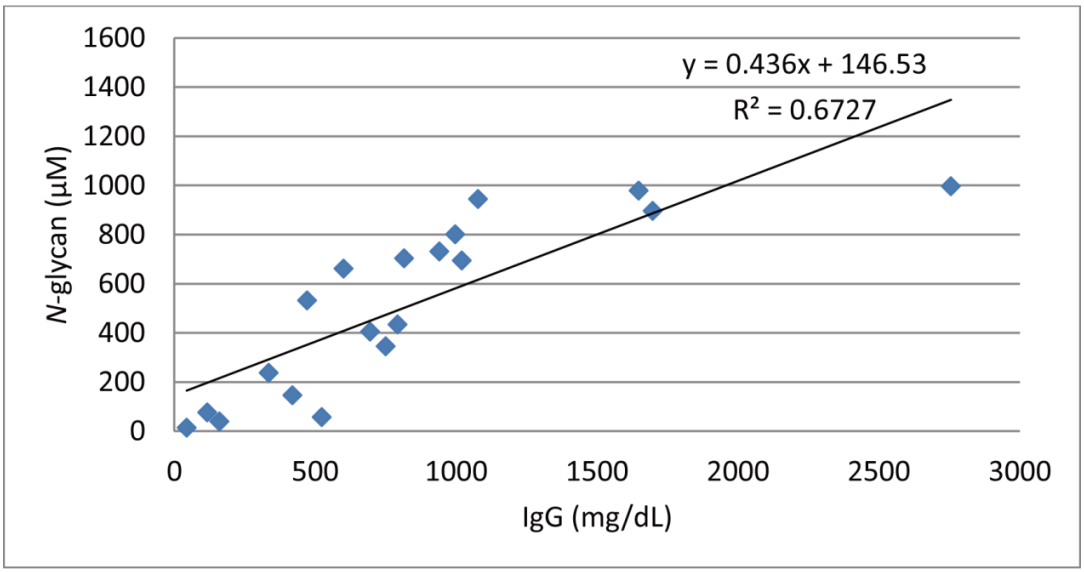

B.

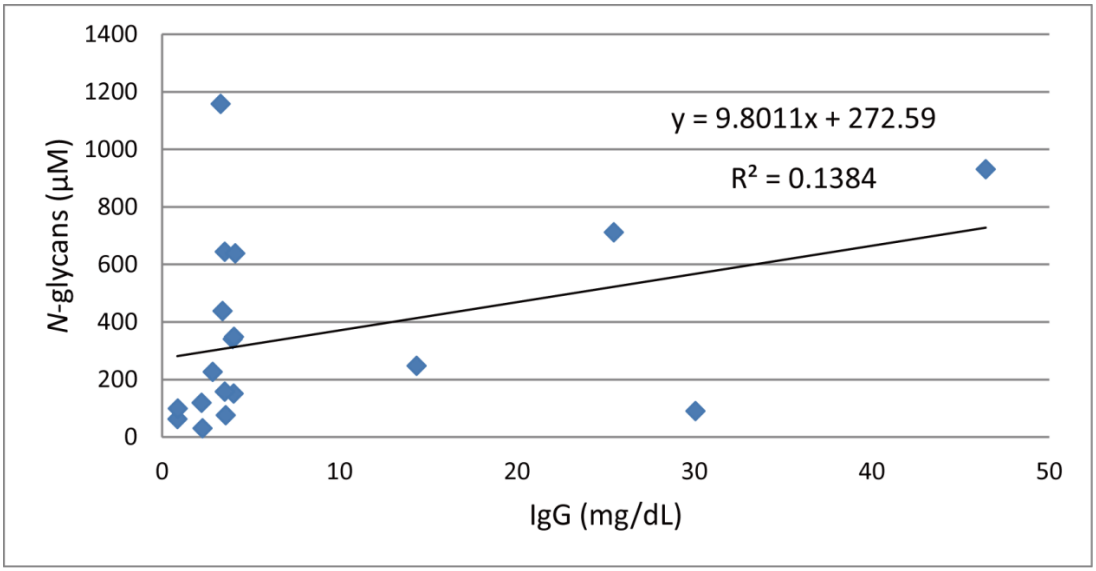

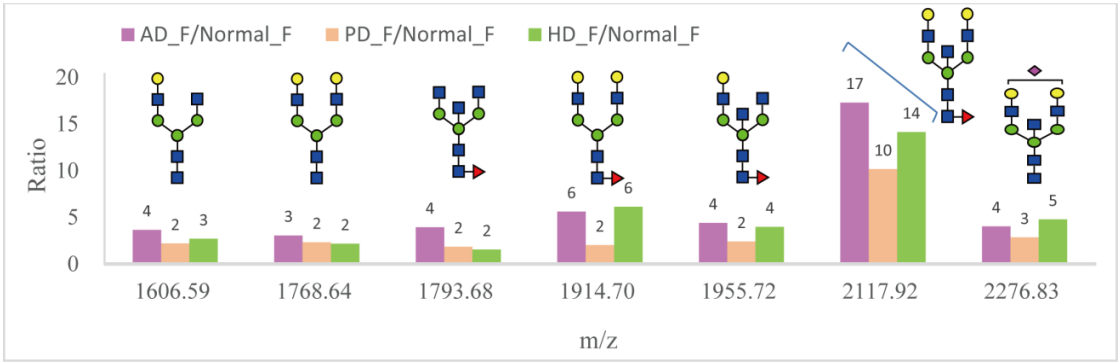

Figure 2.13. Comparison of *N*-glycan and IgG concentrations in human A) Serum (r = 0.82), B) CSF (r = 0.37) and C) Major serum *N*-glycans sourced from IgG.

2.3. Discussion

In this research, I proposed the total glycomics of neurodegenerative diseases for comprehensive structural estimation and quantitative analysis of total glycomes, viz., *N*-, *O*-, and *GSL*-glycans. From the mice brain *N*-glycomics, I found no significant difference in the amount of *N*-glycomes expression levels between the HD transgenic and WT mice. However, in serum, *N*-glycans were found in decreased levels in HD transgenic mice. Core-fucosylated, bisecting-GlcNAc and biantennary complex type *N*-glycans were slightly increased in the brain tissue of HD transgenic mice. I performed glycan-type focus lectin staining to crosscheck *N*-glycan analysis and confirmed that the localization of glycoconjugates in brain tissue were not significantly different between HD transgenic and WT mice. Conventional PAS showed no specific stained regions in brain tissue of HD transgenic and WT mice.

As stated earlier, it's likely that HD might affect significantly cortex as well as striatum, and also even other parts of the body. Comparison of the intra-brain region glycome may uncover the significance of the region-specific sensitivity of the neuronal and glial cells to the cytotoxic effect of the huntingtin aggregates. The total amount of *N*-glycans were found in increased levels in the striatum than in the cortex, which the samples were taken from the same mice brain ($p < 0.001$, Figure 2.8). The increase of *N*-glycans in the striatum is related to higher neuronal numbers [11]. Lower *N*-glycans expression levels in the cortex indicate selective vulnerability of the HD cortices (especially in the later weeks) and accumulation of gangliosides due to the low activity of specific hydrolase enzymes. The difference in total glycomes expression levels between male and female mice is useful finding as it would facilitate sex focused diagnosis and therapeutic targets.

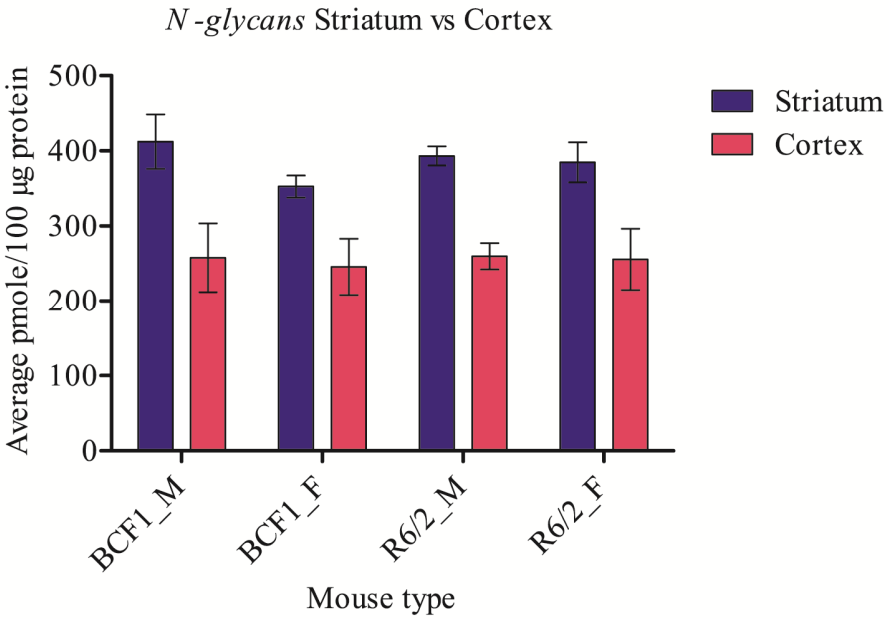

Figure 2.14. Comparison of *N*-glycans in striatum and cortex (R6/2, HD transgenic mice; BCF1, wild type mice; M, male; and F, female).

The decrease mechanism and biochemical effects of HD to other sequelae of diseases, including diabetes mellitus, changes in liver function and the aggregation of proteins in different cellular compartments (as characteristic neurodegenerative diseases neuropathological lesions involve deposition of abnormal proteins) is area of great interest. In addition to glycome profiling of the brain, serum *total-glycomics* provides an alternative method for quantifying the glycome expression levels of HD to help assess the liver function. Furthermore, the alteration of specific glycomes can predict whether HD transgenic mice are predisposed for other sequelae.

It has been known that an ominpresent huntingtin (HTT) protein is responsible for the aggregation of amyloid like proteins, termed as “protein-cancers”, in the bodies of mice. The

gradual increase in the amount of aggregates significantly affects liver (the source of most serum glycoproteins) and pancreas (where the whole sugar metabolism is governed) function. Some researchers believe that age-dependent HD neurological defects are accompanied by progressive decline in glucose tolerance that ultimately leads to diabetes mellitus and insulin deficiency [12]. This hypothesis is further supported by the observation that diabetes frequently develops in HD patients and transgenic mice [13]. In contrast, other researchers also claim that HD does not appear to increase the possible risk of diabetes mellitus, albeit their results do not exclude change in glucose tolerance in end-stage HD patients or in patients with juvenile onset on HD [14]. The present result reveals that the expression levels of FUT8 mRNA were significantly increased in the liver and *N*-glycans possessing alpha1,6-fucose was increased in diabetic mice (db/db) relative to the db/+ of the control group [15]. Core fucosylation by FUT8 might increase the survival rate of HD transgenic mice. Miyoshi *et al*. reported that in HCC, chronic hepatitis and liver cirrhosis, the expression of FUT8 is quite low in comparison to that of a normal liver. Further, increased levels of fucosylated proteins in serum can be used as tumour markers because numerous serum proteins are produced in liver [16,17]. Combined with the current serum *N*-glycomics, I conclude that HD transgenic mice share the same glycosylation effects as diabetic mice and liver function is affected with the progression of the disease. However, identifying the specific protein to which those glycans attach required further investigation.

My result showed significant reduction of glycans in human frontal cortex of neurodegenerative diseases which might be due to an early onset of progressive and severe ß-amyloid deposits, the selective vulnerability of the frontal cortex and then the spreading of the protein aggregates, as the moving aggregates, towards the other parts of the brain. One potential explanation for selective vulnerability is that the gene that triggers protein misfolding is

expressed at higher levels in areas that are affected the most [24]. The neuropathological lesions involved deposition of abnormal proteins, which can be intranuclear, cytoplasmic and extracellular, might indeed contribute for the reduction of *N*-glycans in neurodegenerative diseases [25]. Those abnormal protein aggregates lead to the degeneration of the neurons which come up with not only the loss of the neurons but also causes astrogliosis of the non-neuronal cells. As a result, the loss and functional abnormalities of both of neuronal and non-neuronal cells regulate and/or affect the activities of glycosyltransferases towards alteration in glycosylation. The pathogenesis of neurodegeneration, which are caused by either genetic or environmental cellular stressors, evoke biochemical changes in the brain cells from the cerebral cortex. It was well documented that there were an association between the perturbation of glycosylation machinery and pathology of the number of diseases [26, 27].

The lower amount of *N*-glycans with bisecting GlcNAc and core fucose residues in the frontal cortex of AD can explained by the down regulations of ß1,4- *N*-acetylglucosamine transferase III (GnTIII) and α1,6-fucosyltransferase (FUT8) activity in the brain. This result is in concordant with glycosylation difference reported in normal (PrPC) and pathogenic (PrPSc) prion protein isoforms due to the decrease in the activity of GnT-III in the prion disease process [28]. Moreover, expression of a truncated and inactive GnT-III protein in murine brain leads to the neurological dysfunction [29]. Modification of *N*-glycans by bisecting GlcNAc down regulated Aß secretion [30]. From my result, I suggest that the decrease in bisecting GlcNAc in the frontal cortices of AD might be due to the reverse effect. In frontal cortex, tri-and tetra-antennary *N*-glycans showed no significant difference that no longer process of the GlcNAc-IV and GlcNAc-V enzymes (which are encoded by *MGAT4 and MGAT5*, respectively) and they are

expressed at normal levels, which amplify the outcome of *MGAT3* gene, resulting in reduction bisecting GlcNAc type *N*-glycans in the frontal cortex in Schizophernia [31].

Human serum *N*-glycomics showed an increase in the expression levels of bisecting GlcNAc, core-fucose, tri-and tetra-antennary structures of *N*-glycans in AD compared to the Normal subjects. Beta A4 amyloid deposition in the brain, which is characteristic of AD, may result from either over expression of the amyloid protein precursor (APP) or failure of APP to be correctly processed. AD related abnormalities of APP metabolism (which can increase the Aß concentration and result in Aß deposition) in the CNS might be reflected in the circulation and Aß peptides which are secreted by cells can be detected in plasma and CSF. Study showed that 50% increase in the proportion of 130-kDa APP species in patients with AD. In addition, point mutation in the ß-APP gene found in familial Alzheimer's disease (FAD) kindred results directly in increased generation of the ß-amyloid accompanied by a decrease P3 peptide [32]. Mutant APP contained higher contents of bisecting GlcNAc and core fucose residues compared to wild type APP [33] and tri-and tetra-antennary *N*-glycans are increase in pathogenic prion protein isoforms (PrPSc) compared to the normal (PrPC) prion proteins [28]. Combining so far stated, the elevation of bisecting GlcNAc, core fucose and tri-and tetra-antennary *N*-glycans in AD might be due to an elevation of mutant APP in the circulation, which corresponds to increase in Aß and decrease in P3 peptide – the neuropathological blueprints of AD.

CSF proteomes are produced from the brain, choroid plexus in the brain ventricles originating from the blood, following active and passive transport through the blood brain barrier, and from drainage of interstitial liquid of the nervous system [34]. Since the CSF compartment is in close anatomical contact with the brain interstitial fluids, where biochemical changes related to chronic neurological diseases (CND) are reflected, CSF is a promising source

of biomarkers [35]. In CSF, the total amount of *N*-glycans expression levels were increased in AD, but not in PD and HD, when compared to the Normal subjects. I have also found high amounts of core fucose, bisecting GlcNAc and terminal galactose types of *N*-glycans in AD compared to the Normal subjects. Our result further strengthens of the high presence of "brain type" neutral *N*-glycans in CSF [31, 36-39]. The *N*-glycans difference between genders could be explained by the sex hormone levels that regulate pituitary gland hormones, in which many of them are glycosylated [31].

Two major *N*-glycans (m/z 2117.75 in serum and m/z 1793.67 in CSF) were found in increased levels in female AD, PD and HD compared to the Normal subjects. Futakawa et al. [37] reported that Tf-2 and Tf-1 have unique *N*-glycans and Tf-2/Tf-1 ratio was also used as diagnostic index for idiopathic normal pressure hydrocephalus (iNPH) and AD with their respective controls. In my CSF *N*-glycomics, I found that the ratio of m/z 2117.75 to m/z 1793.67 was significantly decreased in AD, PD and male HD compared to the Normal subjects (data not shown). Since reports declare there were no significant difference in AD CSF transferrin and Aß1-42 levels compared to the nondemented control [40] and such unique glycan (m/z 1793.67) cannot persist in blood due to the existence of specific hepatic clearance mechanism [41], those glycans are the most promising glyco-biomarkers in serum and CSF that were clearly shown a clear-cut difference between neurodegenerative diseases and the normal subjects. This study showed clearly a stronger correlation between the concentration of serum IgG and *N*-glycans. Besides, my results confirmed similar major IgG bound *N*-glycans [42] with gender difference [43]. Taken together, I deduce that the major serum *N*-glycans were sourced from IgG and IgG concentration was found elevated in neurodegenerative diseases compared to

the Normal subjects. Consequently, IgG is a key biological marker of serum of neurodegenerative diseases.

My research proved the alteration of glycome expression levels due to the accumulation of Aß in AD, α-synuclein in PD, and HTT in HD both in brain and circulation. It's obvious that the blood brain barrier (BBB) permeability is significantly increased in AD [44]. In AD, receptor for advanced glycation end products (RAGE) levels at the BBB are increased and low-density lipoprotein receptor related protein-1 (LRP1) levels at the BBB and the capacity of a soluble form of LRP1 (sLRP1) binding of peripheral Aß are reduced, favoring Aß accumulation in the brain [45]. Moreover, RAGE contributes to mechanisms involved in the translocation of Aß from the extracellular to the intracellular space, thereby enhancing Aß cytotoxicity [46]. All are resulting in aggravation of neuronal death and subsequent perturbation of sugar metabolism which in particular reduced the concentration of brain specific *N*-glycans. Moreover, elevated amyloid-ß peptides detected in peripheral tissues, serum, plasma and CSF of neurodegenerative diseases. Increased bisecting GlcNAc delays degradation of β-site APP cleaving enzyme 1(BACE1 or β-secretase) and itself by lysosomes that leads to increase the concentration of Aß [47]. In turn, accumulation of Aß in neuronal cells or specimens (either serum or CSF) triggers aberrant and/or failure of glycosylation in key proteins (yet to be identified) that could end up with an elevated concentration of core fucose, bisecting GlcNAc and tri-and tetra-antennary types of *N*-glycans in AD compared to the Normal subjects, as shown in our data, vividly.

2.4. Experimental Section

2.4.1. Mouse Sample

Animal experiments were conducted under the guidelines and with the approval of the committee on animal experiments of Hokkaido University. B6CBA-Tg (HDexon1)62Gpb/1J, aka R6/2, transgenic mice expressing the *N*-terminal region of a mutant human huntingtin gene [48] were purchased from Jackson Laboratory. R6/2 mice were bred by ovarian transplantation to B6CBAF1 (BCF1) mice by mating with BCF1 male. The length of the trinucleotide repeat was monitored by PCR amplification and gel electrophoresis of the tail DNA of the offspring, and was determined to contain 120-150 repeats. Mice were group housed in individually ventilated shoebox cages with paper bedding and a filter top. Food and water were available *ad libitum.* The neurological phenotypes of the R6/2 mice appeared between 6-9 weeks of age and the mice died at 14-18 weeks. Even though the phenotype is very complex, there are a number of components of the motor disorders. These include resting tremor, movements resembling chorea, stereotypic involuntary movements, mild ataxia, and dyskinesia of the limbs. As the disease progresses, mice are very frequently observed to eating without gaining weight or, in more severe cases, emaciated with an overall loss of muscle bulk [48]. In this study, I used 3 mice of each sex (HD transgenic and control mice) for brain tissues total glycome analysis, 5 mice of each sex (HD transgenic and control mice) for serum total glycome analysis and all experiments were performed twice.

2.4.2. Human Sample

Human tissues/fluids specimen of AD, PD, HD and Normal subjects were obtained from the Human Brain and Spinal Fluid Resource Center (HBSFRC), VA West Los Angeles Healthcare Center, Log Angeles, CA 90073, which is sponsored by NINDS/NIMH, National Multiple Sclerosis Society, USA, and the study was performed in accordance with the Ethics Committees Guidelines for our institution. The frontal, Parietal, Occipital, and Temporal cortices were dissected; serum and CSF were used directly without any prior treatment. We have analyzed 24 human subjects of four brain regions (182.3g), 19 sera (11 male, 8 female) and 19 CSF (9 male, 10 female) samples. All samples were stored at -80 °C until the day of use. The profile of all subjects, viz., sample names, brain sections, gender, autolysis time, age and other necessary information are summarize in Table 2.9.

Table 2.9. Profiles of human samples used in this study

		Weight (g)					
	Tissue	Frontal	Temporal	Parietal	Occipital	Age	Autolysis Time (hr)
Normal	M1	1.8	1.8	2.4	2.3	57	12.6
	M2	1.5	1.8	2.8	1.8	76	22.2
	M3	1.5	1.9	2.4	2.2	67	12.3
	F1	2.1	2.0	2.0	1.7	73	18.5
	F2	1.3	1.8	1.6	1.7	55	19.7
	F3	2.6	1.8	2.0	2.2	75	15.4
AD	M1	1.4	2.4	2.4	1.8	76	9.8
	M2	1.2	1.0	2.4	1.5	76	13.8
	M3	1.4	1.8	1.3	1.5	81	15.8
	F1	2.4	2.3	2.4	1.5	78	19.3
	F2	2.1	1.0	1.6	1.3	45	15.7
	F3	2.2	1.5	1.1	1.5	66	16.2
PD	M1	1.7	1.6	1.1	1.7	82	13.0
	M2	1.8	2.8	2	1.6	87	11.2
	M3	1.9	1.9	2.2	2.0	73	30.6
	F1	1.7	2.3	2.1	1.4	72	14.7
	F2	1.3	2.5	2.6	2.1	64	16.2
	F3	1.7	2.9	1.9	2.1	81	14.8
HD	M1	2.7	1.5	2.1	1.8	37	7.3
	M2	2.5	2.9	2.0	2.1	77	15.3
	M3	1.3	3.0	2.4	2.3	49	12.7
	F1	1.0	2.3	1.6	1.8	68	11.0
	F2	2.2	2.3	1.8	1.8	79	16.0
	F3	1.4	1.4	1.7	1.5	69	8.6

Key: M1, M2, M3 are male sample 1, 2, and 3; F1, F2, F3 are female samples 1, 2, and 3. Orange mark, only tissue; red mark, tissue and serum; green mark tissue and CSF.

2.4.3. Reagents and Equipment

TCEP, trypsin, PAS kit, Mayer's heamatoxylin, DTT, ConA- and SSA-biotin conjugated lectins were purchased from Sigma-Aldrich. PNGase F was purchased from New England Biolabs® Inc. (Ipswich, Massachusettes, USA). Ammonium carbamate (99%) and 1-propanesulfonic acid-2-hydroxyl-3-myristamido (PHM) were obtained from Tokyo Kasei (Chuo-ku, Tokyo, Japan). Chitooligosaccharide mixture was from Seikagaku Biobusiness (Tokyo, Japan). BlotGlyco®H bead was purchased from Sumitomo Bakelite (Tokyo, Japan). MTT and *O*-benzylhydroxylamine hydrochloride (BOA) were from Tokyo Chemical Industry Co., Ltd. Somnopentyl® (Pentobarbital sodium) and Agarose LO3 were purchased from Kyoritsu Seiyaku (Tokyo) and Takara Bio, Inc (Otsu), respectively, of Japan. DSA-, LCA-, PHA-E_4-, and PNA-biotin-conjugated lectins were from J-OIL MILLS, Inc (Chuo-ku, Tokyo, Japan). VECTASTAIN® Elite ABC and ImmPACT DAB (3, 3'-diaminobenzidine tetrahydrochloride) Peroxidase Substrate Kits were from Vector Laboratories (Burlingame, CA, USA). Human IgG ELISA quantification set (Cat. No. E80-1004) was purchased from Bethyl Laboratories, Inc., USA. Immunopen, other reagents and solvents were obtained from Wako Pure Chemicals (Tokyo, Japan) and Kanto Chemical Co., Inc., unless otherwise stated.

MultiScreen Solvinert filter plates and Mass PREP™ HILIC µElution plates were purchased from Millipore and Waters, respectively. The Ozone generator used (NG81-NO3, T-153) was from Nigorikawakogyo, Japan. Slicer VT1000S was obtained from Leica Microsystems Co. Ltd. Our fluorescence digital microscope (BA210EINT) was obtained from

Shimadzu (Tokyo, Japan), and the automated glycan-processing machine (Sweetblot) was obtained from Systems Instruments Corporation (SIC). All mass measurements were performed using MALDI-TOF/MS (Ultraflex III, Bruker Daltonics, Germany).

2.4.4. Perfusion of Mice

For lectin staining, each mouse was injected intraperitoneally with 0.1 mL Somnopentyl® using 26G½ inch needle. The mice were subsequently observed until the mice fell asleep to avoid vasoconstriction reflex and ensured that each mouse survived. Each mouse was fixed on the surgical table with a plastic vat and the abdominal skin was cut with scissors and stripped. The abdominal wall, diaphragm, and costal bone were cut to expose the heart. After the peristaltic pump was switched on and the steady flow of fixing solution (4% paraformaldehyde in 0.1 M phosphate buffer, PB) was confirmed, the right atrial appendage was cut and the needle was quickly inserted into the left ventricle. Perfusion was performed for 10 mins with a fixing solution by a peristaltic pump adjusted to a flow rate of 10 mL/min, until the internal thoracic artery and liver were whitish in color, and the body became rigid. After the neck, head skin and cranial bone were cut, the brain was removed, placed in a tube containing a fixing solution and stored at 4°C. For glycoblotting, perfusion was done with PBS instead of fixing solution. For some experiments using unperfused brain tissues, the tissues were recovered immediately after euthanization by cervical dislocation. The brain tissues for glycoblotting were stored at -80°C until they were used [49].

2.4.5. Embedding, Slicing and Lectin Staining (Avidin-Biotin Complex Method)

The desired portion of the perfused mouse brain tissues (striatum and cortex) were prepared and placed on a glass dish. A 2% agarose LO3/0.1 M PB was poured onto the brain tissue, and the gel was allowed to solidify. Tissue slicing was carried out using a LECIA VT1000S slicer (Leica Microsystems Co. Ltd, Japan, Speed: 7, Frequency: 6.5, and Feed µM: 40) after which the slices were stored at 4°C in a 24-well dish containing 0.1 M PB/0.1% NaN_3. The tissue slices were then washed with PBS and air dried. Each slide was marked with an Immunopen designed to minimize the wastage of antibody and to ensure an efficient immunoreaction. Tissue sections were suspended in a 700 µL biotin-labelled lectin solution (30 µg/mL, except ConA was 10 µg/mL) and was incubated for 1 hr on ice. Each slice was then washed with three times with PBS over a period of 5 mins and was incubated with ABC reagent (700 µL, VECASTAIN® Elite ABC kit standard) for 30 mins. PBS wash was repeated as described above. The tissue was incubated with ImmPACT DAB peroxidase substrate (700 µL) for 2 mins followed by washing in two changes of water in 5 min intervals. Following counter staining with Mayer's haematoxyline for one minute, the tissue was washed with tap water for 5 mins (every wash was carried out immersing in a small bucket containing solvent to avoid being pilled off). Next, the tissue was dehydrated by passing through 70, 80, 90 and 100% ethanol and xylene washes, successively, and in 5 min intervals for each concentration. DAB-labelled slides were mounted in a non-aqueous mounting medium (Entellan New, Merck Millipore, Germany) using a light microscope (Shimadzu BA201ES, Tokyo, Japan). Both the striatum and cortex were viewed at 40X, 100X, and 400X. [49]

PAS staining was performed based on the manufacture's protocol. Briefly, tissue sections were deparaffinized and hydrated in deionized water. The slides contained tissue sections were immersed in Periodic Acid Solution for 5 mins at room temperature. The slides were rinsed in several changes of distilled water and were immersed in Schiff's reagent for 15 mins at room temperature. After the slides were washed in running tape water for 5 mins, the slides were counter stained in Hematoxylin Solution for 90 seconds. The slides were rinsed in running tape water, dehydrated, and cleared. Finally, the slides were mounted in xylene based mounting medium in a light microscope same as described above.

2.4.6. Mouse Serum Preparation

Blood was collected from the heart of 12-week-old mice (n=5 of each sex of HD transgenic and control mice). Briefly, the mice were restrained and the heart was opened after the abdominal bone, diaphragm, and costal bone were cut. About 400-500 µL of blood was collected using 26G½ syringes while the heart was beating. The blood was allowed to clot at 4°C for 16 hours. Then, the clotted blood was centrifuged at 5,000 rpm for 5 mins. The supernatant (serum) was carefully transferred to a new Eppendorf tube and was stored at -80°C until the day of use.

2.4.7. Releasing *N*-Glycans from Brain Tissue Glycoproteins

Perfused mouse (n=3 of each sex for HD transgenic and control mice) and human brain tissues (n=3 of each sex for AD, PD, HD, and normal subjects), sub-fragmented into 2-3 mm squares with razor, were homogenized in a lysis buffer (2% SDS, 5 mM TCEP in 0.1 M Tris-acetate, pH 7.4, 100 mg/mL) using a Polytron at 25,000 rpm (MAX) over a 30 second period three times on ice. I employed 200 µL and 500 µL of tissue homogenates for mice and human *N*-glycomics, respectively. The lysates were centrifuged at 20,400 g (MAX) for 20 mins at 4°C. The amount of protein was quantified from 5 µL of the homogenates via the Bicinchoninic acid (BCA) method using Pierce®BCA protein assay kit (prod# 23227, Thermo Scienctific, USA). Ice-cold acetone (in an amount four times the volume of homogenates) was added and incubated overnight at -20°C in order to precipitate proteins. The precipitate was collected by centrifugation at 20,400 g for 20 mins at 4°C, and washed with 500 µL of ice-cold acetonitrile (ACN). Next, the precipitate was centrifuged as described above and air dried for 5 mins. The precipitate was dissolved in freshly prepared ammonium bicarbonate (ABC, 50 µL, 200 mM) containing 0.1% 1-propanesulfonic acid-2-hydroxyl-3-meristamido (PHM) in 10 mM ABC and the resulting solution was incubated at 37°C for 10 mins in a rotary shaker. Proteins were reduced by 120 mM 1, 4-dithiothrietol (DTT) at 60°C for 30 mins and were alkylated using 123 mM iodoacetamide (IAA) at room temperature in the dark for 1 hour. The mixture was digested using 10 µL trypsin (400 U/µL in 1 mM HCl) at 37°C overnight followed by heat-inactivation of the enzyme at 90°C for 10 mins. After cooling to room temperature, 2 U PNGase F was added and incubated at 37°C overnight (for mice experiment) where as 10 U PNGase F was added and incubated at 37°C for 3 hour (for human experiment). The sample was dried and stored at -30°C

until the day of use. Protein concentration was adjusted to a concentration of 100 µg (in case of mice) and 200 µg (in case of human) protein by using de-ionized water and applied to glycoblotting, as described below. For human brain, *N*-glycans amount were then normalized to 100 µg protein for convenient use.

2.4.8. Releasing *N*-Glycans from Mouse Serum Glycoproteins

Mouse serum (n=5 of each sex for R6/2 and BCF1) and human (19 samples of both sexes) were pretreated for the release of *N*-glycans followed by glycoblotting in order to enrich the *N*-glycans prior to MALDI-TOF/MS and TOF/TOF analysis. Briefly, 10 µL of mouse and human sera were diluted six times in freshly prepared ammonium carbonate (0.33 M) -1-propanesulfonic acid, 2-hydroxyl-3-meristamido (0.4% in 10 mM ABC) – DTT mixture (120 mM in de-ionized water) at a 1:1.5:1 (v/v) ratio. Internal standard (A2amide, 110 pmole) was added and the mixture was incubated at 60°C for 30 mins. Iodoacetamide (IAA, 10 µL of 123 mM) was added and incubated at room temperature for 1 hour in the dark. Trypsin (5 µL, 40 U/µL in 1 mM HCl) was added and the mixture was incubated at 37°C for 1 hour. The digested mixture was heat inactivated (90°C, 10 mins) and cooled to room temperature. PNGase F (5 U) was added and incubated at 37°C for 2 hours. 20 µL of digested mixture was applied directly to glycoblotting.

2.4.9. Glycoblotting (Enrichment, on Bead Esterification, and Labelling Total Glycomes)

500 µL of BlotGlyco® H beads (10 mg/mL) was added to the wells of a MultiScreen Solvinert filterplate and the water was removed by vacuum. Digested mixtures of brain tissue (20 µL) containg 100-500 µg protein (specified in each *N*-, *O*-, and GSL-glycan analysis) and serum IS (A2amide for *N*-glycans, GN4 for *O*- and GSL-glycans, which accurate concentration was known) were added together to each well along with 180 µL of 2% AcOH/ACN. The plate was incubated at 80°C for 45 mins followed by two successive washings using 200 µL each of 2 M guanidine-HCl in 16.6 mM ABC, water and 1% triethylamine in MeOH. After the unreactive hydrazide functional groups were acetyl capped using 10% acetic anhydride in MeOH at room temperature for 30 mins, the remaining acetic anhydride was removed by vacuum. Each well was washed two times with 10 mM HCl, MeOH and dioxane, consecutively. 150 mM MTT was added and incubated at 60°C for 90 mins for on-bead methyl esterification. Next, washing was performed using 200 µL of dioxane, water, methanol and water. For an effective transimination reaction, 20 mM Na(aminooxy-acetyl) tryptophanylarginine methyl ester (aoWR) (for mice brain tissue *N*-glycans and serum *O*-glycans) and 50 mM *O*-benzylhydroxylamine (BOA) (for all mice and human experiments, except stated above) were added and incubated at 80°C for 45 mins. Labeled glycans were eluted with 100 µL water. The aoWR-tagged solution was further purified using a hydrophilic interaction chromatography purification plate (Mass PREP™ HILIC µElution Plate, Waters, MA). The resulting glycan solutions were concentrated by SpeedVac and subsequently dissolved in 10 µL of distilled water.

2.4.10. Mass Spectrometric Analysis

The recovered glycans from either from mice or human brain tissues, serum and CSF, which were dissolved in 10 µl water (in case of mice samples) and directly from 100 µL elute (in case of all human samples), were analyzed after being spotted on MTP 384 target plate (Polished steel TF, Bruker Daltonics) and crystallized together with matrices [10 mg/mL DHB in 30% ACN for aoWR-labeled glycans, DHB/DHB-Na^+(10 mg/mL DHB-Na^+ in 30% ACN) in 9:1 for BOA-labeled glycans]. MALDI-TOF/MS data were acquired on an Ultraflex III (Bruker Daltonics, Bremen, Germany) equipped with a reflector and controlled by the FlexControl 3.0 software package according to the general protocol. All spectra were obtained using reflectron mode with an acceleration voltage of 25 KV, a reflector voltage of 26.3 KV, pulsed ion extraction of 160 ns in the positive mode and sum up to 2,000 shots of each spots. Further fragment analysis was performed by MALDI-TOF/TOF analysis (Bruker Daltonics, Bremen, Germany). Annotation of the MS and TOF/TOF data was done using the FlexAnalysis 3.0 software package (Bruker Daltonics GmbsH, Bremen, Germany, S/N= 6 and quality factor threshold of 30). The experimental masses were used to predict the possible glycan compositions of reported on http://web.expassy.org/glycomod/ and CFG(http://www.functionalglycomics.org). The Lipid Bank(http://lipidbank.jp/) and in-house database were used for GSL-glycans structure. Glycan profiling was performed basically by focusing on exclusively known glycan structures from brain/nervous system and serum of *Mus musculus* and *Ratus norvegicus* and other mammals (especially known glycoforms sourced from human brain). After the peak for the detected glycans were selected, absolute quantification was performed by comparative analysis, i.e., the area under each isotopic peak was normalized to the internal standard. Glycan expression

levels were determined analytically as neurodegenerative diseases versus the control group and the corresponding statistical significance was calculated using the student t-test.

2.4.11. Human Immunoglobulin G (IgG) Quantification

100 µL of diluted Affinity purified Goat anti-Human IgG-Fc coating antibody was added to each well of the ELISA microplates in duplicate and was incubated at room temperature (r.t., 20-25 °C) for 1 hour. The microplate was washed five times with 200 µL washing solution (50 mM Tris, 0.14 M NaCl, 0.05% Tween, pH 8.0), consecutively. A 200 µL blocking solution (50 mM Tris, 0.14 M NaCl, 1% bovine serum albumin, pH 8.0) was added and incubated at r.t. for 30 mins. Each well was washed 5 times with washing solution and then 100 µL of standard and test samples were added and incubated at r.t. for 1 hour. After 5 times successive washing, 100 µL of diluted HRP conjugated Goat anti-Human IgG-Fc detection antibody was added to each well and was incubated at r.t. for 1 hour. The microplate was washed as described above. 3,3',5,5'-tetramethylbenzidine (TMB, 100 µL) substrate solution was added to each well and was allowed to develop color at r.t. in the dark for 15 mins. The reaction was stoppd by 100 µL stop solution (0.18 M sulfurc acid) within 5 mins. Finally, absorbance was measured using the plate reader at 450 nm.

2.5. References

[1] R. Kornfeld, S. Kornfeld, Assembly of aspargine-linked oligosaccharides, Ann. Rev. Biochem. 54 (1985) 631 – 664.

[2] P. Stanley, H. Schachter, N. Taniguchi, N-glycans, in: A. Varki, R. D. Cummings, J.D. Esko, H.H. Freeze, P. Stanley, C.R. Bertozzi, G.W. Hurt, M.E. Etzler (Eds.), Essentials of Glycobiology, 2nd Ed., Cold Spring Harbor Laboratory Press, Cold Spring Harbor, New York, 2008, pp.101 – 114.

[3] W. Morelle, V. Faid, F. Chirat, J.-C. Michalski, Analysis of N-and O-linked glycans from glycoproteins using MALDI-TOF mass spectrometry, in: N.H. Packer, N.G. Karlsson (Eds.), Glycomics: Methods and protocols, Humana Press, New York, 2009, pp.5 – 9.

[4] S.J. North, S. Chalabi, M. Sutton-Smith, A. Dell, S.M. Haslam, M, Mouse and Human Glycomes, in: R.D. Cummings, J.M. Pierce (Eds.), Handbook of Glycomics, Academic Press, New York, 2009, pp 263 – 327.

[5] S.-I. Nishimura, K. kiikura, M. Kurogochi, T. Masushita, M. Fumoto, H. Hinou, R. kamitani, H. Nakagawa, K. Deguchi, N. Miura, K. Monde, H. Konde, High-throughput protein glycomics: Combined use of chemoselective glycoblotting and MALDI-TOF/TOF mass spectroscopy, Angewu.Chem. Int.Ed. 44 (2005) 91 – 96.

[6] Y. Miura, M. Hato, Y. Shinohara, H. Kuramoto, J.-i. Furukawa, M. Kurogochi, H. Shimaoka, M. Tada, K. Nakanishi, M. Ozaki, S. Todo, S.-I. Nishimura, BlotGlycoABC™, an integrated glycoblotting technique for rapid and large scale clinical glycomics, Mol. Cell. Proteomics 7 (2008) 370 – 377.

[7] J.-i. Furukawa, Y. Shinohara, H. Kuramoto, Y. Miura, H. Shimaoka, M. Kurogochi,M. Nakano, S.-I. Nishimura, Comprehensive approach to structural and functional glycomics based on chemoselective glycoblotting and sequential tag conversion, Anal. Chem. 80 (2008) 1094 – 1101.

[8] M. Amano, M. Yamaguchi, Y. Takegawa, T. Yamashita, M. Terashima, J.-i. Furukawa, Y. Miura, Y. Shinohara, N. Iwasaki, A. Minami, S.-I. Nishimura, Threshold in stage-specific embryonic glycotypes uncovered by a full portrait of dynamic *N*-glycan expression during cell proliferation, Mol. Cell. Proteomics 9 (2010) 523 – 537.

[9] K. Hirose, M. Amano, R. Hashimoto, Y.C. Lee, S.-I. Nishimura, Insight into glycan diversity and evolutionary lineage based on comparative Avio-N-glycomics and sialic acid analysis of 88 Egg Whites of Galloanserae, Biochemistry 50 (2011) 4757 – 4774.

[10] Y. J. Chen, D. R. Wing, G. R. Guile, R. A. Dwek, D. J. Harvey, S. Zamze, Neutral *N*-glycans in adult rat brain tissue - complete characterization reveals fucosylated hybrid and complex structures, Eur. J. Biochem. 251 (1998) 691 – 703.

[11] H. Heinsen, M. Strik, M. Bauer, K. Luther, G. Ulmar, D. Gangnus, G. Jungkunz, W. Eisenmenger, M. Götz, Cortical and striatal neurone number in Huntington's disease, Acta Neuropathol. 88 (1994) 320 – 333.

[12] O. A. Andreassen, A. Dedeoglu, V. Stanojevic, D. B. Hughes, S. E. Browne, C. A. Leech, R. J. Ferrante, J. F. Habener, M. F. Beal, M. K. Thomas, Huntington's disease of the endocrine pancrease: Insulin deficiency and diabetes mellitus due to impaired insulin gene expression, Neurobiology of Disease 11 (2002) 410 – 424.

[13] M. Bjorkqvist, M. Fex, E. Renstrom, N. Wierup, A. Petersen, J. Gil, K. Bacos, N. Popovic, J-Y. Li, F. Sundler, P. Brundin, H. Mulder, The R6/2 transgenic mouse model of huntington's disease develops diabetes due to deficient β - cell mass and exocytosis, Human Molecular Genetics 14 (2005) 565 – 574.

[14] T. W. Boesgaard, T. T. Nielsen, K. Josefsen, T. Hansen, T. JØrgensen, O. Pedersen, A. NØrremØlle, J. E. Nielsen, L. Hasholt, Huntington's disease doesn't appear to increase the risk of diabetes mellitus, Journal of Neuroendocrinology 21 (2009) 770 – 776.

[15] N. Itoh, S. Sakaue, H. Nakagawa, M. Kurogochi, H. Ohira, K. Deguchi, S.-I. Nishimura, M. Nishimura, Analysis of *N*-glycan in serum glycoproteins from db/db mice and humans with type 2 diabetes, Am J Physiol Endocrinol Metab 293 (2007) E1069 – E1077.

[16] E. Miyoshi, K. Moriwaki, T. Nakagawa, Biological function of fucosylation in cancer biology, J. Biochem. 143 (2008) 725 – 729.

[17] E. Miyoshi, N. Uozumi, K. Noda, N. Hayashi, M. Hori, N. Taniguchi, Expression of alpha1-6 fucosyltransferase in rat tissues and human cancer cell lines, Int. J. Cancer 72 (1997) 1117 – 1121.

[18] R. Spector, C.E. Johanson, The mammalian choroid plexus, Sci.Am. 261 (1989) 68 – 74, IN: (J.L. Stanta, R. Saldova, W. B. Struwe, J.C. Byrne, F.M. Leweke, M. Rothermund, H. Rahmoune, Y. Levin, P.C. Guest, S. Bahn, P.M. Rudd, Identification of *N*-Glycosylation Changes in the CSF and Serum in Patients with Schizophrenia, J. Proteome Res. 9 (2010) 4476 – 4489).

[19]. H. Tumani, C. Teunissen, S. Süssmuth, M. Otto, A.C. Ludolph, J. Brettschneider, Cerebrospinal fluid biomarkers of neurodegeneration in chronic neurological diseases, Expert Rev Mol Diagn. 8 (2008) 479 – 94.

[20] A. Fogli, C. Merle, V. Roussel, R. Schiffmann, S. Ughetto, M. Theisen, O. Boespflug-Tanguy, CSF N-Glycan Profiles to Investigate Biomarkers in Brain Developmental Disorders: Application to Leukodystrophies Related to eIF2B Mutations, PLoS ONE 7 (2012) e42688.

[21]. S. Futakawa, K. Nara, M. Miyajima, A. Kuno, H. Ito, H. Kaji, K. Shirotani, T. Honda, Y. Tohyama, K. Hoshi, Y. Hanzawa, S. Kitazume, R. Imamaki, K. Furukawa, K. Tasaki, H. Arai, T. Yuasa, M. Abe, H. Arai, H. Narimatsu, Y. Hashimoto, A unique N-glycan on human transferrin in CSF: a possible biomarker for iNPH, Neurobiology of Aging 33 (2012) 1807 – 1815.

[22] A. Hoffmann, M. Nimtz, R. Getzlaff, H.S. Conradt, 'Brain-type' N-glycosylation of asialo-transferrin from human cerebrospinal fluid, FEBS Letters 359 (1995) 164 – 168.

[23]. S. Zamze, D.J. Harvey, P. Pesheva, T.S. Mattu, M. Schachner, R.A. Dwek, D.R. Wing, Glycosylaton of a CNS-specific extracellular matrix glycoprotein, tenascin-R, is dominated by *O*-linked sialylated glycans and “brain-type” neutral *N*-glycans, Glycobiology 9 (1999) 823 – 831.

[24] W.S. Jackson, Selective vulnerability to neurodegenerative disease: the curious case of prion protein, Dis Model Mech. 7 (2014) 21 – 29.

[25] C.A. Ross, M.A. Poirier, Protein aggregation and neurodegenerative disease, Nat Med. 10 (2004) S10 – S17.

[26] R. Barone, L. Sturiale, A. Palmigiano, M. Zappia, D. Garozzo, Glycomics of pediatric and adulthood diseases of the central nervous system, J Proteomics 75 (2012) 5123 – 5139.

[27] J. Jaeken, Congenital disorders of glycosylation (CDG): it's all in it! J Inherit Metab Dis 34 (2011) 853 – 858.

[28] P.M. Rudd, T. Endo, C. Colominas, D. Groth, S.F. Wheeler, D.J. Harvey, M.R. Wormald, H. Serban, S.B. Prusiner, A. Kobata, R.A. Dwek, Glycosylation difference between normal and pathogenic prion protein isoforms, Proc Natl Aca Sci USA. 96 (1999) 13044 – 13049.

[29] R. Bhattacharyya, M. Bhaumik, T.S. Raju, P. Stanley, Truncated, inactive *N*-acetylglucosaminyltransferase III (GlcNAc-TIII) induces neurological and other traits absent in mice that lack GlcNAc-TIII, J. Biol.Chem. 277 (2002) 26300 – 26309.

[30] K. Akasaka-Manya, H. Manya, Y. Sakurai, B.S. Wojczyk, Y. Kozutsumi, Y. Saito, N. Taniguchi, S. Murayama, S. L. Spitalnik, Tamao Endo, Protective effect of N-glycan bisecting GlcNac residues on ß-amyloid production in Alzheimer's disease, Glycobiology 20 (2010) 99 – 106.

[31] J.L. Stanta, R. Saldova, W.B. Struwe, J.C. Byrne, F.M. Leweke, M. Rothermund, H. Rahmoune, Y. Levin, P.C. Guest, S. Bahn, P.M. Rudd, Identification of *N*-Glycosylation Changes in the CSF and Serum in Patients with Schizophrenia. J. Proteome Res. 9 (2010) 4476 – 4489.

[32] M. Citron, T. Oltersdorf, C. Haass, L. McConlogue, A.Y. Hung, P. Seubert, C. Vigo-Pelfrey, I. Lieberburg, D.J. Selkoe, Mutations of the ß-amyloid precursor protein in familial Alzheimer's disease increases ß-protein production, Nature 360 (1992) 672 – 674.

[33] K. Akasaka-Manya, H. Manya, Y. Sakurai, B.S. Wojczyk, S. L. Spitalnik, Tamao Endo, Increased bisecting and core-fucosylated *N*-glycans on mutant human amyloid precursor proteins, Glycoconj J 25 (2008) 775 – 786.

[34] R. Spector, C.E. Johanson, The mammalian choroid plexus. Sci.Am. 261 (1989) 68 – 74. IN: (J.L. Stanta, R. Saldova, W. B. Struwe, J.C. Byrne, F.M. Leweke, M. Rothermund, H. Rahmoune, Y. Levin, P.C. Guest, S. Bahn, P.M. Rudd, Identification of *N*-Glycosylation Changes in the CSF and Serum in Patients with Schizophrenia, J. Proteome Res. 9 (2010) 4476 – 4489).

[35] H. Tumani, C. Teunissen, S. Süssmuth, M. Otto, A.C. Ludolph, J. Brettschneider, Cerebrospinal fluid biomarkers of neurodegeneration in chronic neurological diseases, Expert Rev Mol Diagn. 8 (2008) 479 – 494.

[36] A. Fogli, C. Merle, V. Roussel, R. Schiffmann, S. Ughetto, M. Theisen, O. Boespflug-Tanguy, CSF N-Glycan Profiles to Investigate Biomarkers in Brain Developmental Disorders: Application to Leukodystrophies Related to eIF2B Mutations, PLoS ONE 7 (2012) e42688.

[37] S. Futakawa, K. Nara, M. Miyajima, A. Kuno, H. Ito, H. Kaji, K. Shirotani, T. Honda, Y. Tohyama, K. Hoshi, Y. Hanzawa, S. Kitazume, R. Imamaki, K. Furukawa, K. Tasaki, H. Arai, T. Yuasa, M. Abe, H. Arai, H. Narimatsu, Y. Hashimoto, A unique N-glycan on human transferrin in CSF: a possible biomarker for iNPH, Neurobiology of Aging 33 (2012) 1807 – 1815.

[38] A. Hoffmann, M. Nimtz, R. Getzlaff, H.S. Conradt, 'Brain-type' N-glycosylation of asialo-transferrin from human cerebrospinal fluid, FEBS Letters 359 (1995) 164 – 168.

[39] S. Zamze, D.J. Harvey, P. Pesheva, T.S. Mattu, M. Schachner, R.A. Dwek, D.R. Wing, Glycosylaton of a CNS-specific extracellular matrix glycoprotein, tenascin-R, is dominated by *O*-linked sialylated glycans and “brain-type” neutral *N*-glycans, Glycobiology. 9 (1999) 823 – 831.

[40] M. Taniguchi, Y. Okayama, Y. Hashimoto, M. Kitaura, D. Jimbo, Y. Wakutani, K. Wada-Isoe, K. Nakashima, H. Akatsu, K. Furukawa, H. Arai, K. Urakami, Sugar chains of

cerebrospinal fluid trasferrin as a new biological marker of Alzheimer's disease, Dement Geriatr Cogn Disord 26 (2008) 117 – 122.

[41] G. Ashwell, J. Harford, Carbohydrate-specific receptors in the liver, Annu. Rev. Biochem. 51 (1982) 531 – 554.

[42] G. Chen, Y. Wang, L. Qiu, X. Qin, H. Liu, X. Wang, Y. Wang, G. Song, F. Li, Y. Guo, F. Li, S. Guo, Z. Li, Human Ig G Fc-glycosylation profiling reveals associations with age, sex, female sex hormones and thyroid cancer, J Proteomics 75 (2012) 2824 – 2834.

[43] S. Bekesova, O. Kosti, K.B. Chandler, J. Wu, H.L. Madej, K.C. Brown, V. Simonyan, R. Goldman, *N*-glycans in liver-secreted and immunoglobulin-derived protein fractions, J Proteomics 75 (2012) 2216 – 2224.

[44] A.J. Farrall, J.M. Wardlaw, Blood-brain barrier: Ageing and micorvascular disease-systematic review and meta-analysis. Neurobiology of Aging. 30 (2009) 337 – 352.

[45] R. Deane, R.D. Bell, A. Sagare, B.V. Zlokovic, Clearance of amyloid-ß peptide across the brain-brain barrier: Implication for therapies in Alzheimer's disease. CNS Neurol Disord Drug Targets. 8 (2009) 16 – 30.

[46] K. Takuma, F. Fang, W. Zhang, S. Yan, E. Fukuzaki, H. Duc, A. Sosunov, G. McKhann, Y. Funatsu, N. Nakamichi, T. Nagai, H. Mizoguchi, D. Ibi, O. Hori, S. Ogawa, D.M. Stern, K. Yamada, S.S. Yan, RAGE-mediated signaling contributes to intraneuronal transport of amyloid-ß and neuronal dysfunction, PNAS 106 (2009) 20021 – 20026.

[47] Y. Kizuka, S. Kitazume, R. Fujinawa, T. Saito, N. Iwata, T. C Saido, M. Nakano, Y. Yamaguchi, Y. Hashimoto, M. Staufenbiel, H. Hatsuta, S. Murayama, H. Manya, T. Endo, N.

Taniguchi, An aberrant sugar modification of BACE1 blocks its lysosomal targeting in Alzheimer's disease, EMBO Mol Med 7 (2015) 175 – 189.

[48] L. Mangiarini, K. Sathasivam, M. Seller, B. Cozens, A. Harper, C. Hetherington, M. Lawton, Y. Trottier, H. Lehrach, S. W. Davies, G. P. Bates, Exon 1 of the HD gene with an expanded CAG repeat is sufficient to cause a progressive neurological phenotype in transgenic mice, Cell 87 (1996) 493 – 506.

[49] S. A. Brooks, D. M. Hall, Lectinhistochemistry to detect altered glycosylation in cells and tissues, Methods Mol Biol. 878 (2012) 31 – 50.

Chapter 3

O-Glycomics of Neurodegenerative Diseases

3.1. Introduction

O-glycosylation is a common covalent modification of serine and threonine residues of mammalian glycoproteins, though modification of hydroxyproline and hydroxylysine is observed in limited cases [1]. The *O*-glycans are structurally diverse (i.e., they do not contain a uniform core structure like that of the *N*-linked glycans) and have been functionally implicated in a plethora of biological processes [2]. Mucin glycosylation is based on a relatively simple set of core structures in which *N*-acetylgalactosamine (GalNAc) is linked to the side chain of serine and threonine (Tn antigen) and bears a single ß1,3-linked Gal residue to form a core 1 (T antigen) structure [3]. Interestingly, mammals have genes encoding for approximately 20 different polypeptide-*N*-acetylgalactosaminetransferase (ppGalNAc), all of which transfer GalNAc from UDP-GalNAc to a hydroxyl-containing amino acid [4]. Homologs of ppGalNAcT genes are expressed in all eukaryotic organisms and a high degree of sequence identity exists between mouse and human ppGalNAcTs [1]. The Tn antigen can then be further modified or elongated to produce up to eight core types in mammals. This biosynthetic pathway involves numerous enzymes localized in the Golgi, which contribute to the complexity and variety of *O*-glycosylation [5]. (Figure 3.1)

Because the *O*-glycans are hydrophilic and usually negatively charged, they are not only aiding in water retention but also the mucins serve us lubrication and also help to protect from invasion by microorganisms. From a pathophysiological perspective, *O*-GalNAc modification appears to play a critical role in the immune system, cell-cell interactions, and cancer [6]. The multiply modification of *O*-GlcNAc glycosylation regulates the phosphorylation of Tau protein in site specific manner [7].

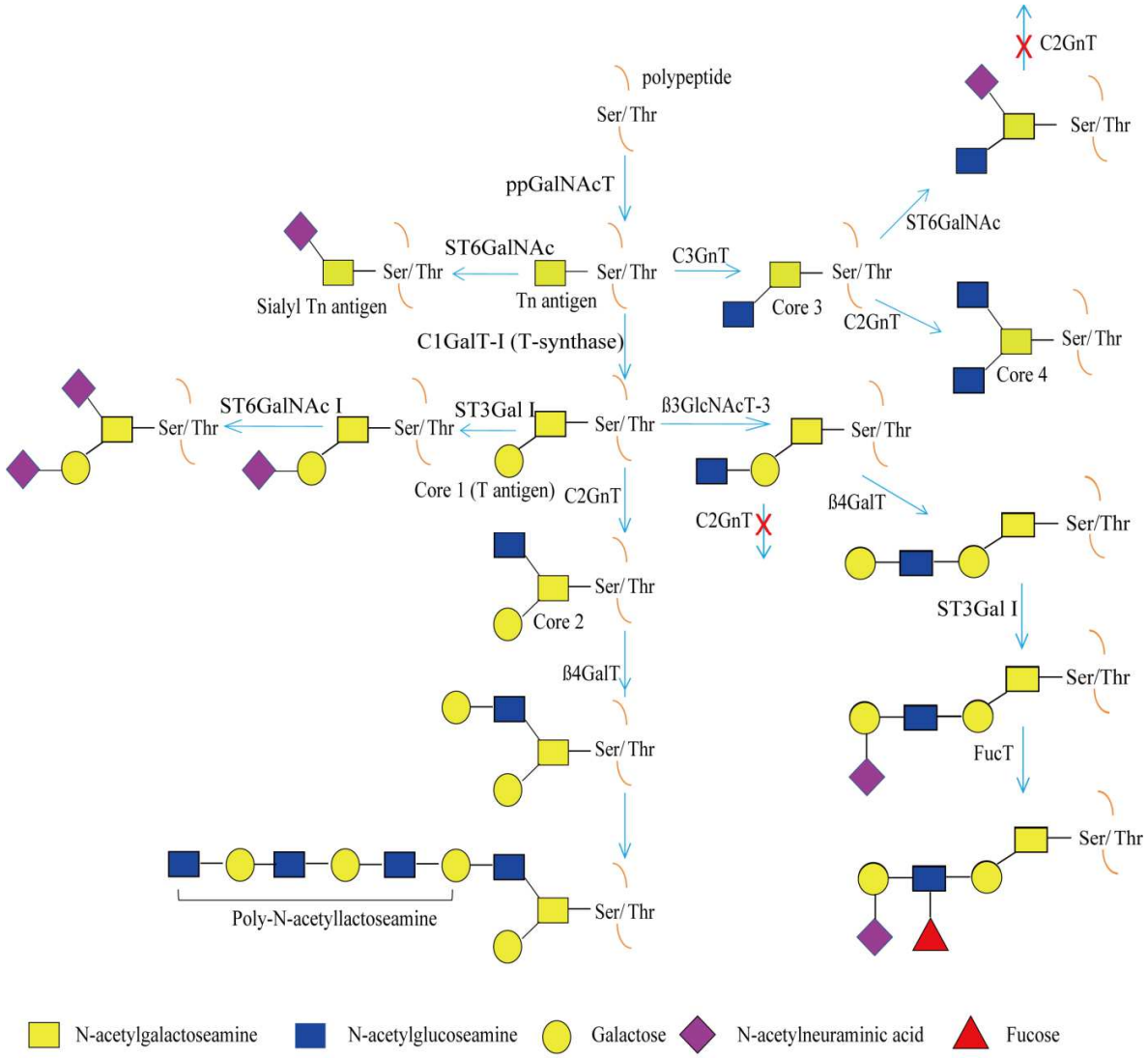

Figure 3.1. Sequential synthesis of complex *O*-linked glycans. The linkage of *N*-acetylgalactosamine to serine or threonine to form the Tn antigen, catalyzed by polypeptide-*N*-acetylgalactosaminyltransferases (ppGalNAcTs), is the basis for all core structures. Core 1 (T antigen), core 2, core 3 and core 4 (the four common core structures) synthesized by core 1 ß1,3-galactosyltransferase (C1GalT-1), core 2 ß1,6-*N*-acetylglucosaminyltransferase (C2GnT), core 3 ß1,3-*N*-acetylglucosaminyltransferase (C3GnT), and core 2/4 ß1,6- *N*-acetylglucosaminyltransferase (C2GnT-2). “X” indicates blocked pathways.

Human serum *O*-glycan analysis is indispensable to estimate the compostion and amount of *O*-glycans for the discovery of biological markers. Mucin-type *O*-glycosylation is one of the most common protein PTM and plays important roles in many biological processes, viz., signal transduction, cell-cell interaction (selectins and their ligands), immunity and angiogenesis. In addition, mucins have been used for identification of disease markers in human ovarian astricites [8] and the Tn and sialyl Tn antigens occur in human and animal pathologies are recognized as disease markers [9].

With this, I put efforts to profile *O*-glycans in neurodegenerative diseases brain tissues and serum using non-reductive ß-elimination by employing ammonium carbamate [10] followed by glycoblotting-based glycan enrichment analysis of *O*-glycans [11-13]. In Chapter 3, I discuss about *O*-glycans (particularly mucin-types) profiled from brain tissues and serum of HD transgenic and WT mice, and also human brain tissue and serum of AD, PD, HD and Normal subjects.

3.2. Results

3.2.1. Brain Tissue and Serum *O*- Glycomics of HD Transgenic and WT Mice

I have profiled the possible mucin type *O*-glycans from the brain and sera of HD transgenic and WT mice. The total amount of mucin type *O*-glycans in the striatum and cortex was found in increased levels in male and decreased in female of HD transgenic mice (Chapter 2 Table 2.2.). The estimated composition of mucin type *O*-glycans in brain tissue(striatum and cortex) and serum were summarized in Table 3.1 and Table 3.2, respectively. Regarding the brain tissue, Tn antigen (HexNAc, m/z 349.1) was only found to have decreased in the cortex of R6/2 ♀ compared to the same section of BCF1 ♀. Core 1 or T antigen (HexNAcHex, m/z 511.221) was exclusively detected in the HD transgenic mice. Core 3 ($HexNAc_2$, m/z 552.2) increased in R6/2 ♂ of in both striatum and cortex whereas it decreased in R6/2 ♀. Levels of HexNAcNeuAc (sialyl Tn, m/z 640.3), which is supposed to be the final product that can no longer be an acceptor for other glycosyltransferases, increased in HD transgenic mice, except in the cortex of the female R6/2 mice (Table 3.1. B).

From 100 µL of serum, mucin type *O*-glycans levels were found in decreased levels in HD transgenic mice, albeit statistically insignificant. However, core 1 (HexHexNAc) decreased in R6/2 as compared to BCF1 and, core 2 ($Hex_1HexNAc_2$) was not detected in HD transgenic mice. In addition to mucin type, we also found other modification such as *O*-mannosyl, *O*-fucosyl, and *O*-GlcNAcylation, all of which are potential markers.

Table 3.1. Composition of brain tissue *O*-glycans (BOA-labeled) of HD Transgenic and control mice ('SC', present in both striatum and cortex; 'S', only in striatum; 'C', only in Cortex; and '-', neither striatum nor cortex.

A) Estimated composition of brain tissue *O*-glycans

		Control		HD	
m/z	Composition	BCF1_♂	BCF1_♀	R6/2_♂	R6/2_♀
349.105	(HexNAc)1	SC	SC	SC	SC
511.221	(Hex)1 (HexNAc)1	-	-	SC	S
552.223	(HexNAc)2	SC	SC	SC	SC
615.307	(Hex)1 (NeuGc)1	C	-	-	-
640.294	(HexNAc)1 (NeuAc)1	SC	SC	SC	SC
656.364	(HexNAc)1 (NeuGc)1	-	C	C	C
657.339	(Hex)1 (HexNAc)1 (Deoxyhexose)1	C	-	-	-
714.411	(Hex)1 (HexNAc)2	-	C	C	C
755.403	(HexNAc)3	-	C	C	C
1590.78	(Hex)3 (HexNAc)4 (Deoxyhexose)1	C	SC	C	C
1793.93	(Hex)3 (HexNAc)5 (Deoxyhexose)1	SC	SC	SC	SC
1899.06	(Hex)4 (HexNAc)4 (Deoxyhexose)2	-	C	-	-
2011.12	(Hex)2 (HexNAc)4 (Deoxyhexose)1 (Neu	C	SC	C	C
2102.1	(Hex)4 (HexNAc)5 (Deoxyhexose)2	SC	SC	SC	SC

B) Amount (pmole ± SD, from 100 µg protein) of selected brain tissue *O*-glycans.

	Striatum		Control		HD	
m/z	Composition	Common name	BCF1_♂	BCF1_♀	R6/2_♂	R6/2_♀
349.11	(HexNAc)1	Tn antigen	34.69 ± 13.99	31.28 ± 16.44	40.38 ± 18.75	28.84 ± 13.53
552.22	(HexNAc)2	Core 3	208.29 ± 78.06	171.09 ± 70.91	293.91 ± 203.38	130.23 ± 67.89
640.29	(HexNAc)1 (NeuAc)1	Sialyl Tn	3.70 ± 2.20	4.53 ± 3.65	17.89 ± 9.81	8.74 ± 3.12

	Cortex					
m/z	Composition	Common name	BCF1_♂	BCF1_♀	R6/2_♂	R6/2_♀
349.11	(HexNAc)1	Tn antigen	19.57 ± 6.65	19.45 ± 5.57	20.15 ± 11.91	11.12 ± 4.61
552.22	(HexNAc)2	Core 3	119.59 ± 94.35	125.81 ± 99.44	142.15 ± 99.44	94.49 ± 35.75
640.29	(HexNAc)1 (NeuAc)1	Sialyl Tn	3.523 ± 2.56	3.58 ± 2.23	5.13 ± 3.65	3.05 ± 1.63

Table 3.2. Estimated composition of serum *O*-glycans (aoWR-labeled) of HD transgenic and control mice (pmole ± SD, "- " is to show not detected).

			Control		HD	
MS_MW	Composition	Common name	BCF1_♂	BCF1_♀	R6/2_♂	R6/2_♀
813.37	(Hex)1 (HexNAc)1	Core 1	3.67 ± 2.08	1.57 ± 1.49	0.31 ± 0.18	0.21 ± 0.03
854.40	(HexNAc)2		0.41 ± 0.29	0.30 ± 0.19	0.20 ± 0.05	0.15 ± 0.07
959.43	(Hex)1 (HexNAc)1 (Deoxyhexose)1		0.07 ± 0.023	0.04 ± 0.00	-	0.02 ± 0.00
975.42	(Hex)2 (HexNAc)1		0.27 ± 0.13	0.15 ± 0.08	0.04 ± 0.01	0.05 ± 0.0
1016.45	(Hex)1 (HexNAc)2	Core 2	0.07 ± 0.01	0.04 ± 0.01	-	-
1057.48	(HexNAc)3		0.21 ± 0.14	0.10 ± 0.01	0.09 ± 0.02	0.10 ± 0.01
1134.48	(Hex)1 (HexNAc)1 (NeuGc)1		0.66 ± 0.47	0.55 ± 0.26	0.39 ± 0.14	0.65 ± 0.50
1137.48	(Hex)3 (HexNAc)1		0.23 ± 0.14	0.21 ± 0.00	0.20 ± 0.02	0.16 ± 0.04
1162.51	(Hex)1 (HexNAc)2 (Deoxyhexose)1		0.09 ± 0.04	0.04 ± 0.01	0.02 ± 0.00	0.02 ± 0.01
1296.53	(Hex)2 (HexNAc)1 (NeuGc)1		0.53 ± 0.19	0.28 ± 0.05	0.26 ± 0.04	0.34 ± 0.16
1455.58	(Hex)1 (HexNAc)1 (NeuGc)2		0.05 ± 0.02	0.12 ± 0.05	0.21 ± 0.07	0.38 ± 0.11
1499.61	(Hex)2 (HexNAc)2 (NeuGc)1		0.16 ± 0.13	0.07 ± 0.00	0.07 ± 0.00	0.05 ± 0.00
1527.64	(Hex)2 (HexNAc)3 (Deoxyhexose)1		0.06 ± 0.00	0.12 ± 0.07	0.07 ± 0.01	0.07 ± 0.02

3.2.2. Human Parietal Cortex *O*-Glycan Analysis of AD, PD and HD and Normal Subjects

From parietal cortex *O*-glycans, 26 *O*-glycans were estimated and their expression levels were quantified. The major *O*-glycans include core 1 (T antigen), Core 3, sialyl Tn, core 4, sialyl T antigen, di-sialyl T and extended core 1 or core 3 (Figure 3.2). The expression levels of the major *O*-glycans are tabulated on Table 3.3. Di-sialyl T is the most abundant mucin-type *O*-glycan in human brain tissue.

Table 3.3. Expression levels of the major *O*-glycans (pmole ± SD, from 100 µg protein) found in human parietal cortex of AD, PD, HD and the Normal subjects (M, male, and F, female).

Common name	m/z	Normal_M	AD_M	PD_M	HD_M
Sialyl T	816.42	5.24 ± 1.67	6.92 ± 2.13	5.45 ± 1.25	8.15 ± 3.78
Di-Sialyl T	1121.62	24.51 ± 7.96	24.18 ± 7.46	29.16 ± 7.16	34.26 ± 13.00
	Total	29.74 ± 9.55	31.10 ± 9.54	34.61 ± 8.31	42.41 ± 16.75

Common name	m/z	Normal_F	AD_F	PD_F	HD_F
Sialyl T	816.42	6.27 ± 0.41	8.10 ± 2.04	7.09 ± 1.04	5.98 ± 1.339
Di-Sialyl T	1121.62	27.29 ± 3.10	39.32 ± 13.32	30.40 ± 6.69	300.82 ± 7.25
	Total	33.56 ± 3.32	47.53 ± 15.31	37.49 ± 7.69	36.80 ± 8.51

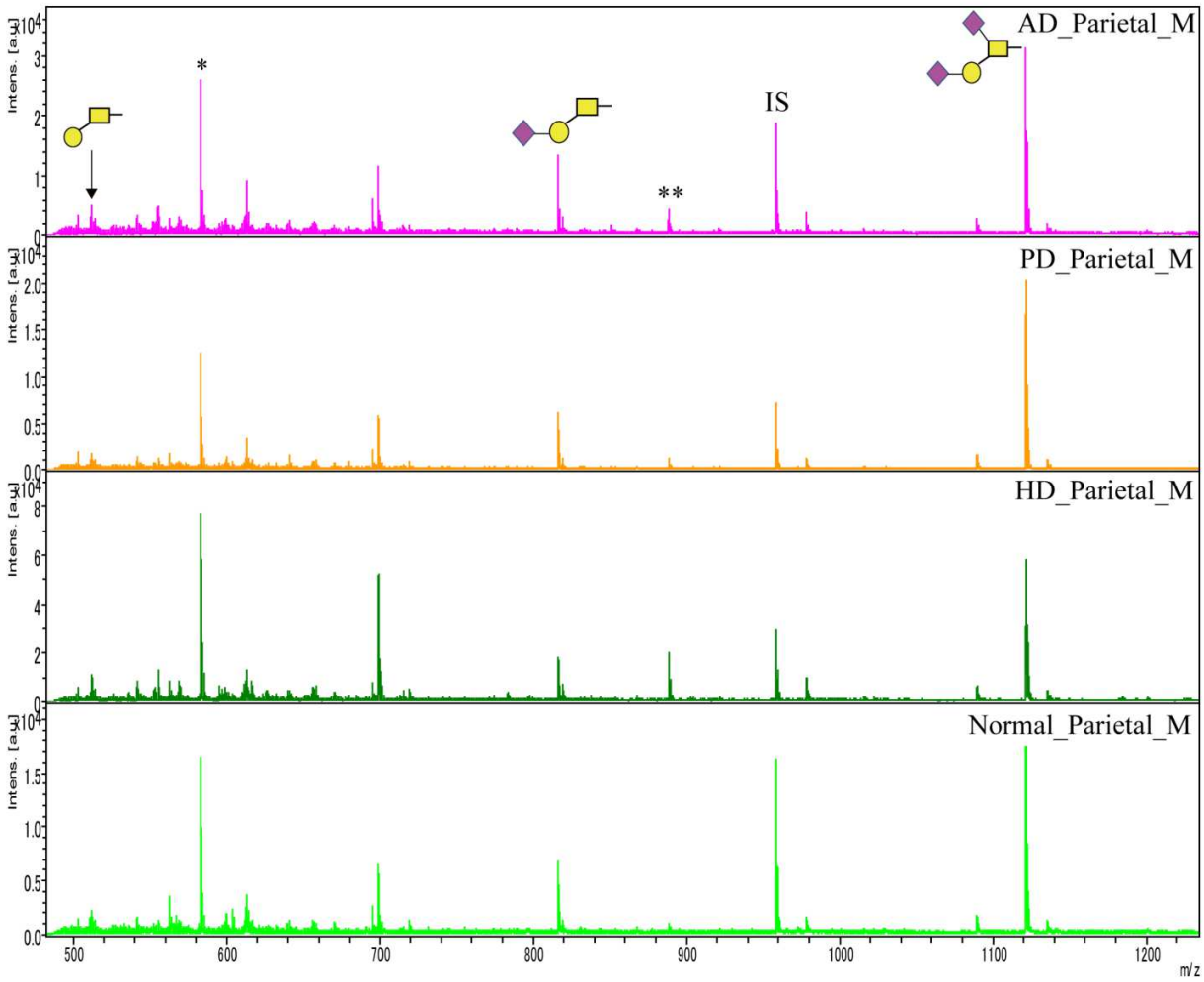
AD_Parietal_M
PD_Parietal_M
HD_Parietal_M
Normal_Parietal_M
Intens. [a.u.]
*
**
IS
500
600
700
800
900
1000
1100
1200
m/z

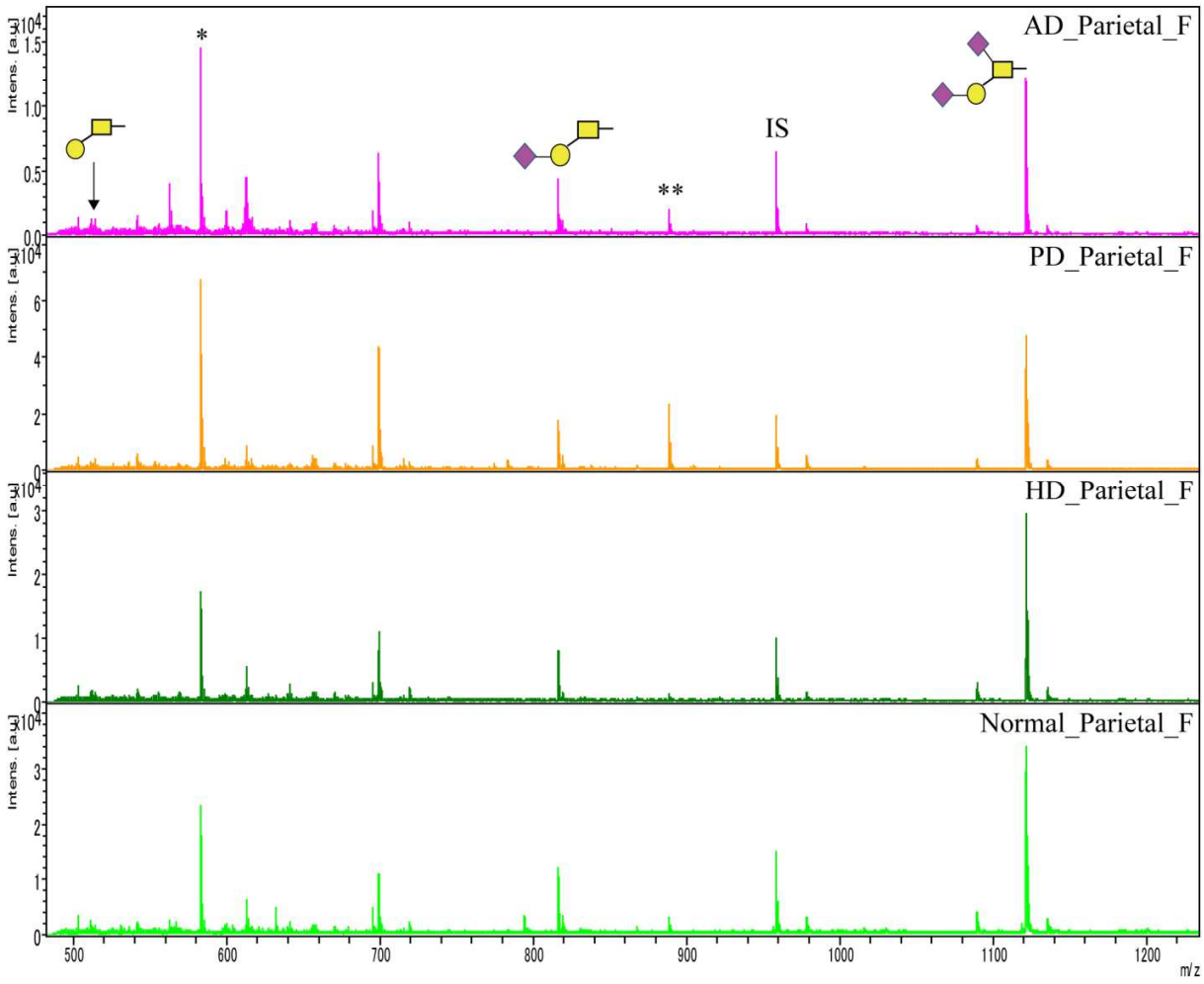

Figure 3.2. MALDI-TOF MS spectra parietal cortex *O*-glycans. Structure of major *O*-glycans showed. "**" the sialylated sugar of "*"; however, the later was not yet identified. IS, internal standard; M, male; and F, female. Glycan cartoons were constructed using the standard Consortium for Functional nomenclature, i.e., yellow square, *N*-acetylgalactosamine; yellow circle, galactose; and purple diamond, *N*-acetylneuraminic acid.

3.2.3. Human Serum *O*-Glycan Analysis of AD, PD and HD and Normal Subjects

Human serum *O*-glycomics is indispensable to estimate the composition and amount of *O*-glycans for the discovery of biological markers. To identify disease specific glyco-biomarkers, the composition of 10 mucin-type *O*-glycans were estimated from human serum of AD, PD, HD and Normal subjects. The major *O*-glycans include core 1 (T antigen), Core 3, Sialyl Tn, core 4, Sialyl T, di-sialyl T and extended core 1 or core 3 (Figure 3.3). The total expression levels of mucin-type *O*-glycans are tabulated on Table 3.4 and it highly dependent on the nature of the samples. Sialyl T is the most abundant mucin-type *O*-glycan (> 76 % in all samples) and sialyl T focus analysis is needed. *O*-glycans expression levels were different in intra-samples. This is because patients were diagnosed not only neurological but also clinical complications. For example, diabetes Type II, hypertension, kidney failure and heart attack. All of these are sequela of CNS disorders. Moreover, their autolysis time was different.

Table 3.4. Amount of *O*-glycans (pmole ± SD) in each human sera of AD, PD, HD and the Normal subjects. " – " cell show that no sample is paired with the brain tissue. AD, Alzheimer's disease; PD, Parkinson's disease; HD, Huntington's disease; Normal, control; M, male and F, female.

Sample name	M1	M2	M3
Normal	31.95 ± 6.17	432.97 ± 0.00	512.80 ± 66.28
AD	282.04 ± 152.63	307.69 ± 24.42	68.44 ± 3.20
PD	10.39 ± 1.28	207.03 ± 16.68	702.47 ± 78.81
HD	–	27.93 ± 1.47	152.25 ± 11.29

Sample name	F1	F2	F3
Normal	822.84 ± 81.00	89.77 ± 1.59	–
AD	529.86 ± 95.33	544.36 ± 7.17	–
PD	–	581.67 ± 64.74	125.06 ± 7.85
HD	432.32 ± 0.00	–	436.51 ± 8.63

A.

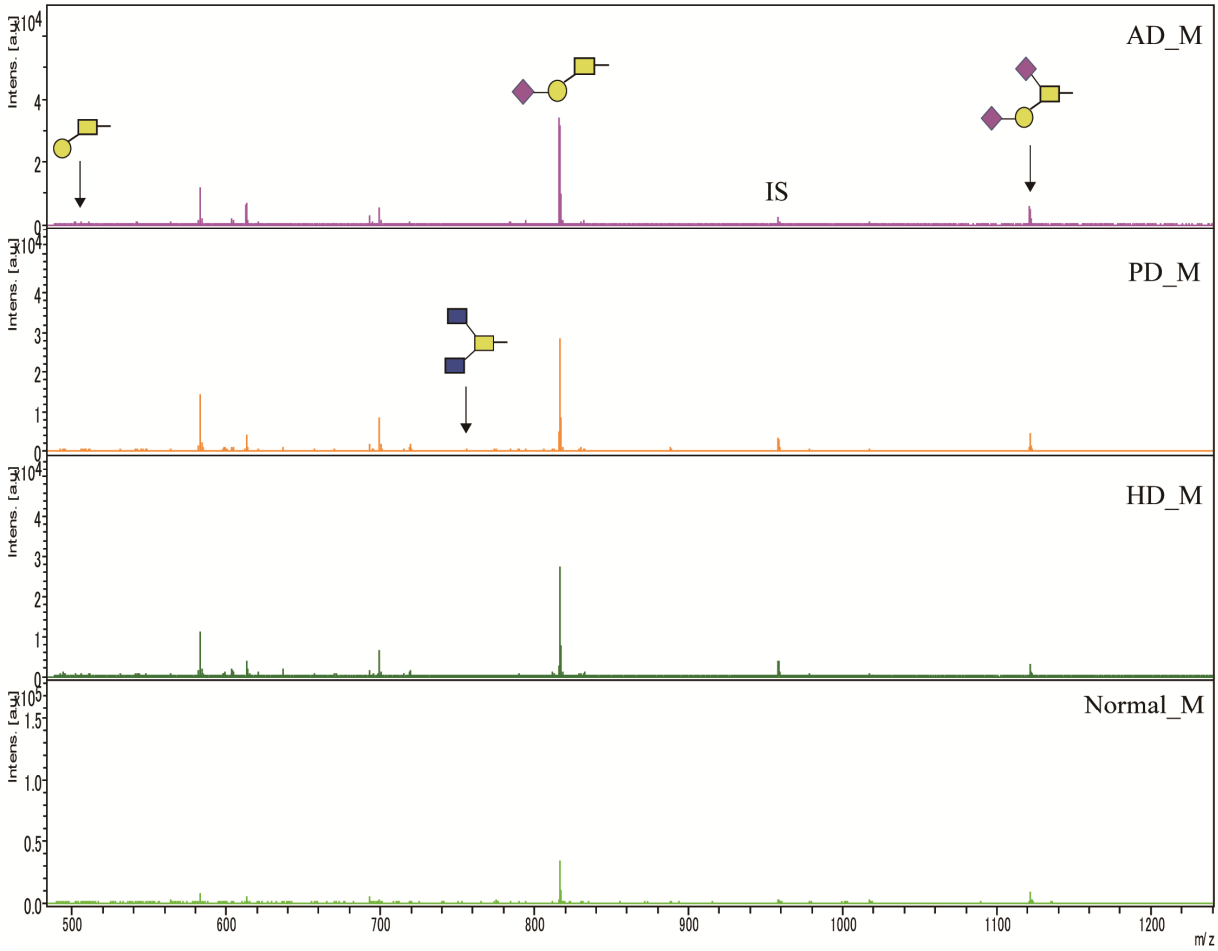
AD_M
IS
PD_M
HD_M
Normal_M
Intens. [a.u.]
m/z
500
600
700
800
900
1000
1100
1200

B.

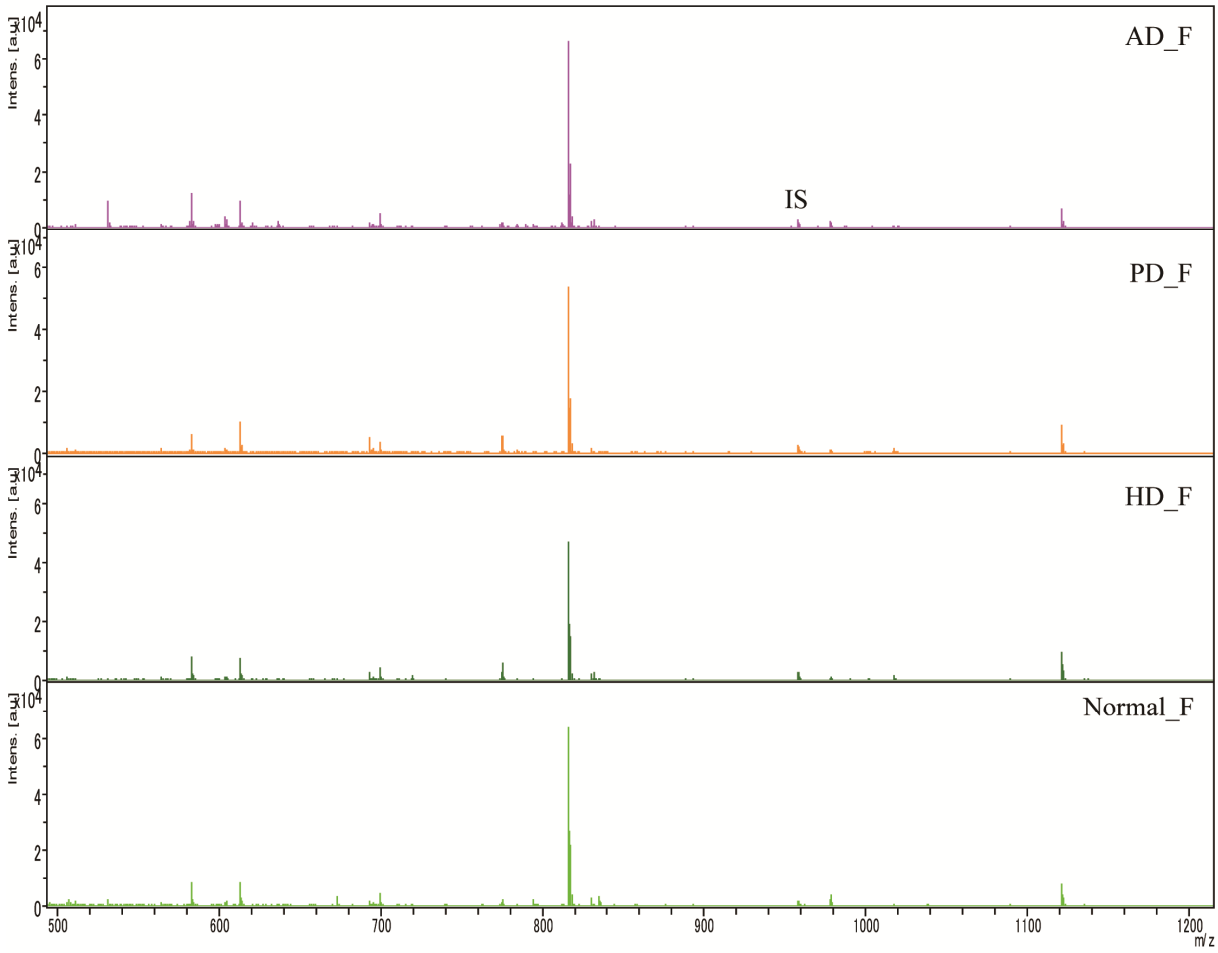

Figure 3.3. MALDI-TOF MS spectra of male (A) and female (B) human serum *O*-glycans. Structure of major *O*-glycans showed. IS, internal standard; M, male; and F, female. Glycan cartoons were constructed using the standard Consortium for Functional nomenclature, i.e., yellow square, *N*-acetylgalactosamine; yellow circle, galactose; and purple diamond, *N*-acetylneuraminic acid.

.

3.4. Discussion

The total amount of *O*-glycans found in the striatum and cortex was elevated in males and lower in females from the HD transgenic mice group compared to the WT mice. I found that the amount of *O*-glycans was reduced in the serum of HD transgenic mice. The most dominant mucin type of *O*-glycan in the brain tissue was found to be Core 3 (GlcNAcβ1→3GalNAc) which was elevated in male HD transgenic mice and lower in female HD transgenic mice compared to the corresponding WT mice group. Consequently, core 3 could serve as a promising mucin type *O*-glycan biomarker for HD pathophysiology. With respect to serum *O*-glycomics, core 1 levels were decreased and, core 2 was not detected in HD transgenic mice at all. The total amount of *O*-glycans released from the striatum of HD transgenic and WT mice were higher relative to the cortex, albeit statistically insignificant (Figure 3.5).

Human brain tissues and sera *O*-glycans analysis have been used to identify disease specific glycosylation alterations. From this study, while di-sialyl T was found the major *O*-glycan in human parietal cortex, sialyl T was found highly expressed in human serum. The ratio of di-sialyl T to sialyl T was found to be high in brain tissue, and the reverse is true in serum. From this particular observation, I could able to deduce that the activity of Core 1 α2-3 sialyltransferase (ST3GalT I) and α2-6 sialyltransferase (ST6GalNAc I) were higher in human serum and brain tissues, respectively.

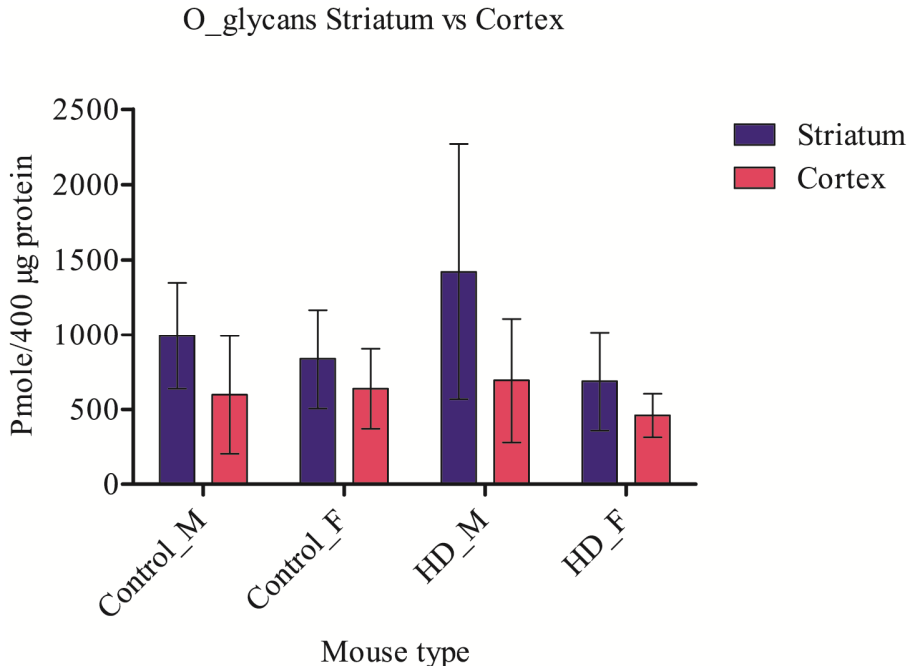

Figure 3.5. Comparison of *O*-glycans between striatum and cortex of HD transgenic and control mice. M, male; and F, female.

3.3. Experimental Sections

3.3.1. Releasing *O*-Glycans from Brain Tissue and Serum Glycoproteins

Sample preparation was performed as described in Chapter 2. Ammonium carbamate ('a' +5 mg, where 'a' is volume (in µL) of original homogenate used) was added to glycoproteins mixture and incubated at 60°C for 40 hrs. The digested mixture was subsequently washed (four times with 500 µL water) and neutralized (one time with 500 µL 150 mM acetic acid) with each process being accompanied by drying via SpeedVac. The dried sample was stored at -30°C until the day of use. 400 µg of protein was used for glycoblotting protocol as described in Chapter 1. The amount of *O*-glycans were then normalized to 100 µg protein for convenient use.

3.3.2. Releasing *O*-Glycans from Human Serum Glycoproteins

50 µL of serum was directly used without prior treatment and was added 50 mg ammonium carbamate. The mixtures was incubated at 60°C for 40 hours. The digested mixture was subsequently washed (four times with 500 µL water) and neutralized (one time with 500 µL 150 mM acetic acid) with each process being accompanied by drying via SpeedVac. 20 µL of digested mixture was applied directly to glycoblotting the same as decribed in Chapter 2.

3.4. References

[1] I. Brockhausen, Schachter, and P. Stanley, O-GalNAc glycans, in Essential of glycobiology (Eds. A. Varki, R.D. Cummings, J.D. Esko, H.H. Freeze, P. Stanley, C.R. Bertozzi, G.W. Hart, and M.E. Etzler, 2nd ed.), Cold Spring Harbor Laboratory Press, Cold Spring Harbor, New York, 2009, pp. 115 – 127.

[2] Lance Wells, *O*-glycan complexity and analysis, in Hand book of glycomics (Eds.: R. D. Cummings, J. M. Pierce), Academic Press, New York, 2009, pp. 263 – 327.

[3] Maureen E. Taylor and urt Drickamer. Introduction to glycobiology. Oxford University Press Inc., New York, pp. 33 – 50.

[4] Kelly G. Ten Hagen, Timothy A. Fritz, and Lawrence A. Tabak, All in the family: the UDP-GalNAc : polypeptide N-acetylgalactoseaminlyl transferases. Glycobiology 2003, 13: 1R-16R.

[5] Tian E, Ten Hagen K. 2009. Recent insights into the biological roles of mucin-type O-glycosylation. Glycoconj J. 26(3):325 – 334.

[6] Franz-Georg Hanisch, O-Glycosylation of the Mucin Type. Biol. Chem., 2001, 382: pp.143 – 149.

[7] Fei Liu, Khalid Iqbal, Inge Glyrundke-Iqbal, Gerald W. Hart, Cheng-Xin Gong, *O*-GlcNAcylationn regulates phosphorylation of tau: A mechanism involved in Alzheimer's disease, PNAS 101 (2004) 10804 – 10809.

[8] N.G. Karlsson, M.A. McGuckin, O-Linked glycome and proteome of high-molecular-mass proteins in human ovarian cancer ascites: Identification of sulfation, disialic acid and O-linked fucose, Glycobiology 22 (2012) 918 – 929.

[9] T. Ju, Y. Wang, R.P. Aryal, S.D. Lehoux, X. Ding, M.R. Kudelka, C. Cutler, J. Zeng, J. Wang, X. Sun, J. Heimburg-Molinaro, D.F. Smith.R.D. Cummings, Tn and sialyl-Tn antigens, aberrant O-glycomics as human disease markers, Proteomics Clin. Appl. 2013, 7, 618 – 631.

[10] Y. Miura, K. Kato, Y. Takegawa, M. Kurogochi, J.-i. Furukawa, Y. Shinohara, N. Nagahori, M. Amano, H. Hinou, S.-I. Nishimura, Glycoblotting – assisted O- glycomics: Ammonium carbamate allows for highly efficient release from glycoproteins, Anal. Chem. 82 (2010) 10021 – 10029.

[11] S.-I. Nishimura, K. kiikura, M. Kurogochi, T. Masushita, M. Fumoto, H. Hinou, R. kamitani, H. Nakagawa, K. Deguchi, N. Miura, K. Monde, H. Konde, High-throughput protein glycomics: Combined use of chemoselective glycoblotting and MALDI-TOF/TOF mass spectroscopy, Angewu.Chem. Int.Ed. 44 (2005) 91 – 96.

[12] Y. Miura, M. Hato, Y. Shinohara, H. Kuramoto, J.-i. Furukawa, M. Kurogochi, H. Shimaoka, M. Tada, K. Nakanishi, M. Ozaki, S. Todo, S.-I. Nishimura, BlotGlycoABC™, an integrated glycoblotting technique for rapid and large scale clinical glycomics, Mol. Cell. Proteomics 7 (2008) 370 – 377.

[13] J.-i. Furukawa, Y. Shinohara, H. Kuramoto, Y. Miura, H. Shimaoka, M. Kurogochi,M. Nakano, S.-I. Nishimura, Comprehensive approach to structural and functional glycomics based on chemoselective glycoblotting and sequential tag conversion, Anal. Chem. 80 (2008) 1094 – 1101.

Chapter 4

Glycosphingolipidomics of Neurodegenerative Diseases

4.1. Introduction

Glycosphingolipids (*GSLs*) are a subtype of glycolipids found in cell membranes of organisms from bacteria to humans, which are further classified into neutral (no charged or ionic group), sialylated (having one or more sialic acid residues), or sulfated [1]. The most abundant negatively charged *GSLs* are the gangliosides and the sulfoglycosphingolipids. Gangliosides are sialic acid containing *GSLs* particularly prevalent in neuronal cells. In nervous system, they contribute to 10-20% of the lipid content [2]. During brain development, the ganglioside pattern changes from the simple gangliosides like GM3 and GD3 to more complex ones like GD1a and GT1b. Non-neuronal cells and mammalian serum are the sources of gangliosides, albeit lower concentration [3]. They belong to the so-called ganglio-, lacto-, and neolacto-series. Other glycolipid series found in human tissues are the globo-, isoglobo-, and muco-series, which are all derived from lactosylceramide [4] (Table 4.1).

Table 4.1. Glycosphingolipids (*GSLs*) series of higher eukaryotes

Glycosphingolipid (GSL) series of higher eukaryotes	
Series	Core structure
Gala	Galα1,4Galß1,1'Cer
Ganglio	Galß1,3GalNAcß1,4Galß1,4Glcß1,1'Cer
Globo	GalNAcß1,3Galα1,4Galß1,4Glcß1,1'Cer
Isoglobo	GalNAcß1,3Galα1,3Galß1,4Glcß1,1'Cer
Lacto	Galß1,3GlcNAcß1,3Galß1,4Glcß1,1'Cer
Neolacto	Galß1,4GlcNAcß1,3Galß1,4Glcß1,1'Cer
Muco	Galß134Galß1,4Galß1,4Glcß1,1'Cer

Glycosphingolipids are synthesized in Golgi apparatus by the combinatorial biosynthesis pathway [5] in which multiple glycosyltransferases involved in the transfer of carbohydrate residues onto a ceramide anchor, which is transferred to the outer leaflet of the plasma membrane. GSLs are not uniformly distributed in the membrane, but cluster in “lipid rafts” [1]. In higher animals, most series are derived from lactosylceramide, in which lactose is ß-glycosidically linked to the 1-hydroxyl group of ceramides except in Gala series that is derived from ß-galactosylceramide [4].

Ceramide (Cer) is the acceptor for UDP-Gal:ceramide β-galactosyltransferase or UDP-Glc:ceramide β-glucosyltransferase in the major pathways to glycosphingolipid biosynthesis in oligodendrocytes and nerve cells, respectively. GalCer is the acceptor for GalCer sulfotransferase, which adds a sulfate group to the C-3 of galactose to form sulfatide. Extension of GlcCer to the major brain gangliosides occurs by the action of UDP-Gal:GlcCer β1,4 galactosyltransferase to make lactosylceramide (LacCer), then CMP-NeuAc:lactosylceramide α2,3 sialyltransferase to make the simple ganglioside GM3. GM3 is a branch point and acts as the acceptor for UDP-GalNAc: GM3/GD3 β1, 4 *N*-acetylgalactosaminyltransferase to generate a-series gangliosides and for CMP-NeuAc: GM3 α2, 8 sialyltransferase to generate GD3 and the b-series gangliosides. Similarly, the action of α2, 8 sialyltransferase on GD3 gives rise to GT3 and the c-series gangliosides. Enzymes for subsequent elongation are common to a-, b-, and c-series gangliosides. In mammals and birds, the major gangliosides in brain are GM1, GD1a, GD1b, and GT1b [1] (Figure 4.1).

In brain, high levels of glycolipid biosynthesis normally accompanied by similarly high rates of glycolipid turnover, which occurs by transport of the glycolipids to the lysosome where they are broken down by specific hydrolases. Genetic lesions leading to the absence or low

activity of practically any one of these hydrolases result in blockage of the breakdown pathways and accumulation of undigested lipids in the lysosomes [6].

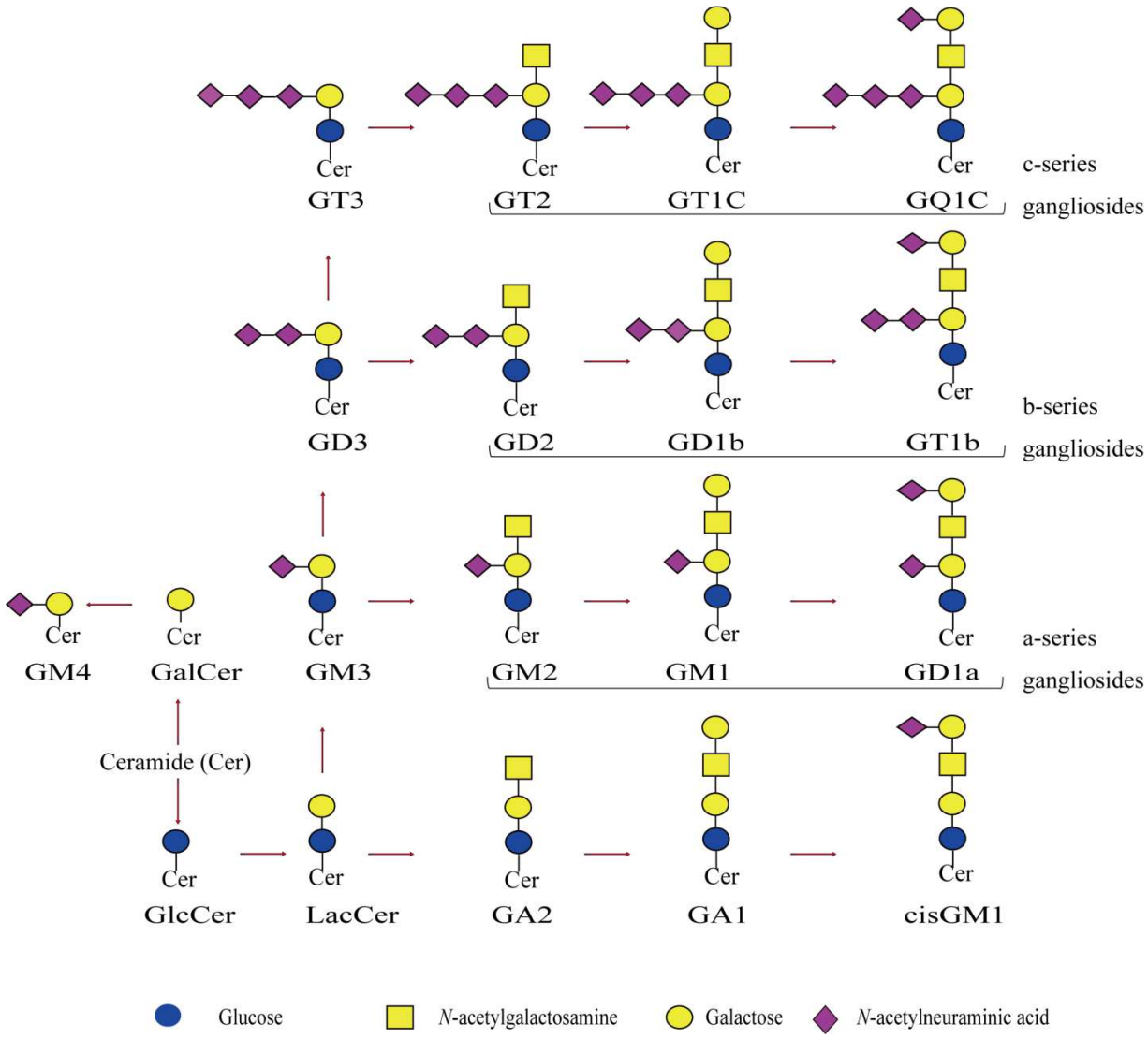

Figure 4.1. Major biosynthetic pathways of brain glycosphingolipids.

The expression levels of *GSLs* are correlated with protein folding diseases [7] and *GSL* abnormalities are one of the etiologies of AD [8]. However, the structural complexity and diversity of cellular glycolipids, differences in abundance, chemical stability and biophysical properties between analytes make *GSL* analysis often neglected [4]. Moreover, the available endoglycoceramidase are inefficient and costly. Here, we have applied the glycosphingolipidomics (*GSL-omics*) approach to analyze the *GSL*-glycans of neurodegenerative diseases sourced from brain tissue and serum by using chloroform/methanol total lipids extraction, liberation of carbohydrate moieties by ozonolysis to give rise to *GSL* aldehydes, which are subsequently fragmented by alkaline treatment [9,10] and glycans enrichment by glycoblotting [11-13].

4.2. Results

4.2.1. Brain Tissue Glycosphingolipidomics of HD Transgenic and WT Mice

The carbohydrate moieties of unprotected (native) *GSLs* were released by extraction of total lipids from brain tissue and serum, with subsequent liberation by ozonolysis giving rise to *GSL*-aldehyde and glycan release by alkaline degradation. Using the glycoblotting technique, *GSL*-glycans were efficiently captured and further structural and quantitative analysis by MALDI-TOF/MS and TOF/TOF analysis was performed. From the brain tissue, I have profiled GM3, GM2, GMl, GD1a, GD2 (except in striatum of male mouse), GA1 (only in the cortex of both sexes) and Type IIA glycosyl ceramide (only in the striatum of male mice). With the exception of the cortex of R6/2 ♂, the total amount of oligosaccharides released from *GSLs* increased in the striatum and cortex of R6/2 ♂ compared to that of BCF1 (Chapter 2 Table 2.2). Focusing on a-series gangliosides expression levels, the relative abundance was found to be GD1a >> GM1 > GM2 > GM3. GD1a is exclusively increased in the striatum (brain region that is most severely affected by HD) (Table 4.2). The possible sequence of GD1a is shown in Figure 4.2. Ganglioside expression levels were found to differ between male and female mice as well as between intra-brain regions.

Table 4.2. Quantitative comparison of a-series gangliosides (pmole ± SD, from 100 µg protein equivalent) in brain tissue of HD transgenic (R6/2) and control mice (BCF1).

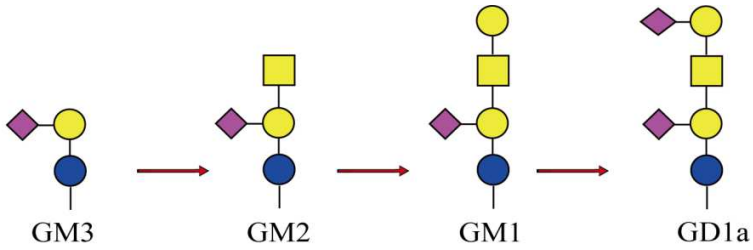

Striatum

Gangliosides	BCF1_♂	BCF1_♀	R6/2_♂	R6/2_♀
GM3	0.552 ± 2.26	1.63 ± 0.18	0.61 ± 1.05	0.65 ± 0.58
GM2	6.97 ± 1.55	15.60 ± 2.99	34.34 ± 10.08	10.83 ± 0.73
GM1	68.22 ± 9.60	120.00 ± 26.14	269.83 ± 64.22	120.05 ± 25.47
GD1a	177.42 ± 23.62	269.96 ± 98.65	531.69 ± 75.76	330.57 ± 107.10

Cortex

Gangliosides	BCF1_♂	BCF1_♀	R6/2_♂	R6/2_♀
GM3	3.48 ± 0.67	1.63 ± 1.26	2.21 ± 1.54	4.40 ± 0.52
GM2	27.70 ± 8.83	16.54 ± 5.02	17.29 ± 5.66	32.64 ± 7.24
GM1	34.47 ± 45.75	266.23 ± 77.60	291.92 ± 64.37	451.21 ± 101.65
GD1a	963.96 ± 147.39	759.69 ± 273.37	791.99 ± 209.37	1222.51 ± 273.00

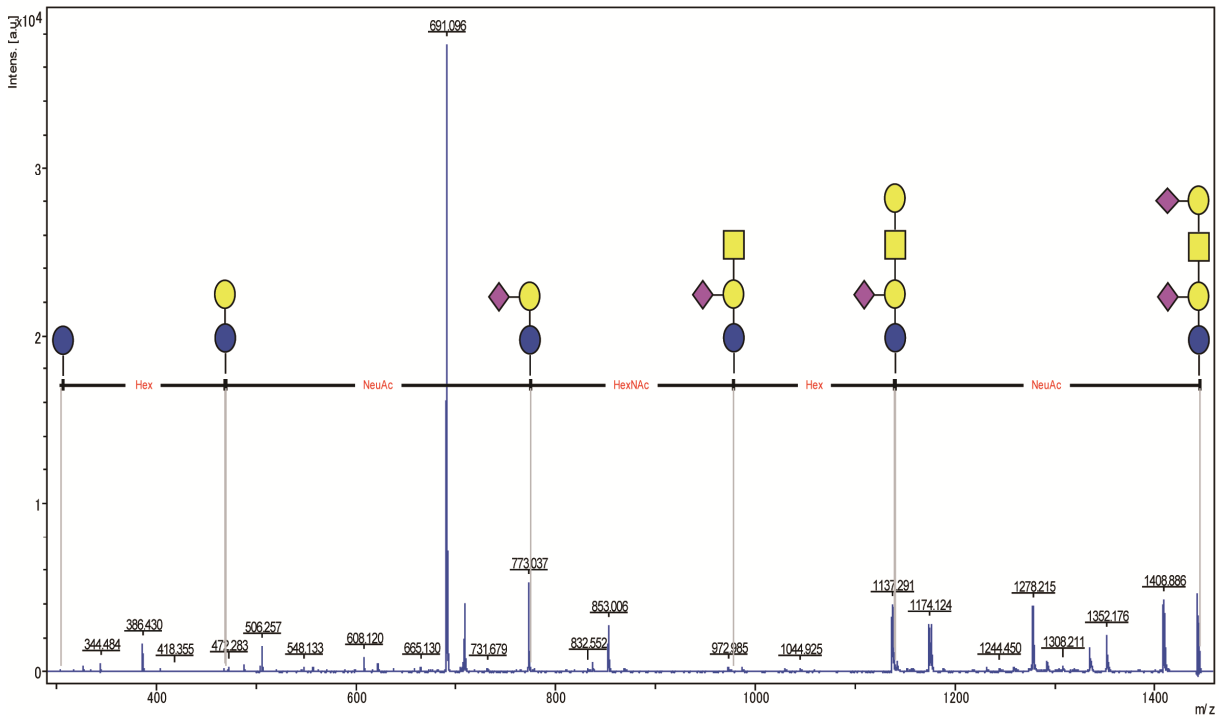

Figure 4.2. TOF/TOF analysis of GD1a (m/z 1445.5, the major peak in brain *GSL*-glycomes)

4.2.2. Serum Glycosphingolipidomics of HD Transgenic and WT Mice

According to the same approach used in the brain GSL-omics, the amount of serum gangliosides (containing NeuAc and NeuGc) and globo-series were estimated (Figure 4.3, and Figure 4.4 for TOF/TOF analysis of GM2-NeuGc). The compositions and amounts of *GSL*-glycans (pmoles ± SD) are summarized in Table 4.3. Total *GSL*-glycans were decreased by 39% and 36% in male and female HD transgenic mice, respectively, compared to that of the control

group mice. This reduction was highly pronounced for NeuGc-containing a-series gangliosides, such as GM2-NeuGc, GM1-NeuGc, GD1a-NeuGc. GM2-NeuGc was found to be the most abundant ganglioside (>76%), decreasing 32% and 40% in male and female HD transgenic mice, respectively, compared to that of the control group mice. From these results, we determined GM2-NeuGc to be a promising candidate as a potential glyco-biomarker in HD and should be studied further.

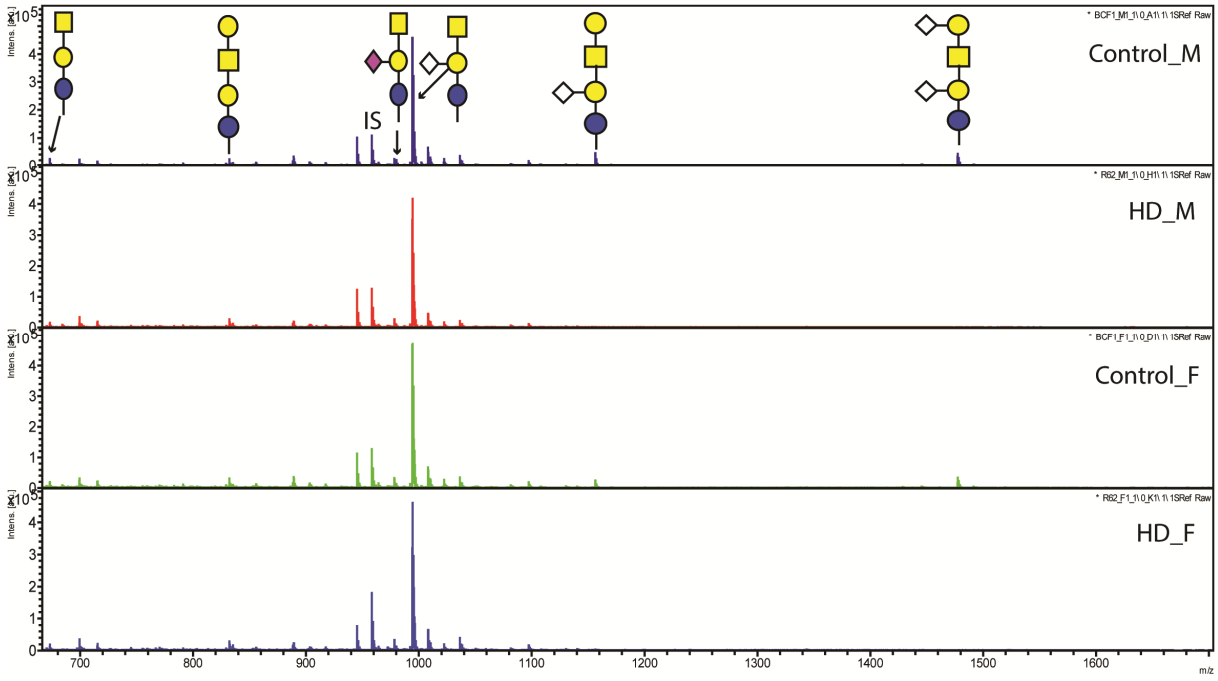

Figure 4.3. MALDI-TOF MS spectrum of serum *GSL*-glycans in R6/2 and BCF1 (IS, internal standard; M, male; and F, female). Glycan cartoons were constructed using the standard Consortium for Functional nomenclature, i.e., blue circle, glucose; yellow circle, galactose;

yellow square, *N*-acetylgalactosamine; purple diamond, *N*-acetylneuraminic acid; and white diamond, *N*-glycolylneuraminic acid.

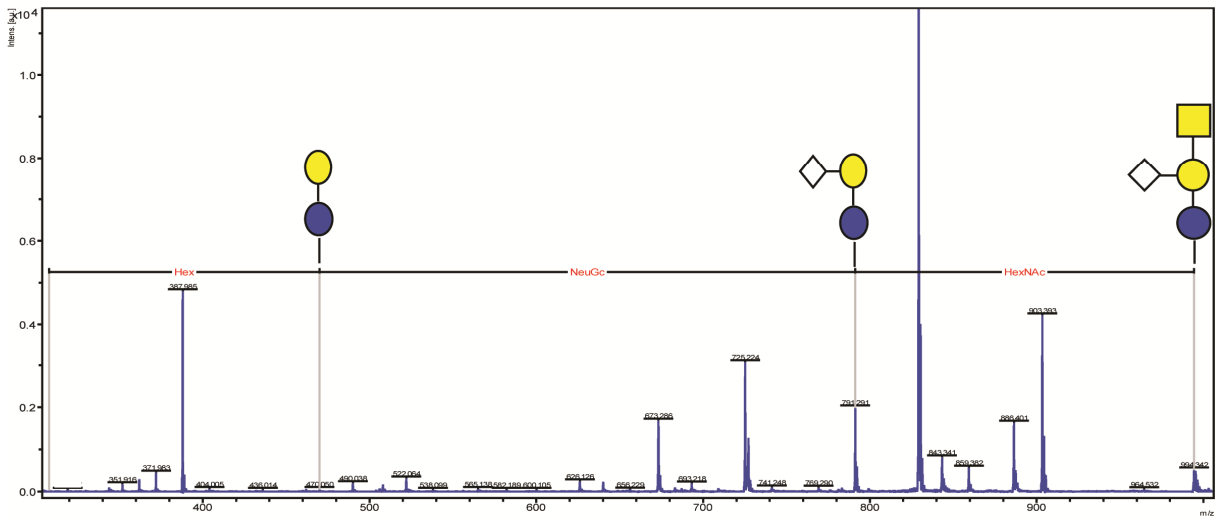

Figure 4.4. TOF/TOF analysis of GM2-NeuGc (m/z 994.3). Glycan cartoons were constructed using the standard Consortium for Functional nomenclature, i.e., blue circle, glucose; yellow circle, galactose; yellow square, *N*-acetylgalactosamine; and white diamond, *N*-glycolylneuraminic acid.

Table 4.3. Serum glycosphingolipidomics. All serum *GSL*-glycans compositions, common names and amounts (pmole ± SD) released from 100 μL of sera from HD transgenic and WT mice are summarized (Hex, glucose or galactose; HexNAc, *N*-acetylgalactosamine; NeuAc, *N*-acetylneuraminicacid; NeuGc, *N*-glycolylneuraminic acid; and ND, not detected).

			Control		HD	
GSL-glycan composition	Common name	MS_MW	BCF1_♂	BCF1_♀	R6/2_♂	R6/2_♀
(Hex)2 (HexNAc)1	GA2	673.2	3.88 ± 0.85	4.88 ± 1.06	2.73 ± 0.59	2.43 ± 0.46
(Hex)2 (NeuAc)1	GM3 (NeuAc)	775.3	0.60 ± 0.22	0.64 ± 0.07	0.54 ± 0.18	0.63 ± 0.14
(Hex)2 (NeuGc)1	GM3 (NeuGc)	791.3	2.22 ± 0.27	1.99 ± 0.34	1.28 ± 0.48	1.21 ± 0.26
(Hex)3 (HexNAc)1	Asialo GM1	835.3	2.47 ± 0.33	2.78 ± 0.26	2.32 ± 0.30	3.08 ± 0.61
(Hex)2 (HexNAc)1 (NeuAc)1	GM2 (NeuAc)	978.4	8.54 ± 1.17	9.05 ± 3.24	7.94 ± 1.54	4.67 ± 1.27
(Hex)2 (HexNAc)1 (NeuGc)1	GM2 (NeuGc)	994.3	247.05 ± 21.27	196.52 ± 46.14	167.49 ± 29.07	118.04 ± 29.92
(Hex)3 (HexNAc)2	Forssman Ag/Globo-5	1038.4	3.13 ± 0.37	2.76 ± 0.57	2.01 ± 0.47	1.93 ± 0.24
(Hex)3 (HexNAc)1 (NeuAc)1	GM1 (NeuAc)	1140.4	1.56 ± 0.19	1.36 ± 0.09	1.18 ± 0.20	1.20 ± 0.27
(Hex)3 (HexNAc)1 (NeuGc)1	GM1 (NeuGc)	1156.4	21.43 ± 4.21	6.26 ± 1.78	1.76 ± 2.06	4.13 ± 3.38
(Hex)3 (HexNAc)2 (Deoxyhexose)1	Type IA/IIA	1184.4	0.76 ± 0.25	ND	ND	ND
(Hex)4 (HexNAc)2	Globo-13	1200.4	0.43 ± 0.08	0.55	ND	0.24
(Hex)2 (HexNAc)1 (NeuGc)2	GD2	1315.5	0.56 ± 0.06	0.38 ± 0.09	ND	0.39 ± 0.08
(Hex)3 (HexNAc)2 (NeuAc)1	GalNAc-GM1 (NeuAc)	1343.5	0.71 ± 0.06	0.60 ± 0.10	0.97 7 0.35	0.57 ± 0.17
(Hex)3 (HexNAc)2 (NeuGc)1	GalNAc-GM1 (NeuGc)	1359.5	ND	ND	ND	0.23 ± 0.10
(Hex)3 (HexNAc)1 (NeuAc)2	GD1a (NeuAc)	1445.5	3.97 ± 0.81	1.82 ± 0.39	1.38 ± 1.12	2.13 ± 1.98
(Hex)3 (HexNAc)1 (NeuAc)1 (NeuGc)1	GD1a (Neu-Ac/Gc)	1461.5	0.92 ± 0.22	0.63 ± 0.16	0.56 ± 0.06	1.08 ± 0.30
(Hex)3 (HexNAc)1 (NeuGc)2	GD1a (NeuGc)	1477.5	26.69 ± 4.93	11.35 ± 3.66	8.38 ± 0.52	11.60 ± 10.54
(Hex)5 (HexNAc)2 (Deoxyhexose)1	Globo-15	1508.5	0.32 ± 0.04	ND	ND	ND
(Hex)4 (HexNAc)2 (NeuGc)1	Ganglio-a-10/-as-9	1521.5	0.26 ± 0.05	0.34 ± 0.09	ND	0.27 ± 0.07
(Hex)3 (HexNAc)2 (NeuGc)2	GalNac-GD1a	1680.6	0.33 ± 0.04	0.34 ± 0.07	0.24 ± 0.04	0.28 ± 0.08
		Total	**325.84 ± 35.44**	**242.26 ± 58.10**	**198.78 ± 36.98**	**154.10 ± 49.87**

4.2.3. Human Brain Glycosphingolipidomics of AD, PD, HD and Normal Subjects.

The human brain is rich in glycosphingolipids (*GSLs*), and gangliosides – sialylated versions of complex *GSL* are abundant in brain and the peripheral nervous system. My effort on profiling and quantifying the expression levels of these carbohydrates were succeeded in discovering the specific gangliosides in brain and serum of HD transgenic and WT brain and serum (GD1a in case of brain tissue and GM2-NeuGc in serum). Proceeding, we have profiled the gangliosides of human brain and serum of AD, PD, HD and Normal subjects (Figure 4.5). Gangliosides were decreased in frontal cortex of AD, PD, and HD brain tissue ($p<0.05$, Table 4.4), except in female PD compared to the Normal subjects. All the female occipital cortices of AD, PD, and HD and parietal cortices of male PD and HD of our experimental samples have shown increased expression levels of gangliosides. Specially, GM1 was significantly lowered in AD of both sex, male PD and HD when compared to the Normal subject (Figure 4.6) Moreover, we have found smaller amounts of GD1a-/GD1b-lactone gangliosides.

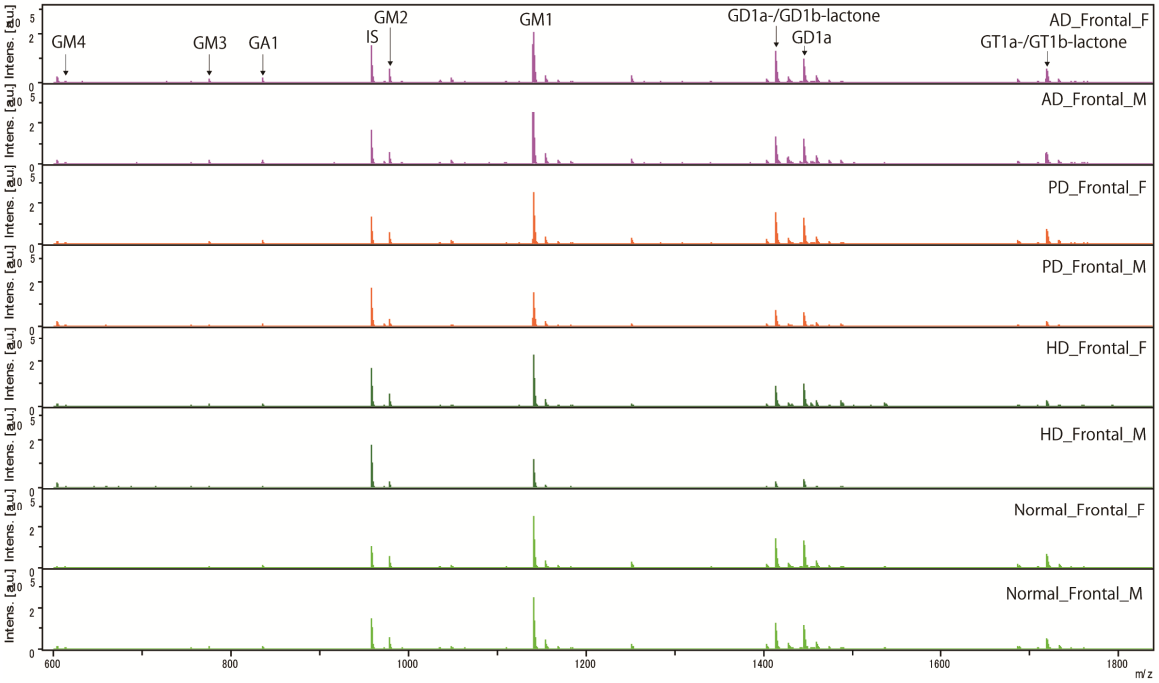
GM4
GM3
GA1
GM2
IS
GM1
GD1a-/GD1b-lactone
GD1a
GT1a-/GT1b-lactone
AD_Frontal_F
AD_Frontal_M
PD_Frontal_F
PD_Frontal_M
HD_Frontal_F
HD_Frontal_M
Normal_Frontal_F
Normal_Frontal_M
Intens. [a.u.]
600
800
1000
1200
1400
1600
1800
m/z

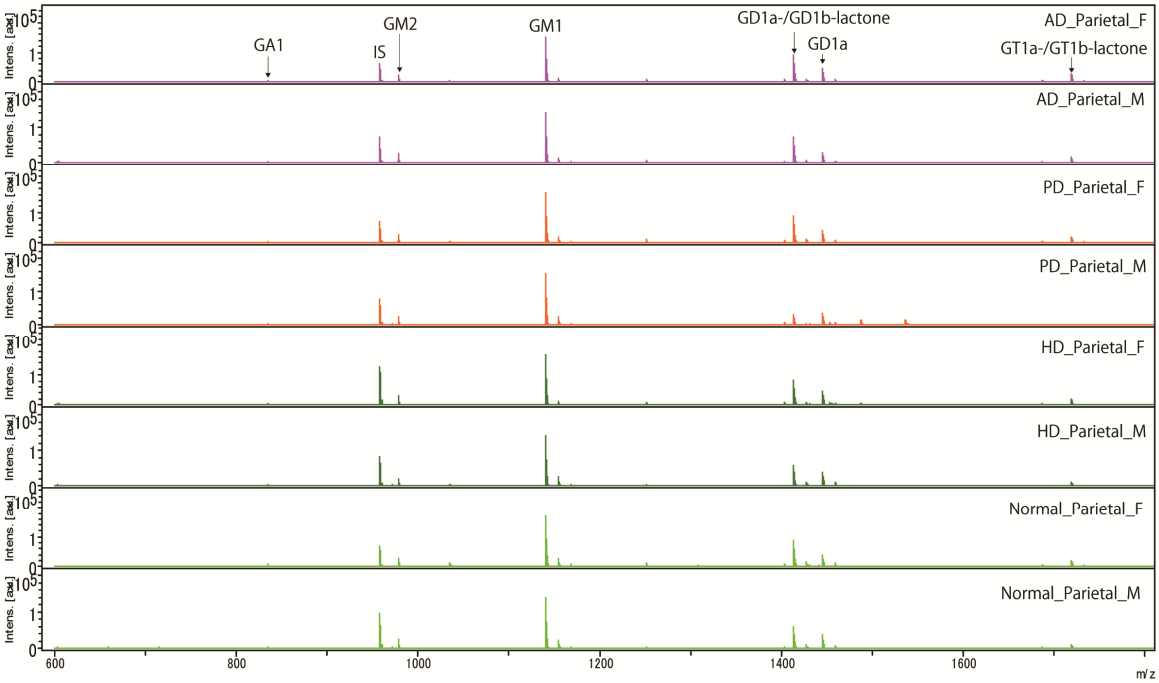
GA1
GM2
IS
GM1
GD1a-/GD1b-lactone
GD1a
GT1a-/GT1b-lactone
AD_Parietal_F
AD_Parietal_M
PD_Parietal_F
PD_Parietal_M
HD_Parietal_F
HD_Parietal_M
Normal_Parietal_F
Normal_Parietal_M
Intens. [a.u.]
600
800
1000
1200
1400
1600
m/z

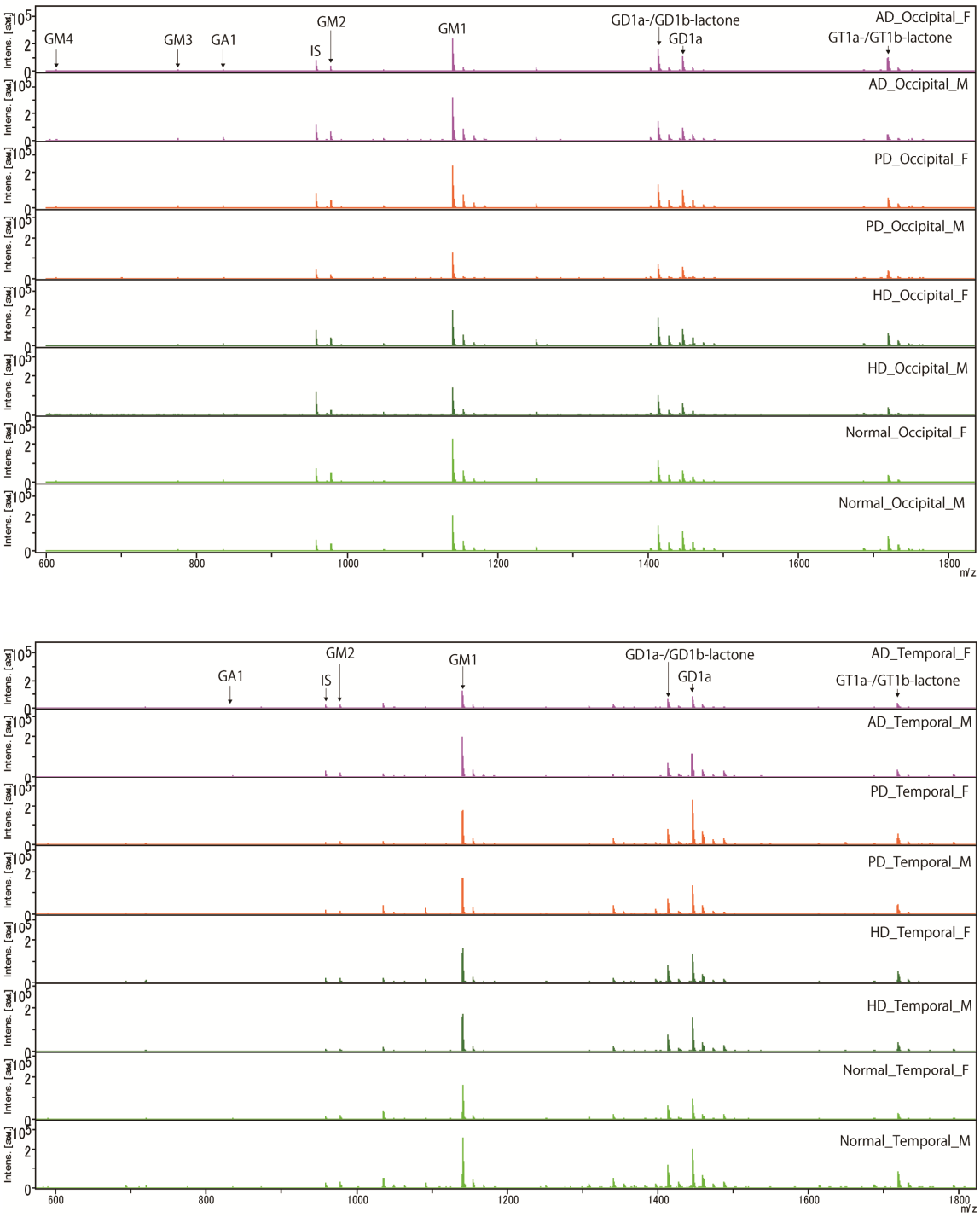

Figure 4. 5. Representative MALDI-TOF MS spectra of human brain tissue GSL-omics.

Table 4.5. Human brain *GSL*-glycans (pmole ± SD, from 100 µg protein equivalent) focused on gangliosides. AD, Alzheimer's disease; PD, Parkinson's disease; HD, Huntington's disease; Normal, as control; M, male; and F, Female.

Cerebral cortices	Normal_M	AD_M	PD_M	HD_M
Frontal	1014.75 ± 206.52	637.49 ± 94.47	429.7725 ± 99.51	394.07 ± 258.12
Parietal	567.15 ± 153.48	622.65 ± 46.58	608.37 ± 63.02	673.65 ± 217.04
Occipital	1241.23 ± 454.25	1342.72 ± 478.70	1248.34 ± 272.60	911.42 ± 336.79
Temporal	6873.56 ± 1081.02	3580.91 ± 1331.59	4636.78 ± 465.11	9762.35 ± 3350.81

Cerebral cortices	Normal_F	AD_F	PD_F	HD_F
Frontal	829.68 ± 148.83	656.19 ± 92.28	881.10 ± 169.49	560.94 ± 50.83
Parietal	617.36 ± 165.59	561.56 ± 151.65	726.24 ± 154.74	563.96 ± 126.51
Occipital	1027.31 ± 318.78	1515.62 ± 359.30	1401.46 ± 338.96	1504.13 ± 290.97
Temporal	3106.71 ± 1901.87	3932.24 ± 1449.97	8129.45 ± 3515.16	4224.82 ± 1036.48

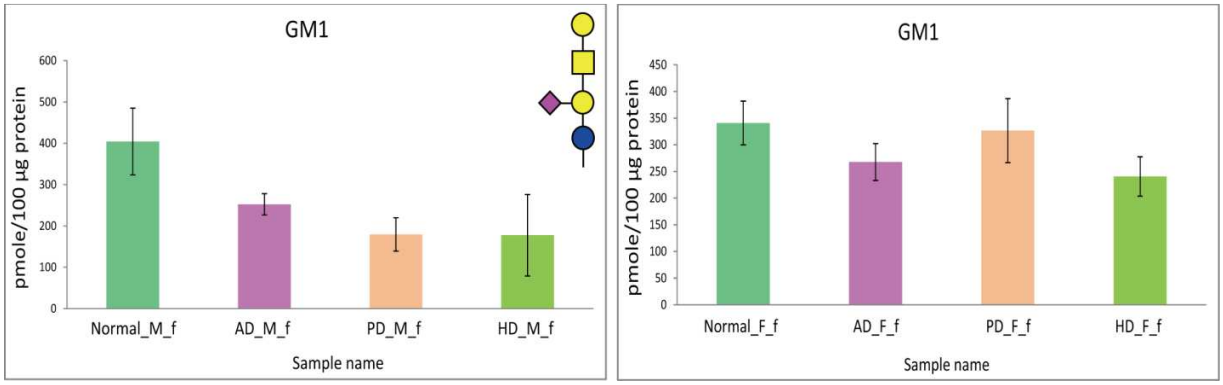

Figure 4.6. concentration of GM1 (pmole, where the bar is SD) in AD, PD, HD and Normal subjects. AD, Alzheimer's disease; PD, Parkinson's disease; HD, Huntington's disease; Normal, as control; M, male; F, Female, and f, frontal cortex.

4.2.4. Human Serum Glycosphingolipidomics of AD, PD, HD and Normal Subjects.

Being amphiphilic and complex in serum with some lipophilic proteins, for example lipoproteins, gangliosides are very informative to understand the sialic acid containing glycosphingolipids. I have analyzed whole *GSL*-glycans release focusing on gangliosides in serum which have direct correlation to those gangliosides in human brain *GSL*-glycan analysis. With this, the amount of gangliosides in human serum of neurodegenerative diseases and their control are shown in Table 4.5. Surprisingly, the increase in the gangliosides expression levels in each serum samples have shown the same trend with the elevation of the *N*- and *O*-glycans expression of same subjects.

Gangliosides were increased in AD, female of PD and female HD while decreased in male PD and HD. I have found higher amount of smaller gangliosides, such as GM2, GM3, and GM4, compared to the larger polysialylated gangliosides (GM1, GD1a, and GT1b). Those simpler gangliosides were highly expressed in AD, and female of PD and female HD. It's a clear observation of *GSL*-glycan expression levels difference between genders as witnessed from the *N*- and *O*-glycan analysis (Chapter 2 and 3).

Table 4.5. Gangliosides concentration (pmole ± SD) in human serum of AD, PD, HD, and Normal subjects. AD, Alzheimer's disease; PD, Parkinson's disease; HD, Huntington's disease; Normal, as control; M, male, and F, Female. The "– "shows that no samples is paired with brain tissues. (Note: *N*-glycans expression levels were different in intra-samples. This is because patients were diagnosed not only neurological but also clinical complications. For example, diabetes Type II, hypertension, kidney failure and heart attack. All of these are sequel of CNS disorders. Moreover, their autolysis time was different. This phenomenon was also observed in case of *N*- and *O*-glycans analysis in Chapter 2 and 3).

Sample name	M1	M2	M3
Normal	14.38 ± 2.40	52.50 ± 5.57	57.31 ± 13.50
AD	93.30 ± 17.20	30.14 ± 13.59	19.95 ± 9.94
PD	7.96 ± 1.61	31.46 ± 2.43	21.48 ± 5.12
HD	–	14.44 ± 3.00	26.91 ± 9.56

Sample name	F1	F2	F3
Normal	37.60 ± 13.40	17.01 ± 10.80	–
AD	49.57 ± 7.20	70.01 ± 44.42	–
PD	–	83.07 ± 19.00	17.87 ± 1.58
HD	54.83 ± 24.79	–	59.93 ± 10.92

4.3. Discussion

The total amount of *GSL*-oligosaccharides were successfully profiled and quantified by using chloroform/methanol extraction, ozonolysis and alkaline treatment for *GSL*-glycan moieties release and glycoblotting–assisted glycan enrichment techniques. The total amount of *GSL*-glycans detected in the striatum of male HD transgenic mice were three times higher than the WT mice; however, those glycans moieties released from the cortex of the same HD transgenic mice were lower than the WT mice. The whole brain regions of the female HD transgenic mice were shown higher amount of *GSL*-glycans relative to WT mice. Except a slight decrease in cortex of male transgenic mice, GD1a was found a drastic increase in HD transgenic mice than the WT mice. Most gangliosides are synthesised by liver and secreted into the serum, and gangliosides compositions altered due to the liver disease of various etiologies. Since serum gangliosides concentration, especially GM2-NeuGc, markedly reduced in mice with the metastatic vasculogenic mimicry (VM) tumor [14], our study can be a further evidence for the alteration of liver functions due to the effect of HD. Therefore, GD1a in brain and GM2-NeuGc in serum found to be the potential glyco-biomarkers in the ganglioside-family. In striatum, while the amount of *GSL*-glycans were higher in female than male WT mice, this phenomenon was found the reverse in HD transgenic mice; and it was vice versa in cortex.

In serum, *GSL*-glycans were higher in male HD transgenic and WT mice than compared to the female mice. I could merely suggest that this particular difference in glycan expression levels is due to hormonal difference and the sensitivity of the HD transgenic mice for over expression of glycomes since sequele of diseases. Apart suggestion, I believe that glycome expression levels within sex need further investigation. In consistence with the result of *N*-

glycome analysis, which is the presence of hybrid type *N*-glycomes that are core fucosylated and with bisecting GlcNAc (peak no. 7, 12, 21, 30) might be due to a novel processing pathway in the brain rather than high level of beta-hexosaminidase activiy [15]; the higher levels of gangliosides in HD model mice were due to inadequate amount of hexosaminidase in lysosomal compartments suggest that HD model mice experienced the same fate as GSL lysosomal storage disease does [15,16].

To emphasize again, comparison of intra-brain region glycome may uncover the significance of the region specific sensitivity of the neuronal and glial cells to the cytotoxic effect of the huntingtin aggregates. With this aim, I found that the total amount of *GSL*-glycans were higher in cortex compared to striatum which was taken from the same mice brain ($p < 0.001$, Figure 4.7). The higher *GSL*-glycans expression indicates how cortex is more affected (especially in the later weeks) and cortex is really important in HD and the accumulation of gangliosides is due to absence or low activity of specific hydrolase enzyme.

From human brain profiling, we have found smaller amounts of GD1a-/GD1b-lactone gangliosides, which were absent in R6/2 and BCF1. As previously also evidenced that GD1b-lactone (GD1b-L) is not artifactually originated but constitutes an authentic product of brain metabolism [17]. The decrease of gangliosides correlates with the degeneration of neurons. In line with my study, which is a significant loss of gangliosides were found in the frontal and male temporal of AD, which proved the previous studies showed losses in both areas [18].

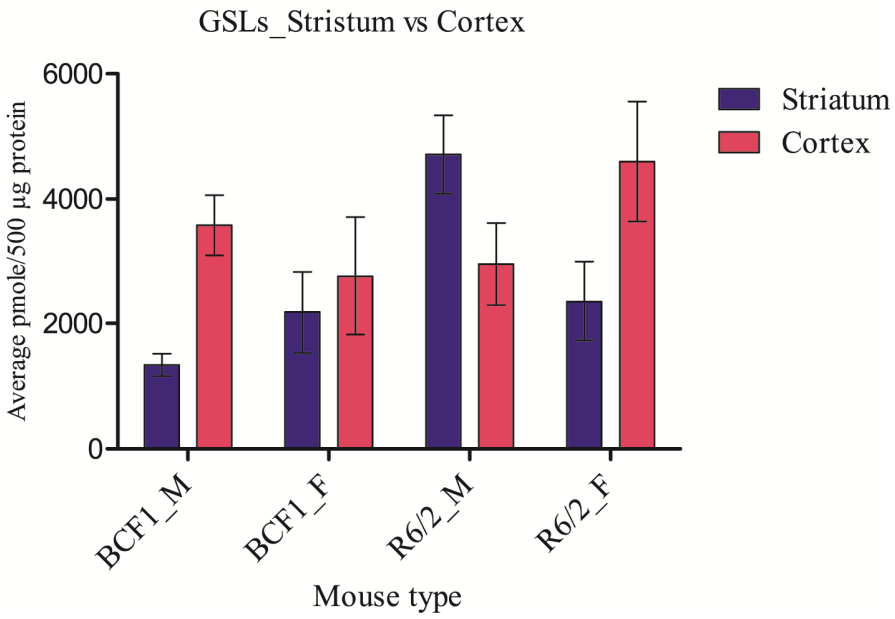

Figure 4.7. Comparison of *GSL*-glycan expression levels in striatum and cortex HD transgenic anc control mice. BCF1, WT mice; R6/2, HD transgenic mice; M, male; and F, female.

The variation is most probably related to different progress of disease reflecting by different ratio of astrogliosis and/or neuronal degeneration. Biochemical findings on gangliosides in AD brains are in agreement with neuroanatomic finding of the most concentrated neuritic plaques in these areas and that the number of neurons in frontal and temporal cortex decreased [19]. The decreased in gangliosides expressions levels was more pronounced in frontal cortex of Alzheimer's disease, which proved that GM1 aggregated with Aß(1-42). Study showed a reduction in gangliosides in the majority of brain regions, including the cerebral cortex, hippocampus, basal telencephalon, and frontal white matter, and especially in the frontal cortex white matter [20]. The decrease in concentration of GM1, especially in Alzheimer's disease, is

due to the presence of membrane-bound Aß(1-42) tightly bind to GM1(GAß), may act as a seed for toxic amyloid fibril formation, and exhibit early pathological changes of AD [21].

Comparing to the control subjects, the elevation of simpler gangliosides in serum AD, such as GM2 and GM3, and the decrease in concentration of larger a-series gangliosides, such as GM1 and GD1a, were might be due to the acceleration of lysosomal degradation of gangliosides, elevated activities of acidic ß-D-galactosidase and reduced sialyltransferase activity; all these changes are associated with Alzheimer's disease [32].

4.4. Experimental Sections

4.4.1. Releasing Glycan Moieties from Brain Tissue GSLs

Perfused mouse and human brain tissues, subfragmented into 2-3 mm squares with razor, were homogenized in PBS (20 mg/mL) using the same method described previously. The lysates were centrifuged at 100 g for 10 mins at 4°C and the supernatant was transferred into another 15 mL Falcon tube. The precipitate was dissolved with 600 µL of PBS, and it was vortexed and sonicated. The mixture was centrifuged at 800 g for 10 mins at 4°C and the supernatant was mixed with the first homogenates. The whole homogenates were centrifuged at 13,000 g for 10 mins at 4°C and the resulting precipitate was again dissolved in 500 µL PBS. 5 µL of this mixture was used for the BCA assay. The remaining solution was centrifuged (13,000 g, for 10 mins at 4°C). The precipitate was dissolved, successively, with a mixture of 3 mL chloroform/MeOH to produce three solutions (1:2, 1:1, 2:1 v/v, for both mouse and human) and chloroform:MeOH:water mixture (2:5:1 v/v, for human brain). Each solution was subsequently was sonicated for 10 mins. Each extraction was followed by centrifugation at 800 g and 4°C and the resulting supernatants were collected in new 15 mL Falcon tube. The resulting supernatants (total lipids) were dried at room temperature via SpeedVac.

The total lipids were suspended in 2 mL (1 mL for mice brain tissue) chloroform/MeOH (1:1 v/v) and sonicated. Ozone was generated from oxygen using a benchtop generator (NG81-NO3, Nigorikawakogyo, Japan) at a flow setting of 1 mL/min. The output from the ozone generator was bubbled for 5 mins and the reaction was quenched by passing N_2 gas in the total lipid suspension for a minute. The pipettes were rinsed with chloroform/MeOH (1:1 v/v) and the

resulting solution was dried by SpeedVac. Next, MeOH:0.5 M sodium methoxide (NaOMe)/MeOH (4:1 v/v) was added to the dried sample and allowed to stand for 30 mins at room temperature. The reaction mixture was transferred to a 1.5 mL eppendorf tube, neutralized with 6 µL concentrated acetic acid and then dried. A sample equivalent to 500 µg (HD transgenic mice) and 400 µg (in human brain tissue) of proteins of mouse and human brain tissues that were adjusted with de-ionized water were used for glycoblotting protocol, the same as decribed in Chapter 2. The amount of *GSL*-glycans were then normalized to 100 µg protein equivalent for convenient use.

4.4.2. Releasing Glycan Moieties from Serum GSLs

A 100 µL of freeze-dried serum was used to analyze serum glycan moieties released from GSLs. Briefly, GSLs were extracted in 3 mL of chloroform/MeOH mixtures at 1:2, 1:1, 2:1 (v/v) and chloroform:MeOH:water mixture at 2:5:1 (v/v) each step was accompanied by sonication for 10 mins and it was centrifuged at 800 g for 10 mins at room temperature. The resulting supernatants of each extraction were collected together in another 15 mL Falcon tube. The rest extraction steps were performed the same as described in section 4.4.1. 20 µL of digested mixture was applied directly to glycoblotting the same as decribed in Chapter 2.

4.5. References

[1] R.L. Schnaar, A. Suzuki, and P. Stanley, Glycosphingolipids, in Essential of glycobiology (Eds. A. Varki, R.D. Cummings, J.D. Esko, H.H. Freeze, P. Stanley, C.R.. Bertozzi, G.W. Hart, and M.E. Etzler, 2nd Ed.), Cold Spring Habor Laboratory Press, Cold Spring Harbor, New York, 2009, pp. 129 – 141.

[2] E. Posse dee Chaves, S. Sipione, Sphingolipids and gangliosides of the nervous system in membrane function and dysfunction, FEBS Lett. 584 (2010) 1748 – 1759.

[3] M. Cotterchio, T.N. Seyfried, serum gangliosides in mice metastatic and non-metastatic brain tumors, J. Lipid Res. 35 (1994) 10 – 14.

[4] H. Farwanah, T. Kolter, Lipidomics of glycosphingolipids, Metabolites 2 (2012) 134 – 164.

[5] T. Kolter, R.L. Proia, K. Sandhoff, Combinatorial ganglioside biosynthesis, J. Biol.Chem. 277 (2002) 25859 – 25862.

[6] M.E. Taylor, K. Drickamer, Introduction to glycobiology, Oxford University Press Inc., New York, pp. 51 – 68.

[7] T. Ariga, M.P. McDonald, R.K. Yu, Role of gangliosides metabolism in the pathogenesis of Alzheimer's disease- a review, J. Lipid Res. 49 (2008) 1157 – 1175.

[8] Q.X. Li, S.J. Fuller, K. Beyreuther, C.L. Master, The amyloid precursor protein of Alzheimer's disease in human brain and blood, J Leukoc Biol. 66 (1999) 567 – 574.

[9] N. Nagahori, M. Abe, S.-I. Nishimura, Structural and functional glycosphingolipids by glycoblotting with aminooxy-functionalized gold nanaoparticles, Biochemistry 48 (2009) 583 – 594.

[10] N. Nagahori, T. Yamashita, M.Amano, S.-I. Nishimura, Effect of ganglioside GM3 synthase gene knockout on the glycoprotein *N*-glycan profile of mouse embryonic fibroblast, ChemBioChem 14 (2013) 73 – 82.

[11] S.-I. Nishimura, K. kiikura, M. Kurogochi, T. Masushita, M. Fumoto, H. Hinou, R. kamitani, H. Nakagawa, K. Deguchi, N. Miura, K. Monde, H. Konde, High-throughput protein glycomics: Combined use of chemoselective glycoblotting and MALDI-TOF/TOF mass spectroscopy, Angewu. Chem. Int. Ed. 44 (2005) 91 – 96.

[12] Y. Miura, M. Hato, Y. Shinohara, H. Kuramoto, J.-i. Furukawa, M. Kurogochi, H. Shimaoka, M. Tada, K. Nakanishi, M. Ozaki, S. Todo, S.-I. Nishimura, BlotGlycoABC™, an integrated glycoblotting technique for rapid and large scale clinical glycomics, Mol. Cell. Proteomics 7 (2008) 370 – 377.

[13] J.-i. Furukawa, Y. Shinohara, H. Kuramoto, Y. Miura, H. Shimaoka, M. Kurogochi,M. Nakano, S.-I. Nishimura, Comprehensive approach to structural and functional glycomics based on chemoselective glycoblotting and sequential tag conversion, Anal. Chem. 80 (2008) 1094– 1101.

[14] M. Cotterchio, T. N. Seyfried, Serum gangliosides in mice with metastatic and non-metastatic brain tumors, J. Lipid Res. 35 (1994) 10 – 14.

[15] Y. J. Chen, D. R. Wing, G. R. Guile, R. A. Dwek, D. J. Harvey, S. Zamze, Neutral *N*-glycans in adult rat brain tissue - complete characterization reveals fucosylated hybrid and complex structures, Eur. J. Biochem. 251(1998) 691 – 703.

[16] K. Sango, M. P. McDonald, J. N. Crawley, M. L. Mack, C J. Tifft, E. Skop, C. M. Starr, A. Hoffman, K. Sandhoff, K. Suzuki, R. L. Proia, Mice lacking both subunits of lysosomal beta-hexosaminidase display gangliosides and mucopolysaccharides, Nature Genetics 14 (1996) 348 – 352.

[17] L. Riboni, S. Sonnino, D. Acquotti, A. Malesci, R. Ghidoni, H. Egge, S. Mingrino, G. Tettamanti, Natural occurrence of ganglioside lactones, J Biol Chem. 261 (1986) 8514 – 8519.

[18] M. Malander-Melin, K. Blennow, N. Bogdanovic, B. Dellheden, J.E. Mansson, P. Fredman, Structural membrane alteration in Alzheimer brain found to be associated with regional disease development; increased density of gangliosides GM1 and GM2 and loss of cholesterol in detergent-resistant membrane domains, J Neurochem. 92 (2005) 171 – 182.

[19] I. Kracun, S. Kalanj, J. Talan-Hranilovic, C. Cosovic, Cortical distribution of gangliosides in Alzheimer's disease, Neurochem Int 20 (1992) 433 – 438.

[20] S. Kalanj, I. Kracun, H. Rosner, C. Cosovic, Regional distribution of brain gangliosides in Alzheimer's disease, Neurol. Croat. 40 (1991) 269 – 281, in T. Ariga, C. Wakade, R.K. Yu, The pathological roles of ganglioside metabolism in Alzheimer's disease: Effects of gangliosides on neruogenesis, Int J Alzheimer's Dis. 2011 (2011) 193618

[21] K. Yanagisawa, A. Odaka, N. Suzuki, Y. Ihara, GM1 ganglioside-bound amyloid beta-protein (A beta): a possible form of preamyloid in Alzheimer's disease, *Nat Med.* 1 (1995) 1062 – 1066.

[22] T. Ariga, M.P. McDonald, R.K. Yu, Role of gangliosides metabolism in the pathogenesis of Alzheimer's disease- a review, J. Lipid Res. 49 (2008) 1157 – 1175.

Chapter 5

Concluding Remarks

Neurodegeneration is the umbrella term that can be applied to several conditions result in progressive loss of neuronal structure and function, and finally neuronal death. All those central nervous system (CNS) disorders result from abnormalities in the processing of proteins and defective processing causes the accumulation of specific neuronal proteins. In addition, this abnormal processing of neuronal proteins can entail misfolding of proteins, consequently, altered post-translational modifications of newly synthesized proteins. Glycosylation is the most prevalent post-translational modifications of proteins in higher organisms essential to modulate a wide range of protein and lipid functions within or on extracellular surfaces of the cell. The atrophy of the neurons due to pediatric and adulthood diseases of the CNS leads to aberrant glycosylation and the biosynthesis pattern of the available glycans is altered. Understanding the glycosylation pattern of *N*-, *O*-, and *GSLs*-glycans, which is affected by either genetic or environmental cellular stressors, can be promising for an easy prognosis. Brain tissue, serum, and CSF specimens from neurodegenerative and age-related diseases have been validated for biomarker discovery. Moreover, direct glycan analysis of human serum without any protein identification represents a new and innovative approach to disease marker. As a first initiative, I have successfully profiled the presumptive compositions and quantified the expression levels of the total glycomes (*N*-, *O*-, and *GSL*-glycans) expressed in the human brain tissue, serum, and CSF of neurodegenerative diseases using glycoblotting-assisted sample preparation combined with MALDI-TOF/MS analysis.

In chapter 2, I have discussed about the composition and amount of *N*-glycans of neurodegenerative diseases. From brain tissue glycomics, I have found no significant difference in the amount of *N*-glycans expression levels between R6/2 and BCF1; however, in serum, *N*-

glycans were found in decreased levels in HD transgenic mice. *N*-glycans were decreased in human brain tissues, but found in increased levels in human serum and cerebrospinal fluids. More pronouncedly, bisecting-GlcNAc and proximal fucose were decreased in AD, PD and HD; however, these glycans were increased significantly in serum and cerebrospinal fluids of AD, female PD and Female HD compared to the Normal subjects. Significant reduction of *N*-glycans in frontal cortex of neurodegenerative diseases might be due to the selective vulnerability of the frontal cortex in which the gene that triggers protein misfolding is expressed at higher levels in areas that are affected the most. *N*-glycan expression levels have strongly correlated with the concentration of serum IgG, but less pronouncedly with the concentration of IgG in CSF. This result proved that most of core-fucosylated, bisecting-GlcNAc and biantennary type of *N*-glycans in human serum are derived from IgG and, noteworthy, IgG as a potential target for biomarker discovery.

Chapter 3 revealed that the total amount of *O*-glycans were elevated and lowered in male and female HD transgenic mice, respectively, compared to the WT mice. The present results clearly indicated that the brain glycomes and their expression levels are significantly gender specific. Core 3 was found in increased levels in male and in decreased levels in both the striatum and cortices of female HD transgenic mice. Furthermore, serum levels of core 1 decreased and were undetected for core 2 for HD transgenic mice. *O*-glycans were not shown any significant difference in human serum of neurodegenerative diseases and the normal subjects. Di-sialyl T and sialyl T were found the major mucin-type *O*-glycans in human brain and serum, respectively, of neurodegenerative diseases. Surprisingly, while the ratio of di-sialyl T to sialyl T is higher in human brain tissues of neurodegenerative diseases, the reverse is true in

serum. Further study focusing on those *O*-glycans, especially sialic acid-focused reverse glycomics, will unravel the mystery of the expression levels difference in human brain and serum of neurodegenerative diseases.

Chapter 4 described the *GSL*-glycans expression levels of neurodegenerative diseases. The striatum HD transgenic mice displayed higher levels of *GSL*-glycans relative to those of the WT mice. GD1a was drastically increased in the striatum of HD transgenic mice. The higher levels of gangliosides in HD model mouse might be due to inadequate amounts of hexosaminidase in lysosomal compartments, suggesting that HD transgenic mice experienced the same symptoms of GSL lysosomal storage disease. Total serum *GSL*-glycans, GM2-NeuGc in parrticular, were decreased in HD transgenic mice compared to the control group mice, in which my study provided further evidence demonstrating the alteration of liver functions due to the effect of HD. Gangliosides were found in decreased levels in human frontal cortex of AD, PD, and HD brain tissue (similar to the *N*-glycans), but in female PD when compared to the Normal subjects. The decrease of gangliosides, particularly a-series gangliosides, resulted from the severe loss of neurons and brain shrinkage, which are the pathological hallmarks of neurodegenerative diseases. The reduction of GM1 in neurodegenerative diseases compared to the normal confirmed the presence of membrane-bound Aß1-42 tightly bind to GM1 (GAß), which acts as a seed for amyloid, and exhibit early pathological changes of AD.

In conclusion, I have proved that total glycomes expression levels were found altered due to the accumulation of ‘amyloid-like proteins’ in neurodegenerative diseases in brain and circulation which is favoring accumulation aggregated proteins in the brain. As a result, neuronal

death aggravated and subsequent perturbation of sugar metabolism which in particular reduced the concentration of brain specific *N*-glycans and gangliosides. Moreover, elevated non-physiologically aggregated proteins detected in peripheral tissues, serum and CSF of neurodegenerative diseases; and aberrant and/or failure of glycosylation of these proteins altered the composition and expression levels of total glycomes.

Finally, I strongly certify that glycome-based analysis of neurodegenerative diseases are one of the down-to-earth and non-invasive approach towards the discovery of the most promising biomarkers in the next-generation neuroscience studies. The present study will be a great assistance in the field of neuroscience and future drug discovery.

Acknowledgments

My sincere gratitude goes to Prof. Shin-Ichiro Nishimura for his resourcefulness, suggestions, and discussions throughout this research work. I am highly grateful to Prof. Toshiaki Koda for reading the manuscript, valuable suggestions, animal experiments training and evaluating my Doctoral dissertation. I offer my gratitude to Prof. Hisashi Haga for his precious time reading, suggestions and evaluation of the Doctoral dissertation.

I am indebted to Dr. Hiroshi Hinou and Dr. Maho Amano for their research suggestions and follow up. I much appreciate the help of Mrs. Keiko Kamimura for her animal experiment guidance, lectin staining and discussion. To one person I owe much of what underlies this work: Mr. Tetsu Ohashi, I owe special thanks for his kindness and help. I thank Medicinal Chemistry Pharmaceuticals Co. Ltd., for their suggestions. I am grateful to all members of Nishimura's laboratory. I would like to thank the Government of Japan for MEXT Scholarship Award for three years.

But words cannot express my acknowledgment of the love and support of my special and respected family: Mrs. Tsehaynesh Tebeje, Assefa Ababa, Alemtsehay Fentawu, Selamawit Tebeje, Ayene Getahun, Tesfaye Sisay and his family. I hope I return more love in kind. To the person who has been encouraging me at all the times, Befakadu Andargie, I am very grateful to you for your brotherly advice all the way during my stay in the land of sun rises.